UNIVERSIDADE FEDERAL RURAL DO SEMI-ÁRIDO
PRÓ-REITORIA DE PESQUISA E PÓS-GRADUAÇÃO
PROGRAMA DE PÓS-GRADUAÇÃO EM MANEJO DE SOLO E ÁGUA
DOUTORADO EM MANEJO DE SOLO E ÁGUA

FRANCISCO ÉDER RODRIGUES DE OLIVEIRA

INFLUENCE OF THE LANDSCAPE ON SOIL CHARACTERISTICS AND SURFACE AND GROUNDWATER IN THE IGUATU-CE CITY

MOSSORÓ
2025

FRANCISCO ÉDER RODRIGUES DE OLIVEIRA

INFLUENCE OF THE LANDSCAPE ON SOIL CHARACTERISTICS AND SURFACE AND GROUNDWATER IN THE IGUATU-CE CITY

Thesis presented to Postgraduate Program in Soil and Water Science of Federal University of Semi-arid Region as a prerequisite for obtaining the Doctorate Degree in Soil and Water Science.

Research Line: Soil and Water Management in the Semi-Arid Region

Advisor: Profª. Dra. Eulene Francisco da Silva

Co-advisor: Profª. Dra. Eveline de Almeida Ferreira

MOSSORÓ

2025

d048i de Oliveira , Francisco Éder Rodrigues .
INFLUENCE OF THE LANDSCAPE ON SOIL CHARACTERISTICS AND SURFACE AND GROUNDWATER IN THE IGUATU-CE CITY / Francisco Éder Rodrigues de Oliveira . - 2025.
121 f. : il.

Orientadora: Eulene Francisco da Silva.
Coorientadora: Eveline de Almeida Ferreira.
Tese (Doutorado) - Universidade Federal Rural do Semi-árido, Programa de Pós-graduação em Manejo de Solo e Água, 2025.

1. Landscape management. 2. Sustainable soil management. 3. Water quality. I. da Silva, Eulene Francisco , orient. II. Ferreira, Eveline de Almeida , co-orient. III. Título.

Ficha catalográfica elaborada por sistema gerador automático em conformidade com AACR2 e os dados fornecidos pelo) autor(a).
Biblioteca Campus Mossoró / Setor de Informação e Referência
Bibliotecária: Keina Cristina Santos Sousa e Silva
CRB: 15/120

O serviço de Geração Automática de Ficha Catalográfica para Trabalhos de Conclusão de Curso (TCC´s) foi desenvolvido pelo Instituto de Ciências Matemáticas e de Computação da Universidade de São Paulo (USP) e gentilmente cedido para o Sistema de Bibliotecas da Universidade Federal Rural do Semi-Árido (SISBI-UFERSA), sendo customizado pela Superintendência de Tecnologia da Informação e Comunicação (SUTIC) sob orientação dos bibliotecários da instituição para ser adaptado às necessidades dos alunos dos Cursos de Graduação e Programas de Pós-Graduação da Universidade.

FRANCISCO ÉDER RODRIGUES DE OLIVEIRA

INFLUENCE OF THE LANDSCAPE ON SOIL CHARACTERISTICS AND SURFACE AND GROUNDWATER IN THE IGUATU-CE CITY

Thesis presented to Postgraduate Program in Soil and Water Science of Federal University of Semi-arid Region as a prerequisite for obtaining the Doctorate Degree in Soil and Water Science.

Research Line: Soil and Water Management in the Semi-Arid Region

Presented in: 27/08/2025.

DEFENSE COMMITTEE MEMBERS

____
Eulene Francisco da Silva, Profª. Dra. (UFERSA)
Advisor

____
Jeane Cruz Portela, Profª. Dra. (UFERSA)
Examiner Member

____
Diana Ferreira de Freitas, Profª. Dra. (UFC)
External Committee Member

____
Rafael Oliveira Batista, Prof. Dr. (UFERSA)
Examiner Member

____
Joaquim Emanuel Fernandes Gondim, Prof. Dr. (UVA)
External Committee Member

To my dad, Francisco Valdetário,

and my uncles and my grandparents (In Memoriam).

To my God, for the grace of calling him father.

To my parents Francisco Valdetário (in memoriam) and Lúcia Rodrigues, for the gift of life.

To my family, for their affection and patience.

To my friends, whom I have been blessed with throughout my life.

For their encouragement and companionship.

I dedicate.

ACKNOWLEDGEMENTS

To God, my eternal Father, for his eternal patience and infinite mercy.

To the Federal Rural University of the Semi-Arid Region (UFERSA) for the opportunity for learning and professional and personal growth.

To Mr. Auricelio Ancelico de Alencar, Mr. Raimundo Alberto da Silva, Mr. José Luiz Alves Bezerra, Mr. Eugênio Alves Gomes, Mr. Dauyzio Alves da Silva, Mr. Benildo Barbosa de Araújo, Mr. Antônio Marcos Pereira da Silva, Mr. Esmael de Souza Vanderlewy, and Mrs. Raquel Pereira da Silva and her husband Francisco Narcélio Alves Nogueira, for all their help with the research, allowing access to their planting areas, interacting, and being patient with the activities carried out by the student.

To my father (*in memoriam*) and my mother, for the educational and professional training that molded me.

To my advisor, Prof. Drª. Eulene Francisco da Silva, for all the trust, assistance, and affection she has given me throughout my academic career.

To the countless unconditional friendships I built at university, represented by the almost daily interaction at the Microbiology and Organic Matter Laboratory, with whom I have a bond of trust, interaction, companionship, many arguments, and daily adventures, but we always lived as a big "Família Buscapé".

To the professors of the Postgraduate Program in Soil and Water Science and Plant Science for the information they shared, which contributed to the knowledge acquired.

To the tenured employee represented by Carolina de Gouveia Mendes da Escóssia Pinheiro and Bruno Caio Chaves Fernandes for their work in promoting the growth of the institution, teaching, and research.

To the outsourced employees Keila Lopes and Roberta, for all the companionship, patience, and affection they have shown me over the years we have worked together.

To my friends Murillo Anderson Barbosa Gonçalves and Régia Marcia da Silva Felipe for all their support, patience, dedication, unforgettable moments, and commitment to believing in me when I didn't believe in myself.

To Brazilian Federal Agency for Support and Evaluation of Graduate Education (CAPES) and the Foundation for the Support and Promotion of Science, Technology, and Innovation of Rio Grande do Norte (FAPERN), for granting scholarships.

To everyone who directly or indirectly contributed to the realization of this study.

“The fear of a new day traps us in a day that has already passed.”

Own authorship

GENERAL ABSTRACT

OLIVEIRA, Francisco Éder Rodrigues. **Influence of the landscape on Soil characteristics and surface and Groundwater in the Iguatu/CE city.** 2025. 119p. Thesis (D.Sc in Soil and Water Management) – Federal Rural University of the Semi-Arid (UFERSA), Mossoró-RN, 2025.

Climate change and anthropogenic pressures intensify environmental challenges in semi-arid regions, altering landscape dynamics, degrading soils, and compromising water resources. The aim of this research study was to evaluate the influence of landscape change, analyze soil characteristics and surface and groundwater quality in Iguatu, Ceará, Brazil. First chapter investigated the dynamics of climate, agriculture, and land use over 37 years (1985–2023) through historical climate series, socioeconomic data, and remote sensors. Second chapter evaluates soil quality in agricultural and livestock areas by collecting samples at depths of 0–10 cm and 10–20 cm in different systems: corn-bean consortium, corn monoculture, banana cultivation, guava-horticulture consortium, and pastures with *Urochloa mosambicensis* under dairy cattle grazing, compared with preserved Caatinga fragments as a reference. Chemical attributes, organic carbon fractions, enzymatic activities (β-glucosidase, arylsulfatase, and dehydrogenase), and micromorphological features were analyzed, complemented by multivariate statistics (PCA, HCA, and Pearson correlation). In third chapter, the water quality of sedimentary basin wells and crystalline basement (G1–G4, G6, G8–G10), sections of the Jaguaribe River (R7, R11, and R13), and the Orós Reservoir (OR5) was characterized. Analyses encompassed physicochemical and microbiological parameters, ions, heavy metals, and irrigation suitability indices, supported by multivariate statistical approaches. Over a 37-year period (1985–2023), remote sensing and socioeconomic data revealed the intensification of droughts, reduction of water bodies, decline in agricultural production, rural exodus, and expansion of livestock farming, alongside severe deforestation and landscape fragmentation. Analyses showed that intensification of land use negatively affected soil quality, with a reduction in the labile and recalcitrant fractions of soil organic carbon and in enzymatic activities in intensive monoculture and fruit tree systems. The pasture showed structural stability and carbon management potential due to the longer permanence of the roots in the soil. Water quality assessments, including physical-chemical and microbiological parameters of surface and groundwater, indicated seasonal variability, with risks of salinity and sodicity during dry periods. Microbial contamination during the rainy season was the most significant among the study points. Multivariate analyses confirms that the lithology of the rock formations in the study area and the soil management practices have a critical influence on hydrogeochemical processes, limiting the irrigation potential of several sources. The results indicate interaction between climate variability and changes in land use, which have intensified environmental degradation, threatening soil and water sustainability. Thus, we highlight urgency of adopting integrated natural resource management strategies, more sustainable land use practices, and continuous water monitoring to strengthen resilience, promote natural resource conservation, and support socioeconomic sustainability in Brazil's semi-arid region.

Keywords: Landscape management. Sustainable soil management. Water quality.

RESUMO GERAL

OLIVEIRA, Francisco Éder Rodrigues. **Influência da paisagem nas características do solo e das águas superficiais e subterrâneas no município de Iguatu/CE.** 2025. 119p. Tese (Doutorado em Manejo de Solo e Água) – Universidade Federal Rural do Semi-Árido (UFERSA), Mossoró-RN, 2025.

Mudanças climáticas e pressões antrópicas têm intensificado os desafios ambientais em regiões semiáridas, alterando a dinâmica da paisagem, degradando solos e comprometendo os recursos hídricos. O objetivo desse trabalho foi avaliar a influência da mudança da paisagem, analisar as características do solo e qualidade das águas superficiais e subterrâneas em Iguatu, Ceará, Brasil. O primeiro capítulo investigou a dinâmica climática, agrícola e uso da terra ao longo de 37 anos (1985–2023), por meio de séries históricas de clima, dados socioeconômicos e sensoriamento remoto. O segundo capítulo avaliou a qualidade do solo em áreas agrícolas e pecuárias por meio da coleta de amostras nas profundidades de 0–10 cm e 10–20 cm em diferentes sistemas: consórcio milho-feijão, monocultivo de milho, cultivo de banana, consórcio goiaba-horticultura e pastagens de *Urochloa mosambicensis* sob pastejo de bovinos leiteiros, comparados a fragmentos preservados de Caatinga como referência. Foram analisados atributos químicos, frações da matéria orgânica, atividades enzimáticas (β-glucosidase, arilsulfatase e desidrogenase) e características micromorfológicas, complementados por análises estatísticas multivariadas (PCA, HCA e correlação de Pearson). No terceiro capítulo, foi feita uma caracterização da qualidade da água de poços de bacia sedimentar e do embasamento cristalino (G1–G4, G6, G8–G10), trechos do rio Jaguaribe (R7, R11 e R13) e Açude Orós (OR5). Foram realizadas análises físico-químicas e microbiológicas, concentração de íons e metais, além de índices de aptidão para irrigação, apoiados por métodos estatísticos multivariados. Os dados de sensoriamento remoto e socioeconômicos revelaram a intensificação das secas, a redução dos corpos d'água, o declínio da produção agrícola e a expansão da pecuária, juntamente com o desmatamento severo e a fragmentação da paisagem. As análises demonstraram a intensificação do uso da terra, que afetou negativamente a qualidade do solo, com redução das frações lábeis e recalcitrantes do C orgânicas do solo e das atividades enzimáticas em sistemas intensivos de monocultivo e fruteiras. A pastagem demonstrou estabilidade estrutural e potencial de manejo de carbono, devido à maior permanência das raízes no solo. Avaliações da qualidade da água, abrangendo parâmetros físico-químicos e microbiológicos das águas superficiais e subterrâneas, evidenciaram variabilidade sazonal, com riscos de salinidade e sodicidade nos períodos de estiagem. A contaminação microbiana na estação chuvosa foi a mais expressiva nos locais de estudo. Análises multivariadas confirmaram que tanto a litologia das formações rochosas das áreas de estudo quanto o manejo adotado no solo exercem influência crítica nos processos hidrogeoquímicos, limitando o potencial de irrigação em diversas fontes. Os resultados demonstram interação entre a variabilidade climática e as mudanças no uso da terra, intensificando a degradação ambiental, ameaçando a sustentabilidade do solo e da água. Portanto, ressaltamos a urgência da adoção de estratégias de gestão integrada de uso dos recursos naturais, com manejos mais sustentáveis do uso do solo e monitoramento contínuo da água, para fortalecer a resiliência, promover a conservação de recursos naturais e apoiar a sustentabilidade socioeconômica na região semiárida brasileira.

Palavras-chave: Dinâmica da paisagem. Manejo sustentável do solo. Qualidade da água.

FIGURE'S LIST

CHAPTER I

CHAPTER II

CHAPTER III

TABLE'S LIST

CHAPTER I

CHAPTER II

CHAPTER III

SUMMARY

GENERAL INTRODUCTION

The semi-arid region is a land of long dry spells and irregular rainfall, and it's sensitive to big changes in its landscape. The high temperatures, uneven rainfall, and not-so-weathered soil mean this region is at high risk for environmental degradation (Araújo, 2011). Anthropic actions have had major impacts on semi-arid landscapes through the intense process of replacing natural areas with various types of land use. Progressive replacement of Caatinga vegetation areas with pasture/agriculture areas has been observed, causing environmental degradation (Oliveira *et al*., 2021). These problems must be mitigated through public policies aimed at sustainable management of natural resources.

Variability in rainfall distribution, coupled with prolonged droughts and high temperatures, and sandy, shallow soils, intensifies soil degradation. When this happens at the highest levels, it causes social, economic, political, and environmental impacts, which are interrelated over the years (Bezerra *et al*., 2020). These natural effects are even more concerning because in the semi-arid region, farming practices are carried out without conservation measures, which can change how the soil responds to water infiltration. The loss of vegetation cover leaves the soil exposed to impact of raindrops, promoting surface micro-compaction and reduced soil porosity, impeding infiltration and thus the recharge of subsurface aquifers. Which in turn increases surface runoff, promoting river contamination and increasing salt concentrations in water used for irrigation (Paiva *et al*., 2017). Monitoring groundwater and surface water, in association with spatial dynamics, is essential for providing an effective response to area managers.

The modification of the landscape in rural areas in Iguatu-CE city been taking place for decades. The local economy is heavily based on rain-fed and irrigated agriculture, and beef and dairy cattle farming. Between the 1930s and the early 1980s, however, cotton cultivation was the main source of income driving the local economy, until it declined due to the attack of the boll weevil (Anthonomus grandis) on crops, and a drop of the price paid for cotton. At that time, the municipality was already a major producer of rice and bananas irrigated by surface water, as well as rainfed crops such as corn and beans (Holanda, 2021).

From the 2000s onwards, the first conventional irrigation systems for pasture irrigation fruit tree irrigation began to be implemented in agricultural areas with the aim of increasing crop productivity. Along with the possibility of increasing production came the exploitation of new areas that were still unused and largely unmodified. The new technology used by farmers led to increased degradation of areas considered unsuitable for planting, because they were located on rocky soils of the crystalline shield. During this period, there was an increase in the replacement of environmental reserve areas and forests bordering the Jaguaribe River, the municipality's main water source, with rain-fed and irrigated agricultural systems. The biggest issues with irrigation water quality are related to salinity, since too many soluble salts in the soil reduce the amount of water available to plants, as well as sodicity, which can cause serious soil sealing problems, and the toxicity of some specific ions (Dias *et al*., 2016).

Soil is considered a dispersed, multiphase, and heterogeneous system, with properties that enable its use as a productive medium for crops. The natural filter formed by the soil matrix, with its chemical and physical adsorption properties, and the activity of plants and microorganisms, may act as a means of intercepting salts, posing a risk of salinization when irrigated with poor-quality water (Porto Filho *et al*., 2011).

Use and occupation of land for agricultural and livestock purposes has exacerbated changes in the landscape of the Semi-Arid region. The removal of forest areas for rain-fed and irrigated planting, and pastures for animal husbandry has grown a lot. These spatial and temporal changes in land use and occupation, however, alter the entire landscape of the entire surrounding area that is directly and indirectly related to these locations. The geological formation of soils, which directly influences fertility and agricultural management practices, are along with landscape transformations in the Semi-Arid region, such as disorderly land use and irregular climatic events such as water scarcity (Coelho *et al*., 2016).

Analysis of physical and chemical attributes, organic fractions, and environmental characteristics are indispensable tools when it comes to the use, management, and occupation of land for agriculture and livestock farming. With this information, it is possible to indicate the most sustainable management practices for the Brazilian semi-arid region, focusing on Iguatu-CE city, where there has been a drastic change in the landscape due to agricultural exploitation and real estate growth.

The study aimed to analyze the impacts of landscape changes in the municipality of Iguatu/CE over four decades, and to analyze the influence of the landscape on the physical, chemical, and microbiological quality of river water and underground wells used for irrigation purposes.

REFERENCES

ARAÚJO, S. M. S. A REGIÃO SEMIÁRIDA DO NORDESTE DO BRASIL: Questões Ambientais e Possibilidades de uso Sustentável dos Recursos. **Revista Rios Eletrônica**, v. 5 n. 5, p. 89 - 98, 2011.

BEZERRA, A. C.; SILVA, J. L. B.; SILVA, D. A. O.; BATISTA, P. H. D.; PINHEIRO, L. C.; LOPES, P. M. O.; MOURA, G. B. A. Monitoramento Espaço-Temporal da Detecção de Mudanças em Vegetação de Caatinga por Sensoriamento Remoto no Semiárido Brasileiro. **Revista Brasileira de Geografia Física**, v. 13, n.01, p. 286-301, 2020.

HOLANDA, C. T. L. **A cultura do algodão e as relações sociais de produção no campo no município de Iguatu (1970 a 1985).** 2021. 112 p. Trabalho de Conclusão de Curso (História). Universidade Estadual do Ceará.

COELHO, V. H. R.; MONTENEGRO S. M. G. L.; ALMEIDA, C. N.; LIMA, E. R. V.; RIBEIRO NETO, A.; MOURA, G. S. S. Dinâmica do uso e ocupação do solo em uma bacia hidrográfica do semiárido brasileiro. **Revista Brasileira de Engrenaria Agrícola e Ambiental**, v. 18, n.1, p.64-72, 2014.

DIAS, N. S.; BLANCO, F. F.; SOUZA, E. R.; FERREIRA, J. F. S.; SOUSA NETO, O N.; QUEIROZ, Í. S. R. de. Efeitos dos sais na planta e tolerância das culturas à salinidade. In: GHEY, H. R. et al. (Eds.). Manejo da salinidade na agricultura: estudos básicos e aplicados. 2a ed. Fortaleza: **INCTSal**, 2016. p. 504.

OLIVEIRA, M. K. S.; FERREIRA, E. A.; ALMEIDA, N. V.; SILVA, E. F.; VASCONCELOS, A. A. Dinâmica Espaço-Temporal da Paisagem Semiárida no Município de Apodi/RN e seus Condicionantes Socioeconômicos e Ambientais. **Revista Brasileira de Geografia Física**, v. 14, n. 04, 2446-2464, 2021.

PAIVA, L. G. G.; SANTOS, J. L.; FREITAS, L. C. B.; VERÍSSIMO, C. U. V. VASCONCELOS, S. M. S. Análise espaço-temporal do uso e da ocupação associada à impermeabilização do solo na microbacia do Rio Granjeiro, CE. **Revista de Geologia**, Fortaleza, v. 30, n. 1, p. 95-114, 2017.

PORTO FILHO, F. Q.; MEDEIROS, J. F. de; CHEYI, H. R.; DIAS, NILDO da S.; SOUSA, P. de S.; DANTAS, D. C. Evolução da salinidade e do pH de um solo sob cultivo de melão irrigado com água salina. **Revista Brasileira de Engenharia Agrícola e Ambiental**, v.15, n.11, p.1130-1137, 2011.

CHAPTER I: DROUGHTS, LIVESTOCK EXPANSION, AND FOREST DEGRADATION: A 37-YEAR ASSESSMENT OF LANDSCAPE CHANGE IN A SEMIARID MUNICIPALITY OF BRAZIL[1]

ABSTRACT

Climate change has intensified extreme events, such as prolonged droughts in semiarid regions, with severe socioeconomic impacts, particularly in economies dependent on agriculture. In this context, we examined the effects of climate variability on productive and environmental dimensions in Iguatu (Ceará), a representative municipality of the Brazilian semiarid region, over a 37-year period (1985–2023). Our results confirm the intensification of droughts, reduction in water bodies, and decline in agricultural production, contributing to rural exodus and unregulated urban growth. In contrast, livestock farming, particularly cattle and sheep, expanded significantly, increasing pasture areas to 42% of the municipality by 2023. The lack of significant correlation between most agricultural production series and climate descriptors may indicate the role of factors including irrigation, government subsidies, and management practices, which enhance production resilience to climate variability. Meanwhile, forest cover was severely reduced and heavily fragmented. Our findings underscore the critical environmental degradation in the region and emphasize the importance of integrated strategies to mitigate climate change impacts. We recommend reforestation on rural properties combined with sustainable agricultural practices, such as intensive livestock farming, pasture rotation and fallow periods, reduction in slaughter age, and crop-livestock-forest integration. These measures have the potential to strengthen the resilience of the Brazilian semiarid region, promoting natural resource conservation and supporting local economic sustainability.

Keywords: Climate change; Forest fragmentation; Agriculture; Pasture.

[1]Oliveira, F. É. R., Ferreira, E. A., Fernandes, Tavares, V. N. S., Araújo, Y. A., Lima, J. L., ... & amp; Silva, E. F. Droughts, livestock expansion, and Forest degradation: A 37-year assessment of landscape change in a semiarid municipality of Brazil. Science of The Total Environment, 986, 179733, 2025.
PUBLISHED ARTICLE

1 INTRODUCTION

Climate change is driving profound shifts in global climate systems, altering temperature regimes, precipitation patterns, sea levels, and the frequency of extreme events such as droughts and floods (Clarke et al., 2022; Gampe et al., 2024; Zhang et al., 2024). These changes are particularly pronounced in arid and semiarid regions (Allan and Douville, 2024), where climate shifts lead to more drastic impacts and more severe droughts (El Kenawy et al., 2020; Han et al., 2021; Adamo et al., 2022). For instance, in the Brazilian semiarid region, droughts have become more frequent, prolonged, and intense, particularly during the 2010s (Marengo et al. 2017, 2018; Santana and Santos, 2020; Brito et al. 2021). We observed that during this decade, certain areas endured an extreme and prolonged drought (2012 to 2017), leading to marked reductions in seasonal rainfall, with several rainy months recording less than 20% of the expected. This scenario becomes even more concerning when considering that, unlike other semiarid regions, such as the Sahel in Africa or the southwestern United States, the Brazilian semiarid region supports a population of over 26 million people, of whom 85% live under conditions of social vulnerability, with the economy predominantly reliant on agriculture and livestock, particularly small-scale family farming (Lemos, 2020; Marengo et al., 2020). With projections of increasingly frequent and severe droughts (Jenkins and Warren, 2015; Tripathy et al., 2023), understanding potential impacts on local communities and ecosystems and anticipating adaptive responses is essential to address these escalating climatic pressures.

The intensification of droughts in Brazil's semiarid region has severely impacted water resources, leading to substantial reductions in river, stream, and reservoir volumes and an estimated economic loss of $30 billion between 2012 and 2016 (Marengo et al., 2017; 2018). The region contains approximately 481 medium- to large-sized reservoirs, with the largest located in Ceará. During critical periods, such as between 2012 and 2017, these reservoirs were reduced to less than 5% of their capacity (Pereira et al., 2023), and many smaller imperatidams dried up entirely. Additionally, thousands of intermittent streams—vital for local water supply—practically disappeared. This water scarcity triggered an agricultural crisis, exacerbated by pest infestations affecting crops like cotton and guava, alongside insufficient public policies and technological support (Mattos et al., 2020; Ashokkumar et al., 2021; Sampaio et al., 2022). This situation left small-scale farmers extremely vulnerable, with reductions of up to 75% in essential crops like corn, beans, potatoes, and cassava during the

2012-2017 drought (Santana and Santos, 2020). In view of negative climate projections (Jenkins and Warren, 2015; Tripathy et al., 2023), public policies must support sustainable agricultural practices while promoting equitable and rational water use to enhance food security and the resilience of communities in Brazil's northeastern semiarid region.

Despite the extreme drought that marked the past decade, livestock farming in Brazil's semiarid region has expanded significantly, particularly with the growth of mixed herds of goats and sheep, which are primarily raised in semi-intensive and extensive systems (Santana and Santos, 2020; Paiva et al., 2022). Goats and sheep have energy demands that are only about 10% of those needed by cattle, and they are more drought-resistant and well-adapted to the arid climate, making them a viable option for the Brazilian semiarid (Askar et al., 2021). Expansion of cattle-based livestock systems has imposed intensifying pressure on natural resources, leading to the conversion of savanna forests into pasture areas and deforestation for firewood and fence posts. Grazing and animal trampling impact the regeneration of native vegetation, reducing plant diversity, leading to local extinctions, and triggering soil erosion and land degradation, thereby accelerating desertification processes (Wu and Tiessen, 2002; Ribeiro et al., 2015; Sobrinho et al., 2016; Schulz et al., 2019). Although livestock farming has become a viable economic alternative to non-mechanized family farming, its unregulated expansion without sustainable management practices or effective public policies has intensified forest fragmentation, soil degradation, and water scarcity (Morales-Barquero et al., 2015). The lack of regulation and monitoring of land and water use, combined with intensifying climate change, threatens the region's socioecological resilience, endangering both local ecosystems and community well-being.

The agricultural crisis in the semiarid region, exacerbated by intense droughts, has driven rural exodus, leading to the rapid expansion of urban centers. As a result, cities have expanded in an unregulated manner, often at the expense of Caatinga vegetation, which is cleared to accommodate urban infrastructure (Espindola et al., 2017; Correia Filho et al., 2022; Brito et al., 2023). Deforestation further compromises the region's ecosystem services by reducing water retention capacity and increasing vulnerability to droughts (Liu et al., 2017; Brito et al., 2023). The expansion of impervious surfaces due to urban growth intensifies surface runoff while decreasing aquifer recharge, worsening water scarcity (+). Additionally, urban expansion has led to public health issues, including improper waste disposal and an increase in diseases associated with poor sanitation infrastructure (Ferreira et al., 2021; Marinho et al., 2022). This scenario is particularly concerning in the semiarid region, where both water availability and quality are already limited and often contested among urban, agricultural, and domestic demands (Brito et al., 2023). The rapid urbanization, driven by the agricultural crisis and the lack of land-use planning policies, not only intensifies pressure on natural resources but also deepens social and environmental inequalities, creating a vicious cycle of ecological degradation and social exclusion (Carneiro et al., 2021).

In this study, we investigate changes in agricultural and livestock production, as well as land use classes, in response to extreme climatic variations such as prolonged and severe droughts in the municipality of Iguatu, Ceará, over a 37-year period (1985–2023). Located in a region of high socioeconomic vulnerability, Iguatu embodies the challenges faced across the Brazilian semiarid region, including a long-standing tradition of family-based agriculture and recurrent droughts. Additionally, this municipality reflects the intense pressure on natural resources and the heavy dependence on rainfall for economic activities, characteristics shared by other semiarid municipalities. As such, Iguatu serves as an ideal model for understanding socio-environmental responses to extreme climatic variations and their impacts on ecosystems and local communities, offering insights that can be extrapolated to the broader Brazilian semiarid region and other arid and semiarid areas worldwide. Our approach provides an integrated examination of the complex interactions between climate, agriculture, livestock farming, and forest degradation. Furthermore, this study is among the first to integrate these factors using long-term time series data for the Brazilian semiarid region. We hypothesize that extreme drought events have substantially altered regional land-use dynamics by depleting surface water resources, constraining the productivity and spatial extent of annual crops, and concurrently driving an expansion of cattle-based livestock systems, trends that became particularly pronounced during the 2010s. We also anticipate that native vegetation, especially forested areas, will undergo cumulative degradation driven by both the recurrence of extreme droughts and increasing socioeconomic and urban pressures. Our findings have the potential to provide a solid foundation for the development of public policies aimed at sustainable land management and climate adaptation.

2 MATERIALS AND METHODS

2.1 Study Area

The microregion of Iguatu is in the south-central part of the semiarid Ceará State, within the Jaguaribe River Basin, covering an area of 1,035 km². In 2022, the municipality had a population of 98,064 people, with 77.34% residing in urban areas and 22.66% in rural zones (IBGE, 2022). According to Köppen’s classification, the region's climate is categorized as hot semiarid (BSh), with an average annual temperature of 28°C and an accumulated annual precipitation of 996.6 mm. Rainfall is concentrated between December and May, while evapotranspiration reaches 1,902.5 ± 117.8 mm per year, with the highest rates occurring between August and January (Alvares et al., 2013; INMET, 2024).

Geomorphologically, Iguatu is part of a semiarid lowland basin (Sertaneja Depression), characterized by flat to gently undulating terrain with slightly incised landforms and altitudes ranging between 198 and 461 meters. The predominant soil classes include Argisols, Vertisols, Latosols, and Neosols (Fig. 1). The vegetation consists of a deciduous, xerophytic biome called Caatinga, with low-stature trees, twisted trunks, and thorny branches, averaging 5 meters in height. The dominant plant families are *Fabaceae*, *Euphorbiaceae*, and *Cactaceae*, with notable species including bromeliads, *Xique-xique* (*Pilosocereus gounellei*), *Mandacaru* (*Cereus jamacaru*), *Embiratanha* (*Poincianella pyramidalis*), *Acácia* (*Vachellia farnesiana*), *Juazeiro* (*Ziziphus joazeiro*), *Macambira* (*Encholirium spectabile*), *Maniçoba* (*Manihot glaziovii*), *Umbu* (*Spondias tuberosa*), and *Mimosa* (*Mimosa tenuiflora*) (Reis et al., 2021).

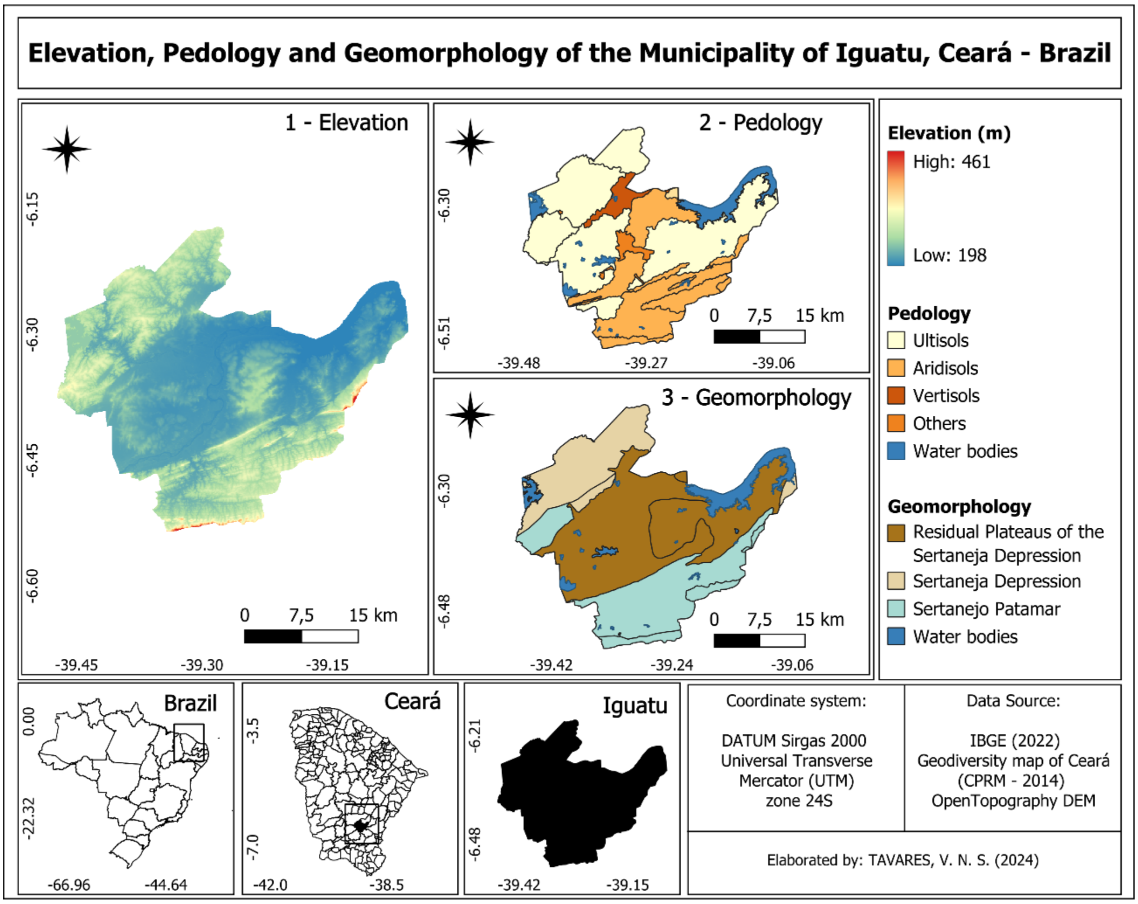

Figure 1. Altitude, Pedology, and Geomorphology Map of Iguatu Municipality, Ceará, Brazil.

2.2 Climatic Variations, Landscape Changes, and Agricultural Production Over the Last 37 Years

We assessed climatic variations in the municipality of Iguatu using time series data on annual accumulated precipitation (mm) and mean, minimum, and maximum annual air temperatures (°C) from 1985 to 2022. Monthly precipitation data were obtained from the Ceará Foundation for Meteorology and Water Resources (FUNCEME, 2022). Drought periods were characterized using the Standardized Precipitation Index (SPI), based on the duration and intensity of these events (McKee et al., 1993). In the studied semiarid region, seasonal meteorological drought typically lasts for eight months (June to January). Based on this timeframe, we classified a prolonged drought as a consecutive dry period lasting at least 14 months, as this includes a rainy season without precipitation. A month was considered dry if its SPI value was lower than -0.5 and wet if it was higher than 0.5 (Wang et al., 2022). Additionally, we evaluated drought intensity, calculated as the sum of SPI values recorded during dry periods, divided by the number of dry months (Wang et al., 2022).

We analyzed temporal trends in key agricultural products (rice, cotton, sugarcane, beans, cassava, sweet potatoes, bananas, guava, watermelon, and tomatoes) and livestock production (cattle, sheep, goats, and swine), both individually and collectively (combining total agricultural and livestock production). The IBGE does not provide information on whether the crops were irrigated or rainfed. However, historically, crops such as rice, sugarcane, beans, sweet potato, and fruit trees have predominantly been cultivated under irrigation. Agricultural and livestock production data were obtained from the Brazilian Institute of Geography and Statistics time series database (IBGE, 2022) for the municipality of Iguatu from 1985 to 2023. To detect trends in these time series, we applied the Modified Mann-Kendall test (Yue and Wang, 2004). This test was selected because it effectively identifies trends in time series affected by autocorrelation, a common characteristic in long-term climatic and agricultural datasets. The Modified Mann-Kendall test incorporates a variance correction to adjust for significant serial correlations, making it more robust for detecting trends in time series with dependencies between consecutive observations. Furthermore, this method calculates the effective sample size by considering serial correlation coefficients across all lags, ensuring greater accuracy in trend analysis. To interpret the results, we used Kendall's Tau and Sen's Slope parameters. The Tau coefficient indicates the strength and direction of the trend, with positive values signifying an increasing trend and negative values indicating a decline. Sen's Slope, in turn, quantifies the magnitude of the trend, allowing us to estimate the average rate of change over the study period.

To examine the relationship between agricultural and livestock production and climate, we performed simple and cross-correlation analyses between production time series and climatic descriptors (annual mean SPI, annual total SPI, mean annual precipitation, and accumulated annual precipitation), with no time lag and with a one-year lag. Simple correlations identified direct associations between climatic variables and agricultural production within the same year, while cross-correlations captured the potential effect of the previous year's climate on current production. This approach provides a comprehensive analysis of both immediate and delayed responses of agricultural activities to climatic variations in the semiarid region.

The SPI was calculated using the "SPEI" package (Beguería and Vicente-Serrano, 2017) for a 12-month time scale. The Modified Mann-Kendall test was performed using the "modifiedmk" package with the "mmky" function (Yue and Wang, 2004). Lagged climatic descriptors were generated using the lag() function from the "dplyr" package. All graphical representations were created using the "ggplot2" package in R software, version 4.41.

2.3 Multitemporal Analysis of Vegetation Cover Changes in Iguatu

To quantify the spatial and temporal changes in the municipality's landscape, we used land use and land cover rasters classified by the MapBiomas project (Collection 7.0) for the years 1985, 2005, 2015, and 2022, which were downloaded from Google Earth Engine. The classified rasters were then processed in QGIS 3.18, where we identified nine land use and land cover classes: dense forest, savanna forest, grassland vegetation, pasture, agricultural use mosaic, temporary crops, urban areas, non-vegetated areas, and water bodies. To simplify the interpretation of temporal changes, we grouped similar classes (*mosaic of agricultural uses + temporary crops*, *grassland vegetation + pasture*, *non-vegetated areas + urban areas*), resulting in three broader categories: agriculture, pasture, and urban area.

To assess temporal changes in the municipality's landscape, we calculated composition metrics, including total area (km²) and percentage of coverage for all classes. Additionally, we evaluated fragmentation descriptors such as the number of fragments, the area of the largest fragment (km²), and the average fragment size (km²) for the dense forest and savanna forest classes. These metrics were compared across the years 1985, 2005, 2015, and 2022, as well as for the overall difference between 2022 and 1985. Fig. 2 shows the flowchart illustrating the study's methodology.

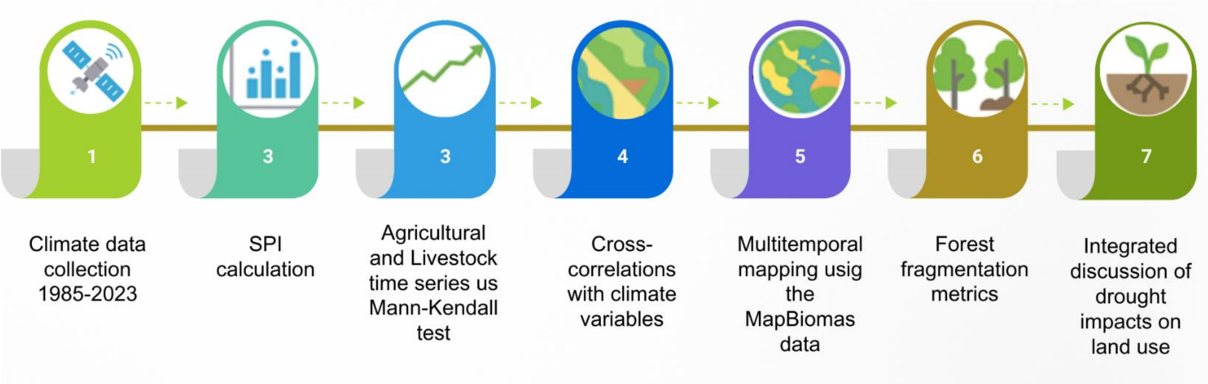

Figure 2. Flowchart illustrating the study's methodology.

3 RESULTS

3.1 Temporal Climatic Variation

Between 1985 and 2023 the climate in the municipality of Iguatu-CE exhibited significant fluctuations, particularly in precipitation levels. Annual accumulated precipitation varied widely, ranging from a maximum of 2,076 mm in 1985 to a minimum of 582.5 mm in 1993 (Fig. 3). Over the 37-year period analyzed, 21 years recorded precipitation levels below the historical average (1,045 mm). Notably, 1992, 1993, 2001, 2005, 2015, 2016, 2017, and 2022 were the driest years in the dataset, with annual precipitation below 767 mm (Fig. 3A). Conversely, years with precipitation above the historical average included 2011 and 2021, which recorded more than 1,500 mm of accumulated rainfall.

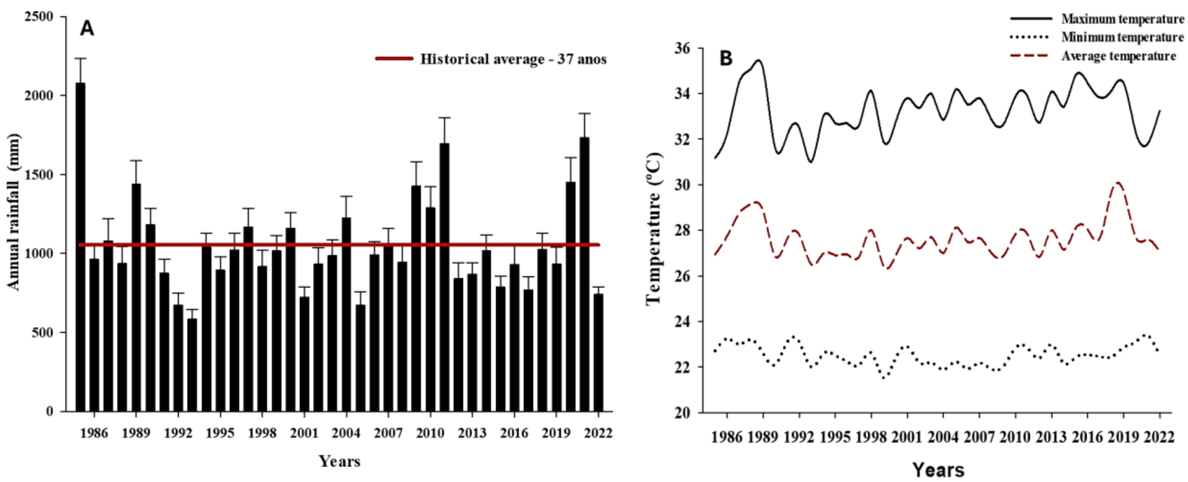

Figure 3. Temporal variation in annual accumulated precipitation (A) and maximum, mean, and minimum temperature values (B) in the municipality of Iguatu-CE between 1985 and 2022. The red line represents the historical average accumulated precipitation over the 37-year series (A).

In contrast to precipitation, temperature trends (minimum, mean, and maximum) remained relatively stable over time. The mean values and standard deviations for maximum, minimum, and mean temperatures were 33.2 ± 1.0 °C, 22.5 ± 0.44 °C, and 27.6 ± 0.79 °C, respectively (Fig. 3B).

When analyzing the duration and intensity of drought events over the past 37 years, we identified 11 extreme drought events (either very prolonged and/or very severe). Among these, five were classified as prolonged droughts, lasting between 29 (1991–1994) and 16 (2012–2013) consecutive months with SPI values below -0.5. These events, along with the 2015–2017 drought, were the most significant in the historical record (Fig. 4).

The first event (1991–1994) was not only the longest but also the most severe (drought severity = -0.49) and most intense (drought intensity = -1.69), with SPI values dropping as low as -4.0 in some months. Although the second set of events (2012–2014 and 2015–2017) had lower intensity (drought intensity = -1.18 and -0.8), with SPI values ranging from -0.5 to -2.9, they occurred in quick succession, with only nine months of regular precipitation between them (Fig. 4). This short recovery period was insufficient to replenish the region's water bodies, exacerbating water scarcity.

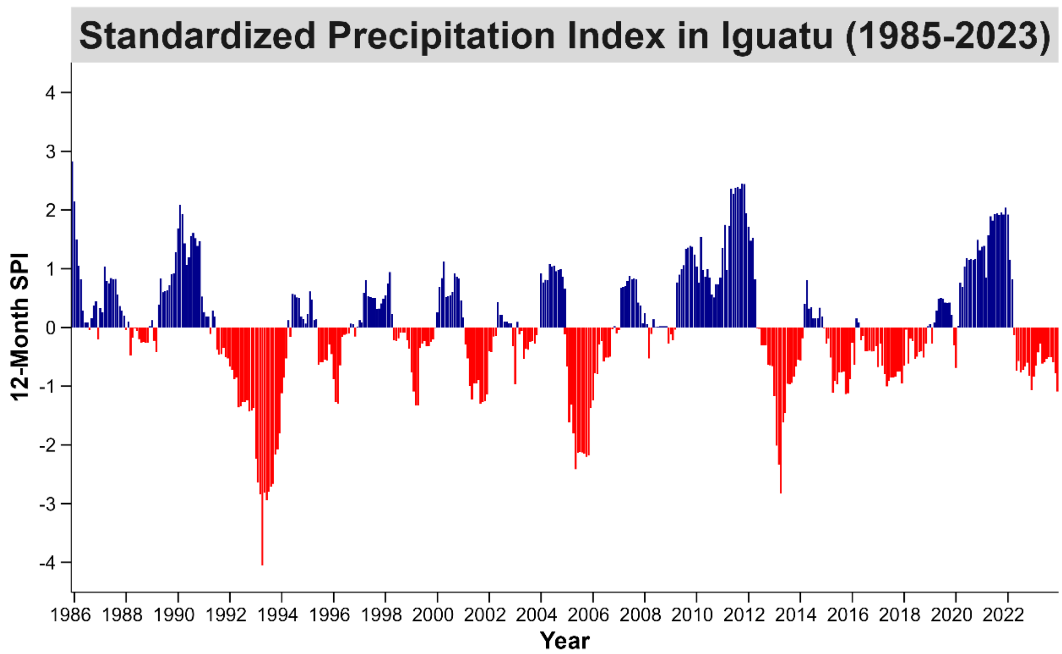

Figure 4. Temporal variation of the Standardized Precipitation Index (SPI) for the municipality of Iguatu-CE, Brazil, from 1985 to 2022. Blue bars represent positive precipitation deviations corresponding to wet months, while red bars indicate negative deviations, representing dry months.

3.2 Temporal Trends in Agriculture and Livestock in Iguatu

Temporal trend analyses revealed varied responses across the 10 agricultural crops and livestock production categories (Figs. 5, 6, and 7). Among all crops, rice exhibited the strongest declining trend (T = -0.75), with an average reduction of -879.6 tons per year (Fig. 5). Cotton and beans showed similar rates of decline (T = -0.39 and T = -0.42), with annual decreases of -31.19 and -40 tons, respectively. Sugarcane and cassava production also declined, at rates of approximately -15 and -9.3 tons per year (T = -0.36 and T = -0.29). In contrast, sweet potato production showed no clear linear trend (SS = 0, T = 0.32). All linear decline trends observed in rice, cotton, beans, sugarcane, and cassava were statistically significant ($P < 0.01$; Fig. 5).

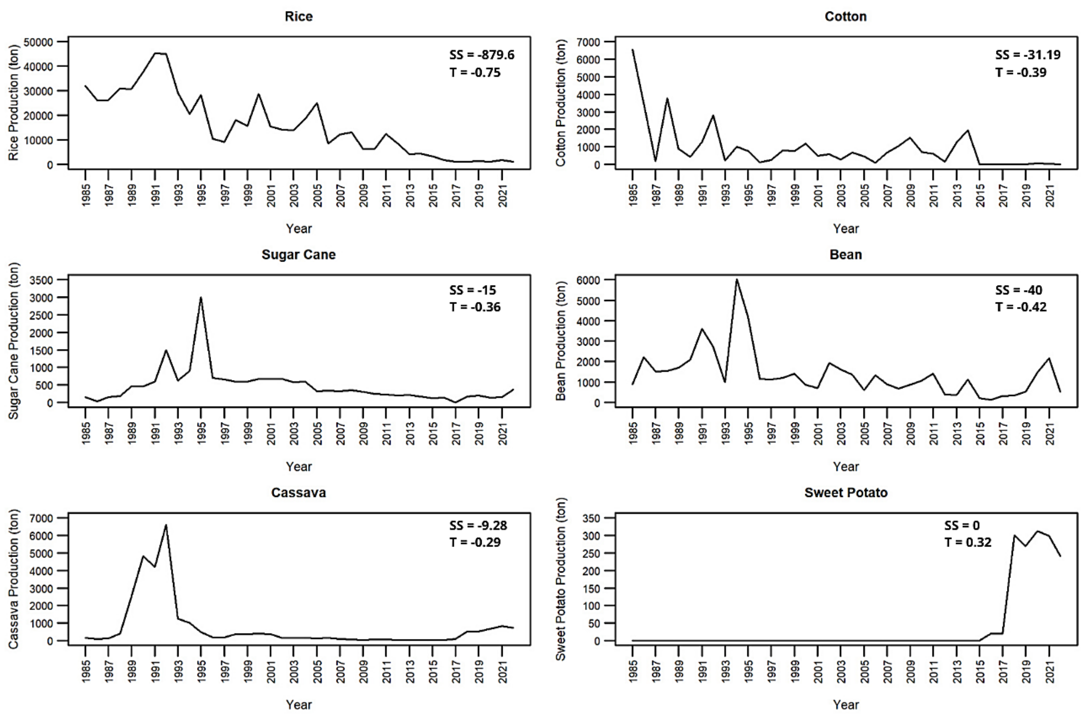

Figure 5. Time series of perennial crop (cotton) and temporary crops (rice, sugarcane, cassava, beans, and sweet potatoes) production in the municipality of Iguatu-CE, Brazil, from 1985 to 2021. SS = Sen's Slope, T = Tau.

Conversely, banana and guava crops showed a significant increasing trend (T = 0.70, $P < 0.01$; T = 0.44, $P < 0.01$; Fig. 6), with annual growth rates of 379.5 banana bunches and 2.27 tons of guava. However, despite the statistical trend indicating growth, guava production has been in decline since 2014. Meanwhile, watermelon and tomato crops exhibited a positive trend (SS = 2.20 and SS = 0.62), but their linear relationships were weak and not statistically significant (T = 0.24, *P* = 0.08; T = 0.07, *P* = 0.38; Fig. 6).

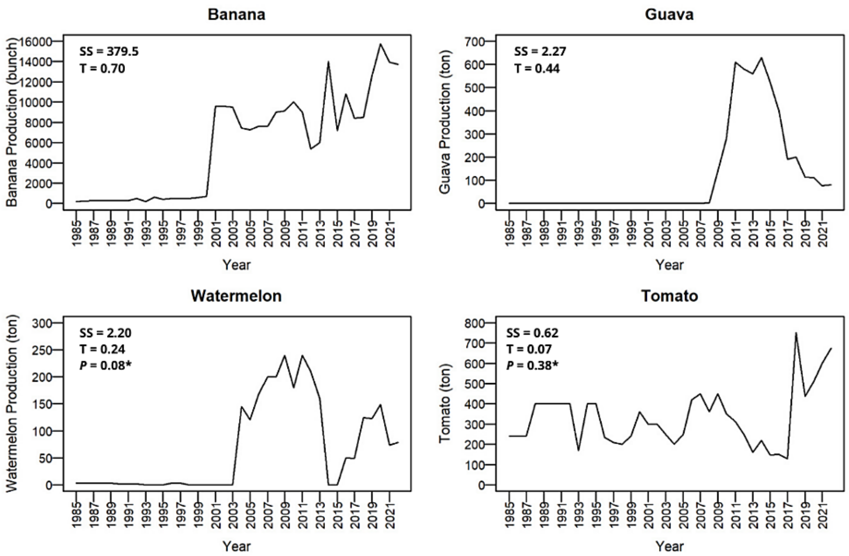

Figure 6. Time series of perennial crop (banana and guava) and temporary crop (melon and tomato) production in the municipality of Iguatu-CE, Brazil, from 1985 to 2021. SS = Sen's Slope, T = Tau. P values indicate non-significant linear trends.

Regarding livestock production, there was a strong investment in cattle farming (Fig. 7), with an annual increase of 1,042.3 head of cattle (T = 0.76; *P* < 0.01; Fig. 7). Despite a historically positive trend in sheep farming (SS = 153.3; T = 0.63), production declined post-2017 and stabilized at lower levels through 2021. Goat production exhibited a marginally significant increasing trend, with an annual growth rate of 20.7 individuals (T = 0.27, *P* = 0.06), while pig production showed no significant linear trend, fluctuating over time with periods of increase and decrease (T = -0.06, *P* = 0.36; Fig. 7).

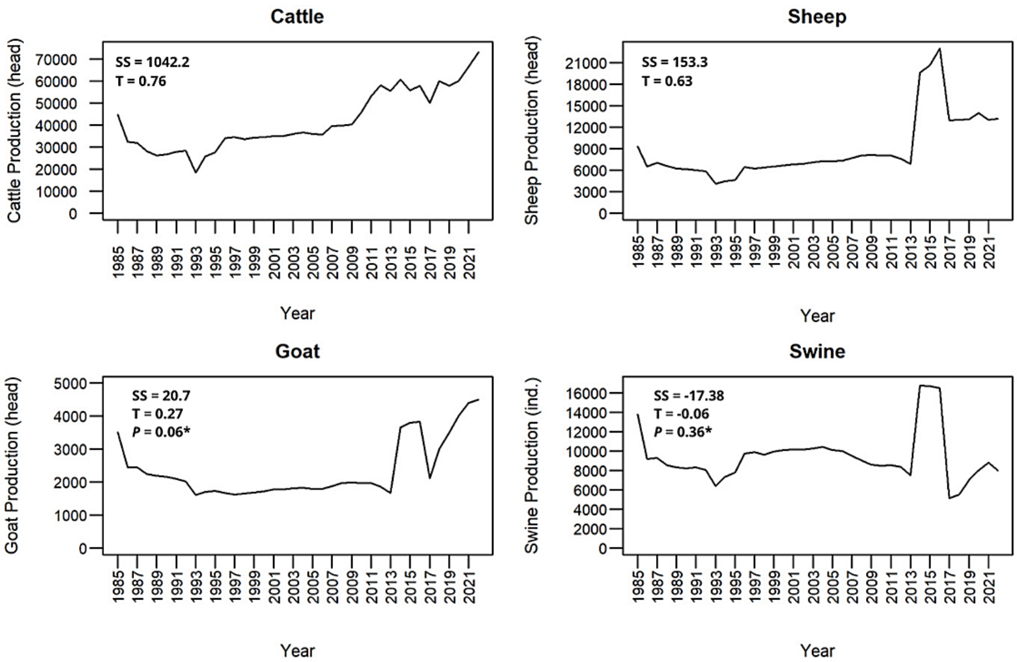

Figure 7. Time series of livestock production (cattle, goats, sheep, and swine) in the municipality of Iguatu-CE, Brazil, from 1985 to 2021. SS = Sen's Slope, T = Tau. P values indicate non-significant linear trends.

When analyzing temporal trends by grouping crop production under the category "Agriculture" and all livestock production under "Livestock Farming," a significant declining trend was observed in agricultural production (T = -0.53), whereas livestock production showed a growth trend (T = 0.74; Fig. 8).

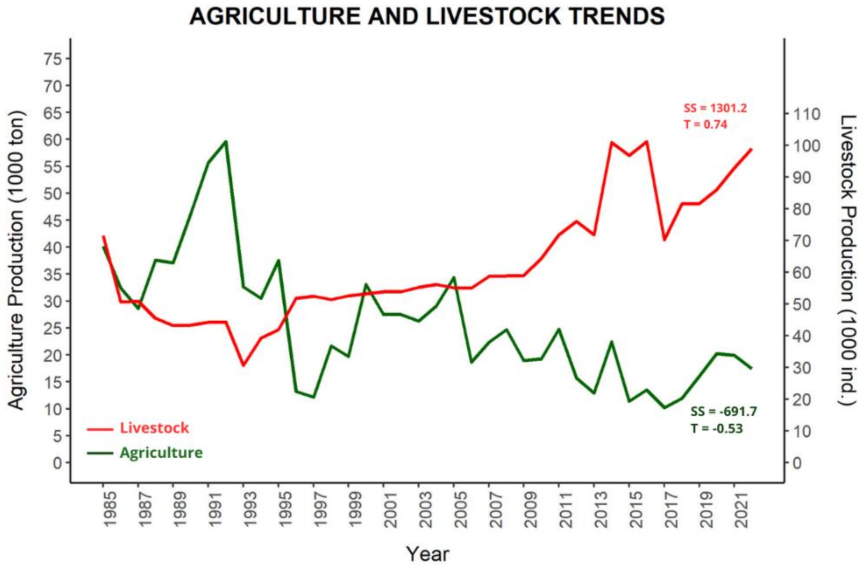

Figure 8. Time series of the "Agriculture" and "Livestock" categories. Agriculture includes the total crop production, while livestock comprises the sum of cattle, goats, sheep, and swine in the municipality of Iguatu-CE, Brazil, from 1985 to 2021. SS = Sen's Sl ope, T = Tau.

Most agricultural and livestock time series did not show significant correlations with the climatic descriptors used (mean precipitation, annual accumulated precipitation, mean SPI, and total annual SPI) for the same year or with a one-year temporal lag. However, watermelon production was positively correlated with mean and accumulated precipitation of the same year (r = 0.34, P = 0.04; r = 0.32, P = 0.05), while tomato production was correlated with total and mean SPI (both r = 0.32, P = 0.05) and mean precipitation of the same year (r = 0.32, P = 0.05). Additionally, cattle production showed a positive and significant correlation with the mean and accumulated precipitation of the previous year (both r = 0.35, P = 0.03).

3.3 Spatiotemporal Dynamics of the Landscape in Iguatu Municipality

The classified land use and land cover maps (1985, 2005, 2015, and 2022) reveals a reduction in forest vegetation (dense and savanna forests). In contrast, there was an increase in pasturelands and urban areas. Deforestation was particularly evident in areas near the sedimentary basin, where agricultural and livestock activities expanded (Fig. 9). The most preserved areas remained near crystalline shields, likely due to the presence of shallow soils with physical and chemical limitations that hinder land management. In 2005, a new water body, the Trussu Reservoir, appears in the northwestern region of the map. This reservoir was constructed to support water supply in the south-central region of Ceará. From 2015 onward, temporary crops became more visible, urban areas expanded in the central region of the map, and water bodies reduced.

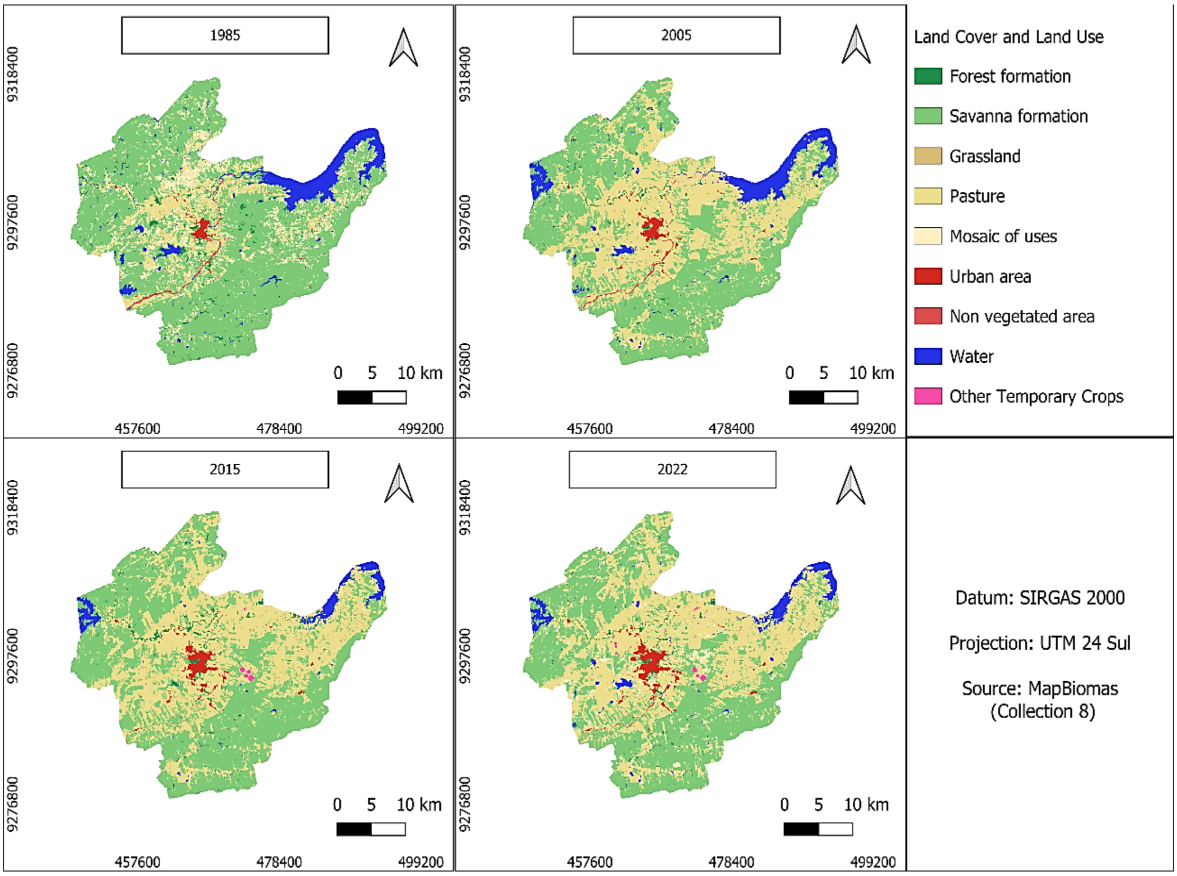

Figure 9. Temporal evolution of land use and land cover in Iguatu, Ceará, Brazil, from 1985 to 2022, as depicted in the maps.

The landscape of the municipality of Iguatu has undergone significant changes in its composition over the past 37 years, marked by a reduction of 207 km² of forest cover (20.5%) and an increase of 291.5 km² (28.9%) in pasture areas. Notably, by 2022, 41.7% of the municipality’s total area was occupied by pasturelands. Conversely, agricultural areas and water bodies experienced reductions of 5.7% and 3.5%, respectively. Although urban areas accounted for only 2% of the municipality's total area, their extent nearly doubled during this period (Table 1).

Table 1. Area (km²) and percentage of land cover (%) for major land use and land cover classes in Iguatu, Brazil, from 1985 to 2022. Forest = dense forest + woodland savanna forest. The change column (1985-2022) shows the net gain or loss in area for each class. Negative values indicate area reduction.

Year	Forest		Pasture		Agriculture		Urban		Water	
	Area (km²)	%	Area (km²)	%	Area (km²)	%	Area (km²)	%	Area (km²)	%
1985	681.9	67.6	128.6	12.8	117.4	11.6	11.3	1.1	68.9	6.8
2005	500.8	49.7	395.4	39.2	36.2	3.6	13.4	1.3	62.2	6.2
2015	525.3	52.1	427.4	42.4	13.2	1.3	15.5	1.5	26.5	2.6
2022	474.8	47.1	420.1	41.7	59.8	5.9	20.2	2.0	33.1	3.3
1985-2022	-207.1	-20.5	291.5	28.9	-57.6	-5.7	8.9	0.9	-35.8	-3.5

When analyzing the fragmentation process of dense forest and woodland savanna forest in the municipality over the past 37 years, we observed a drastic reduction of nearly 202.7 km² (20.1%) in woodland savanna forest and the near-total loss of dense forest, which now accounts for less than 1.6% of the municipality's total area, reaching below 1% in 2005 (Table 2). The reduction in dense forest area was accompanied by a decline in the number of fragments (-89), as both the mean fragment size and the largest fragment remained consistently small (less than 1 km², except in 2015). This pattern, in contrast to woodland savanna forest, suggests that dense forest is nearing extirpation in the Iguatu landscape. Conversely, in woodland savanna forest, the number of forest fragments increased from 805 (1985) to 1,176 (2022), while the size of the largest fragment decreased by 167 km², and the mean fragment size was reduced by nearly 50% (Table 2). These findings indicate a high degree of landscape degradation in Iguatu by 2022, particularly in sedimentary areas that have been increasingly converted into pasturelands (Fig. 7).

Table 2. Configuration metrics of savanna vegetation in Iguatu-CE, Brazil, analyzed for 1985, 2005, 2015, and 2022. The percentage (%) represents the savanna's proportion of the municipal area. Metrics include the number of savanna patches (Number), the area of savanna patches (Number), the area of the largest patch (Largest), and the mean patch size (Mean). The change column (1985-2022) shows the net gain or loss in area for each class. Negative values indicate area reduction.

Years	Type of Vegetation	Area (km²)	%	Number	Largest (km²)	Mean (km²)
1985	Forest	14.42	1.43	458	0.7	0.03
	Savanna	667.4	66.2	805	356.7	0.83
2005	Forest	9.5	0.94	349	0.9	0.02
	Savanna	491.3	48.7	1080	212.6	0.45
2015	Forest	15.8	1.56	452	2.75	0.03
	Savanna	509.6	50.5	1327	246.4	0.38
2022	Forest	10.1	1.01	369	0.46	0.02
	Savanna	464.7	46.1	1176	189.8	0.39
1985-2022	Forest	-4.32	-0.42	-89	-0.24	-0.01
	Savanna	-202.7	-20.1	371	-167	-0.44

4 DISCUSSIONS

In this paper we investigated how climate variability and socioeconomic pressures have influenced agricultural production, livestock expansion, and forest cover in a Brazilian semiarid region over 37 years. We found that while most agricultural production declined, these reductions were not directly linked to drought patterns. Instead, prolonged droughts severely impacted water resources, land use, and forest cover, leading to shifts in production patterns. Annual crops such as rice, cotton, cassava, and sugarcane declined, particularly in the 2010s, likely due to cumulative water crises. In contrast, irrigated fruits like bananas expanded, driven by irrigation and agricultural technologies. Livestock production, especially cattle farming, grew substantially, contradicting our initial hypothesis, while goat farming showed moderate increases. This shift coincided with pastureland expansion, reinforcing a transition toward livestock-based land use. Meanwhile, forest areas declined and became increasingly fragmented, with average fragment sizes decreasing by 50%. The combined effects of extreme droughts and land-use pressures accelerated forest degradation, supporting our hypothesis that climate events and socioeconomic factors intensify ecosystem loss.

However, land-use change and agricultural production are deeply interconnected processes and should not be treated as isolated phenomena. In dryland regions such as the one examined in this study, the decline in agricultural activity alongside the expansion of livestock production represents a systemic adaptation to prolonged drought conditions. These shifts are not coincidental; rather, they reflect a deliberate reconfiguration of land-use strategies, whereby farmers reduce investments in water-intensive cropping systems and transition toward more drought-resilient, livestock-based practices. Analyzing these dynamics separately would obscure the synergistic nature of land-use adaptation, in which spatial and functional land-use adjustments directly respond to climatic pressures, resource constraints, and risk mitigation needs. Moreover, an increasing literature reviews underscores the importance of integrated frameworks that capture the feedback between land-use dynamics and agricultural outputs, offering a more comprehensive understanding of climate vulnerability and the resilience of food systems (Wijerathna-Yapa and Pathirana, 2022; Ahmed, 2023; Allan et al., 2023).

The historical precipitation analysis for the municipality of Iguatu, covering the period from 1985 to 2023, revealed a marked recurrence of severe drought episodes. Eleven events were identified, each characterized by either extended durations exceeding eight consecutive months or by extremely arid conditions, as indicated by Standardized Precipitation Index (SPI) values below -2.0. Five droughts were classified as prolonged, persisting for more than 16 months. The most critical episodes occurred between 1991–1994 and 2015–2017, lasting 29 and 26 months, respectively. These findings underscore the chronic and systemic nature of hydrological stress in this semi-arid region and highlight the increasing exposure of agroecosystems to sustained climatic extremes. Such long-lasting droughts have profound implications for soil moisture dynamics, crop failure risks, and long-term land-use decisions.

This climatic pattern is strongly influenced by the El Niño phenomenon, which intensifies droughts in Northeast Brazil, as well as in other global semiarid regions (e.g., the Southwest Pacific, Southern Africa, and South Asia). Conversely, La Niña typically brings above-average rainfall to these regions (Jimenez et al., 2021; Zhao et al. 2024). Our findings align with recent scientific projections (Jenkins and Warren, 2015; Tripathy et al., 2023), which indicate an increase in the frequency of prolonged droughts in recent decades, driven by global climate change. This trend is highly concerning, as the recurrence of extreme droughts poses a growing threat to the socio-economic and ecological stability of the

Brazilian semiarid region. Urgent action is required to develop adaptive policies that can anticipate and mitigate the adverse effects of these extreme events, especially given projections of increasing drought frequency and intensity in the future (Marengo et al., 2020).

The prolonged droughts that have affected the Brazilian semiarid region in recent decades have had devastating consequences, intensifying conflicts over water use between its 26 million inhabitants and the predominant agricultural and livestock activities (Costa et al. 2023). One of the most severe effects of declining precipitation in the region is the reduction of surface water bodies. In our study, for example, we observed a 3.5% decrease in the surface area of water bodies in the municipality, despite the construction of the Trussu Reservoir, which, in theory, should have expanded water availability (Silva et al., 2023a). In semiarid regions, reservoirs and dams are essential for urban water supply, livestock watering, and agricultural irrigation, becoming even more critical during drought years when rivers and intermittent streams dry up. However, during extreme droughts such as the 2012–2017 event, many large reservoirs experienced a decline in storage levels to less than 5%, while numerous smaller dams dried up completely (Pereira et al., 2023), resulting in severe economic, social, and ecological losses (Marengo et al., 2017; Cunha et al. 2019). Small-scale farmers, particularly those reliant on rainfed agriculture, suffered significant crop failures, impacting both the local economy and social well-being. The Brazilian Ministry of National Integration estimated economic losses of approximately US$6 billion in the agricultural sector alone (Marengo et al. 2017). During these critical periods, many farmers depended on government support to sustain their activities in the face of extreme water shortages (Magalhães et al. 2021; Silva et al., 2021a). These impacts underscore the urgent need for effective climate mitigation and adaptation strategies in highly vulnerable regions such as the Brazilian semiarid Northeast.

Among the ten main agricultural products in Iguatu, five exhibited a significant decline (rice, cotton, beans, sugarcane, and cassava). Rice was the most affected, with an annual reduction of 879.6 tons, primarily due to water scarcity, as this crop has high water demand (Pineda Suárez and Sánchez Román, 2018). Additional contributing factors include high production costs, low technological adoption, and increased imports in the state. Cotton also experienced a sharp annual decline (31.19 tons per year), attributed to a combination of factors, including the devaluation of agricultural commodities, infestations of the cotton boll weevil (*Anthonomus grandis*), and limited technical assistance, which have broadly impacted the Northeast region (Mattos et al., 2020).

The expansion of fruit cultivation in Brazil’s Northeast in recent decades has been significantly driven by the adoption of advanced irrigation technologies. In semi-arid regions, where persistent water scarcity severely limits agricultural potential, techniques such as drip irrigation, sprinkler systems, and the efficient management of surface reservoirs have enabled year-round crop production. This transformation has not only improved yields and overall productivity but has also promoted crop diversification and allowed the integration of previously unproductive or marginal lands into agricultural use. Banana cultivation showed the most substantial increase, expanding from 198 bunches in 1985 to 13,720 in 2022, facilitated by its proximity to tributaries of the Jaguaribe River and the Trussu and Orós reservoirs (Lopes et al., 2014). This crop demonstrated high economic returns, with profit margins of up to 66%.

Conversely, guava production, which expanded rapidly between 2009 and 2014, declined in 2015 due to root-knot nematode (*Meloidogyne enterolobii*) infestations, which significantly reduced yields (Ashokkumar et al., 2021; Sampaio et al., 2022). The results indicate a transition toward economically viable crops, likely driven by the declining performance and sustainability of traditional agricultural systems. This adaptive shift reflects producer strategies in response to prolonged environmental and economic pressures. The trend highlights the growing importance of crop selection under changing climatic and resource conditions. Such dynamics underscore the interplay between land-use decisions and resilience in dryland agroecosystems. These insights contribute to a broader understanding of sustainable adaptation pathways in vulnerable agricultural landscapes. Additionally, efficient water resource management, access to credit, and irrigation technology adoption played a key role in supporting the growth of these crops, highlighting the importance of technological innovation and sustainable water management as essential adaptation strategies for the semiarid region (Silva et al., 2021b; Silva et al., 2023a).

Contrary to our prediction, cattle ranching exhibited the most significant growth among the time series analyzed, with a notable increase of 1,301 head of cattle per year, despite the climatic adversities described. Historically, the south-central region of Ceará has been occupied primarily by cattle farming and subsistence agriculture, both of which developed with little regard for natural resource conservation (Oliveira and Oliveira, 2022). Traditionally, extensive cattle management was practiced, with free-range grazing on native Caatinga vegetation, including herbaceous plants, shrubs, and small trees, as well as their sprouts (Ferreira et al., 2009; Nunes et al., 2016). Over time, alternative forage crops were introduced, such as buffel grass, forage cactus, leucaena, forage watermelon, gliricidia, and pigeon pea, reinforcing cattle ranching as a key economic activity in the formation of villages and towns, which later evolved into urban centers. Despite the overall growth trend in cattle production in Iguatu, similar to other regions of Ceará (Sousa et al., 2021), climatic instability in recent decades has negatively impacted milk production in the 20 municipalities with the highest dairy production rates in the state, particularly in areas with low technological development (Lemos et al., 2022). However, the expansion of pasturelands, diversification of planted forage species, and adoption of irrigation technologies could explain why Iguatu has deviated from the production declines reported in other municipalities in the state.

The significant expansion in sheep and goat farming highlights a strategic shift toward small ruminant production in semi-arid regions. Climatic conditions have directly influenced livestock production systems in the Brazilian semi-arid region. Drought events, in particular, severely constrain cattle farming due to its high water demand (15–30 L animal^{-1} day^{-1}) and reliance on extensive pasture areas. Prolonged dry periods reduce forage availability and significantly increase the marginal costs of feed supplementation (e.g., irrigated grass and silage), rendering cattle production economically unsustainable for small- and medium-scale farmers. In response to these climatic pressures, producers have adapted by shifting toward livestock species better suited to semi-arid conditions. Goats and sheep, for example, are hardy animals that require 60–70% less water than cattle and are well adapted to the xerophytic vegetation of the Caatinga Biome, reducing dependence on irrigated forage. Additionally, swine production, especially under intensive (confined) systems, allows for more efficient water use per kilogram of meat produced. Swine can also be fed on locally available agricultural by-products such as maize and cassava, further improving system sustainability. These adaptive strategies explain the marked expansion of goat, sheep, and swine farming between 2013 and 2017.

However, despite the statistical trend indicating an increase in sheep production, the number of sheep declined in recent years, from approximately 23,000 individuals in 2016 to 13,200 in 2021 and 2022. Livestock farming in Iguatu currently follows a mixed-exploitation model, in which cattle, sheep, and goats coexist in rural areas. Although these animals are adapted to a diet based on grass/herbaceous and shrubs natural vegetation, they exhibit distinct feeding preferences and selectivity, with goats being more selective and preferring shrub vegetation, while sheep favor grasses, like cattle (Mota et al., 2018; Fonseca et al., 2014; Gilbert and Dwyer, 2024).

Other factors that may have contributed to the growth of herds in the municipality include improvements in animals health conditions, the adoption of nutritional and reproductive management techniques, and the support of various public institutions such as the National Rural Learning Service (*Serviço Nacional de Aprendizagem Rural* – SENAR), the Brazilian Micro and Small Business Support Service (*Serviço Brasileiro de Apoio às Micro e Pequenas Empresas* – SEBRAE), the Technical Assistance and Rural Extension Company (*Empresa de Assistência Técnica e Extensão Rural* – EMATER), and the Iguatu Department of Agriculture. Over the past five years, livestock activity has also expanded due to the formation of rural associations and access to rural credit programs, particularly through the "Sustainable Regional Development (DRS)" of Banco do Brasil, a Brazilian public bank.

The growth of livestock herds in Iguatu has increased the demand for pastures, leading to the expansion of grassland areas and the consequent deforestation of forests and savanna vegetation. This process has exacerbated environmental degradation risks, including desertification, soil erosion, and salinization (Silva et al., 2023b; Vieira et al., 2023)

While livestock farming contributes to economic development, its expansion may heighten food system vulnerabilities by displacing other productive activities, intensifying pressure on water resources, and accelerating ecosystem degradation, particularly deforestation and desertification. These concerns underscore the urgent need for sustainable management practices that balance livestock productivity, food production, and natural resource conservation. The urban expansion of Iguatu, although accounting for only 2% of the municipality's total area, more than doubled between 1985 and 2022, reflecting a rapid urbanization process. This growth was driven by the dismantling of public institutions for Rural Technical Assistance (ATER), which contributed to the migration of rural populations to urban centers due to the lack of adequate technical support in the countryside and the subsequent decline in agricultural job opportunities across various regions of Northeast Brazil (Espindola et al., 2017; Silva et al., 2018). Additionally, government incentives for housing finance promoted the rapid expansion of villages and districts in Iguatu, leading to the creation of new residential and commercial zones.

The expansion of urban infrastructure, while fostering economic development, likely intensified the degradation of already deforested areas due to the conversion of abandoned croplands and pastures into new residential subdivisions and urban infrastructure. This urbanization process places significant pressure on natural resources, particularly by compromising water quality (with increased concentrations of inorganic compounds such as NO_3^- and NH_4^+/NH_3) and reducing the availability of potable water (Cerqueira et al., 2019; Bhering et al., 2021). The lack of urban planning has led to several ecological issues, including diffuse pollution of water bodies due to increased surface runoff from impervious areas, improper disposal of solid waste, and groundwater contamination (Pereira et al., 2021; Silva et al., 2023a). The expansion of impervious surfaces, exposed soils, and urban infrastructure—alongside vegetation loss and prolonged drought—has diminished groundwater recharge and compromised long-term water availability (Montenegro and Ragab, 2012; Bendito et al., 2023). In the semiarid Northeast, where water is scarce and climate variability is high, declining water quality and quantity underscore the need for sustainable land-use planning. A holistic approach to urban development is essential to safeguard water-related ecosystem services while balancing economic growth and environmental conservation.

The marked expansion of pasturelands in Iguatu, accounting for nearly 29% of the municipal territory, reflects a systemic land-use shift driven by intensified livestock production and cultivation of perennial crops such as banana and guava. This shift has occurred largely at the expense of native vegetation, particularly savanna and dense forest formations, the latter now reduced to a marginal 1% of the area. These changes are not merely the outcome of productive land demands but are compounded by the increasing frequency and intensity of prolonged droughts, which accelerate arboreal mortality in the Caatinga biome (Campos et al., 2020). The convergence of anthropogenic pressure and climatic stressors suggests a critical trajectory of ecological simplification, reduced carbon stocks, and potential degradation of ecosystem resilience. Such findings underscore the urgency of integrating adaptive land management and forest conservation policies tailored to the unique vulnerabilities of semiarid environments.

The extensive deforestation in Iguatu, driven by pasture expansion, agricultural conversion, and the local demand for firewood and fencing materials, has transformed nearly 34% of the landscape, leading to the decline of native vegetation and a severe erosion of ecosystem services (Silva et al., 2017; Antongiovanni et al., 2020). This dynamic not only undermines local biodiversity and food security, as reflected in the reduced availability and diversity of fruits, but also contributes to broader environmental consequences such as forest degradation and climate instability (Raiesi and Beheshti, 2022; Faria et al., 2023). Moreover, the pronounced fragmentation of savanna and dense forests—from 1985 to 2022—indicates a critical loss of structural integrity and ecological connectivity. The reduction in fragment number and area, including a 47% decline in the size of the largest savanna patch, suggests increasing habitat isolation, which may compromise species persistence and ecosystem resilience under continued anthropogenic and climatic stressors.

The pronounced fragmentation and reduction of native vegetation observed in Iguatu raise critical ecological concerns, consistent with broader evidence from semiarid landscapes.

The decline in both the size and number of forest fragments compromises biodiversity, as fragment size is directly linked to species richness and viability, particularly for large-bodied fauna (Fahrig, 2003; Godefroid and Koedam, 2003; Vieira-Alencar et al., 2023). This structural simplification limits habitat availability increases population isolation, and restricts dispersal, ultimately reducing genetic variability and accelerating extinction risks due to inbreeding and genetic drift (Wiegand et al., 2005; Püttker et al., 2020; Buchmann et al., 2013; Edelsparre et al., 2018; Fletcher Jr. et al., 2018). Furthermore, intensified edge effects in smaller patches expose interior habitats to thermal stress, desiccation, and increased predation (Mendes and Prevedello, 2020; Willmer et al., 2022), while shrinking home ranges heighten competition and vulnerability to parasitism (Rybicki et al., 2020). In combination with the expansion of pastures and grazing pressure from extensive livestock systems, these processes reflect a trajectory of ecosystem degradation like other dryland regions under mounting anthropogenic and climatic stress (Morales-Barquero et al., 2015; Blicharska et al., 2024), threatening not only local biodiversity but also the ecological resilience required to buffer future environmental change.

To mitigate the environmental and socio-economic impacts in the Brazilian semiarid region, which are expected to worsen with climate change, it is essential to implement conservation of the remaining forest fragments and restoration strategies, particularly in degraded areas and riparian forests. The Brazilian Forest Code, updated in 2012, mandates that rural properties preserve native vegetation in specific areas of their land, known as Permanent Preservation Areas (PPAs) and Legal Reserves (RLs). PPAs are primarily located along watercourses, springs, and steep slopes, playing a critical role in water resource conservation, biodiversity protection, and erosion and landslide control (Brandão and Lima, 2002). LRs, on the other hand, correspond to a designated portion of rural properties where native vegetation must be maintained to safeguard biodiversity and ecosystem services (Metzger et al., 2019). The required LR percentage varies by region, with rural properties in the Caatinga and other Brazilian biomes required to maintain 20% of their area as LR, except in the Amazon, where the requirement can reach 80%.

One of the most significant changes introduced by the 2012 Forest Code was the amnesty granted to landowners who had deforested PPAs and LRs before July 2008, allowing them to register their properties in the Rural Environmental Registry (RER) without the obligation of reforestation. Since 2012, RER has become a mandatory tool, facilitating environmental monitoring of rural properties and enabling the enforcement of forest restoration measures. Given the current environmental and climate crisis, it is crucial to reassess and reformulate the Forest Code, ensuring that the reforestation of PPAs and LRs is mandatory across all rural properties in Brazil. This is particularly important considering that the most profound and impactful land use and cover changes in Brazil occurred before 2008 (Morton et al., 2006; Grecchi et al., 2013).

Beyond forest restoration, mitigating the environmental impacts of livestock farming is also possible through the adoption of sustainable agricultural practices. One example is regenerative livestock farming, which involves intensive animal rotation and pasture cycling, allowing soil regeneration in fallow areas while also reducing the need for chemical inputs and consequently increasing productivity per hectare (LaCanne and Lundgren, 2018). Additionally, reducing the slaughter age of cattle (youthful slaughter), typically between 1 and 1.5 years, improves biomass conversion efficiency, enhances meat quality, and lowers greenhouse gas emissions per animal (Skidmore et al., 2022).

Another approach that can enhance the sustainability of livestock systems is the crop-livestock-forest integration system. This method combines crop cultivation, livestock production, and forestry within the same property, creating an efficient and sustainable production cycle (Brown et al., 2022; Bilotto et al., 2024). The presence of wooded areas within these systems provides shade and resting areas for livestock, which can reduce water consumption by up to 10% and increase milk production by 10–20% (Domingos et al., 2013; Giro et al., 2019; Novelli et al., 2022). In semiarid regions, shaded areas can also lower temperatures by up to 6°C, improving animal welfare and reducing water stress (Carvalho et al., 2019). The adoption of these practices not only boosts profitability by optimizing land use but also encourages reforestation in PPAs and LRs, making agricultural production more sustainable and reducing the need for further deforestation. When combined with effective public policies and government incentives, these approaches can promote more balanced socio-economic development, while simultaneously slowing climate change and strengthening the ecological resilience of Iguatu and the Brazilian semiarid region.

5 CONCLUSIONS

This 37-year landscape assessment in a semiarid municipality of Brazil reveals that drought, land use change, agricultural practices, and public policies are intricately connected in shaping socioecological transitions. Our findings demonstrate that recurrent extreme droughts, marked by prolonged water scarcity, catalyzed a systematic reorganization of land use: from water-intensive annual crops toward more drought-resilient livestock systems. This transformation was not merely a reactive shift but rather a structural adaptation to escalating hydroclimatic stress, exacerbated by insufficient public support and weak land governance.

Agricultural decline, particularly in staple crops, coincided with a striking expansion in pasturelands and livestock herds, driving extensive deforestation and severe fragmentation of native vegetation. While irrigation and subsidies enabled isolated fruit crops (e.g., bananas), these interventions were insufficient to buffer broader agroecosystem vulnerabilities. The disjunction between climatic variables and agricultural output trends further suggests the overriding influence of management decisions and policy incentives in modulating land-use responses to climate extremes.

By conceptualizing land-use change as an emergent outcome of the interactions between climate pressures, rural management decisions, and agricultural policy, this study reveals the systemic nature of adaptation in semiarid landscapes. The shift from crop-based systems to extensive livestock farming in Iguatu was not only a response to water scarcity but also a reflection of deeper structural constraints, like limited institutional support, fragmented governance, and historically unsustainable land practices. Without strategic intervention, this trajectory is likely to perpetuate ecological degradation, biodiversity loss, and increased socio-environmental vulnerability. Thus, we call for an urgent reorientation of policy frameworks to support integrated landscape management, one that promotes sustainable intensification, ecological restoration, and land-use planning grounded in climate resilience. Such an approach is essential not only to reverse the ongoing degradation of Brazil's semiarid regions, but also to ensure the long-term sustainability of ecosystems and rural livelihoods facing an increasingly unpredictable climate.

REFERENCES[2]

Adamo, N., Al-Ansari, N., Sissakian, V., Jehad Fahmi, K., Ali Abed, S., 2022. Climate Change: Droughts and Increasing Desertification in the Middle East, with Special Reference to Iraq. *Engineering*. 14:235–273. https://doi.org/10.4236/eng.2022.14702

Ahmed, M., 2023. Climate Change and Farming System: A Review of Status, Potentials, and Further Work Needs for Disaster Risk Reduction. In: Ahmed, M., Ahmad, S. (eds) Disaster Risk Reduction in Agriculture. Disaster Resilience and Green Growth. Springer, Singapore. https://doi.org/10.1007/978-981-99-1763-1_1

[2] First chapter followed the Reference format Science of the Total Environment

Allan, R.P., Douville, H., 2024.An even drier future for the arid lands. *Proc. Natl. Acad. Sci*. 121, e2320840121. https://doi.org/10.1073/pnas.2320840121

Allan, R. P., Arias, P. A., Berger, S., Canadell, J. G., Cassou, C., Chen, D., et al., 2023. Intergovernmental panel on climate change (IPCC). Summary for policymakers. In *Climate change 2021: The physical science basis. Contribution of working group I to the sixth assessment report of the intergovernmental panel on climate change* (pp. 3-32). Cambridge University Press.

Alvares, C.A., Stape, J.L., Sentelhas, P.C., Gonçalves, J.D.M., Sparovek, G., 2013. Köppen's climate classification map for Brazil. *Meteorol. Z.*, 22, 711-728. DOI 10.1127/0941-2948/2013/0507

Antongiovanni, M., Venticinque, E.M., Matsumoto, M., Fonseca, C.R. 2020. Chronic anthropogenic disturbance on Caatinga dry forest fragments. *J. Appl. Ecol.* 57, 2064–2074. https://doi.org/10.1111/1365-2664.13686

Askar, A.R., Salama, R., El-Shaer, H.M., Raef, O., 2021. Effects of supplementary feeding level on digestion and energy utilization by sheep and goats grazing arid-area rangelands. Anim. Feed Sci. Technol. 271, 114695. https://doi.org/10.1016/j.anifeedsci.2020.114695

Ashokkumar, N., Poornima, K., Kalaiarasan, P., Jeyakumar, P., Uma, D., Kavino, M., Dharani, S., Kothai, S., 2021. Induction of defence-related proteins by selected plant growth regulators and biocontrol agents against guava root knot nematode, *Meloidogyne enterolobii*. *J. Nematol.* 53, 1–15. https://doi.org/10.21307/jofnem-2021-081

Beguería, S., Vicente-Serrano, S.M., 2017. SPEI: Calculation of the Standardized Precipitation-Evapotranspiration Index. R package version 1.8.1.

Bendito, B.P.C., Chaves, H.M.L., Scariot, A., 2023. Erosion and Sedimentation Processes in a Semiarid Basin of the Brazilian Savanna under Different Land Use, Climate Change, and Conservation Scenarios. *Water*, 15, 563. https://doi.org/10.3390/w15030563

Bhering, A.P., Antunes, I.M.H.R., Marques, E.A., Paula, R.S., 2021. Geological and hydrogeological review of a semiarid region with conflicts to water availability (southeastern Brazil). *Environ. Res.* 202, 111756. https://doi.org/10.1016/j.envres.2021.111756

Bilotto, F., Harrison, M.T., Vibart, R., Mackay, A., Christie-Whitehead, K.M., Ferreira, C.S., et al., 2024. Towards resilient, inclusive, sustainable livestock farming systems. *Trends Food Sci. Technol.* 152, 104668. https://doi.org/10.1016/j.tifs.2024.104668

Blicharska, M., Haddad, F., Riccardi, T., Smithers, R.J., 2024. Global presumed drylands: drivers, pressures, state, impacts, responses. *J. Environ. Plan. Manag.* 0, 1–28. https://doi.org/10.1080/09640568.2024.2351424

Brandão, S.L., Lima, S.C., 2002. Diagnóstico ambiental das áreas de preservação permanente (app), margem esquerda do rio Uberabinha, em Uberlândia (MG). *Caminhos Geogr.* 3, 41–62. https://doi.org/10.14393/RCG3715299

Brito, H.C. de, Rufino, I.A.A., Barros Filho, M.N.M., Meneses, R.A., 2023. Use of spatial data in the simulation of domestic water demand in a semiarid city: the case of Campina Grande, Brazil. *Urban Sci.* 7, 120. https://doi.org/10.3390/urbansci7040120

Brito, Y.M.A., Rufino, I.A.A., Braga, C.F.C., Mulligan, K., 2021. The Brazilian drought monitoring in a multi-annual perspective. *Environ. Monit. Assess.* 193, 31. https://doi.org/10.1007/s10661-020-08839-5

Brown, K., Schirmer, J., Upton, P., 2022. Can regenerative agriculture support successful adaptation to climate change and improved landscape health through building farmer self-efficacy and wellbeing? *Curr. Res. Environ. Sustain.* 4, 100170. https://doi.org/10.1016/j.crsust.2022.100170

Buchmann, C.M., Schurr, F.M., Nathan, R., Jeltsch, F., 2013. Habitat loss and fragmentation affecting mammal and bird communities-the role of interspecific competition and individual space use. *Ecol. Inform.* 14, 90–98. https://doi.org/10.1016/j.ecoinf.2012.11.015

Campos, D.A., Andrade, E.M., Castanho, A.D.A., Antonino, A.C.D., Montenegro, S.M.G.L., 2020. Biomass dynamics in a fragment of Brazilian tropical forest (Caatinga) over consecutive dry years. *Appl. Sci.* 10, 7813. https://doi.org/10.3390/app10217813

Carmin, J., 2012. Climate change: urban impacts and responses. *Wiley Interdiscip. Rev. Clim. Change.* https://doi.org/10.1002/9780470670590.wbeog076

Carneiro, E., Lopes, W., Espindola, G., 2021. Linking urban sprawl and surface urban heat island in the Teresina–Timon conurbation area in Brazil. *Land* 10, 516. https://doi.org/10.3390/land10050516

Carvalho, C. da C.S., Souza, A.C. de, Ferreira, H.C., Pacheco, F.L., Lima, G.S., 2019. Using infrared thermography to measure the body surface temperature of crossbred cows and calves in the semiarid region of Minas Gerais, Brazil. *J. Anim. Behav. Biometeorol.* 7, 132–136. https://doi.org/10.31893/2318-1265jabb.v7n3p132-136

Cerqueira, T.C., Mendonça, R.L., Gomes, R.L., Oliveira, P.T.S., Rodrigues, D.B.B., 2019. Effects of urbanization on water quality in a watershed in northeastern Brazil. *Environ. Monit. Assess.* 192, 65. https://doi.org/10.1007/s10661-019-8020-0

Clarke, B., Otto, F., Stuart-Smith, R., Harrington, L., 2022. Extreme weather impacts of climate change: an attribution perspective. *Environ. Res. Clim.* 1, 012001. https://doi.org/10.1088/2752-5295/ac6e7d

Correia Filho, W.L.F., Oliveira-Júnior, J.F., Santos, C.T.B., Souza, L.A., 2022. The influence of urban expansion in the socio-economic, demographic, and environmental indicators in the city of Arapiraca-Alagoas, Brazil. *Remote Sens. Appl. Soc. Environ.* 25, 100662. https://doi.org/10.1016/j.rsase.2021.100662

Cunha, A.P.M.A., Zeri, M., Deusdará Leal, K., Costa, L., Cuartas, L.A., Marengo, J.A., Tomasella, J., Vieira, R.M., Barbosa, A.A., Cunningham, C., Cal Garcia, J.V., Broedel, E., Alvalá, R., Ribeiro-Neto, G., 2019. Extreme Drought Events over Brazil from 2011 to 2019. *Atmosphere* 10, 642. https://doi.org/10.3390/atmos10110642

Domingos, H.G.T., Maia, A.S.C., Souza, J.B.F., Loureiro, C.M.B., 2013. Effect of shade and water sprinkling on physiological responses and milk yields of Holstein cows in a semiarid region. *Livest. Sci.* 154, 169–174. https://doi.org/10.1016/j.livsci.2013.02.024

Edelsparre, A.H., Shahid, A., Fitzpatrick, M.J., 2018. Habitat connectivity is determined by the scale of habitat loss and dispersal strategy. Ecol. Evol. 8, 5508–5514. https://doi.org/10.1002/ece3.4072

El Kenawy, A.M., Al Buloshi, A., Al-Awadhi, T., Al-Busaidi, M., 2020. Evidence for intensification of meteorological droughts in Oman over the past four decades. *Atmos. Res.* 246, 105126. https://doi.org/10.1016/j.atmosres.2020.105126

Espindola, G.M., Carneiro, E.L.N.C., Façanha, A.C., 2017. Four decades of urban sprawl and population growth in Teresina, Brazil. *Appl. Geogr.* 79, 73–83. https://doi.org/10.1016/j.apgeog.2016.12.018

Fahrig, L., 2003. Effects of habitat fragmentation on biodiversity. *Annu. Rev. Ecol. Evol. Syst.* 34, 487–515. https://doi.org/10.1146/annurev.ecolsys.34.011802.132419

Faria, D., Morante-Filho, J.C., Baumgarten, J., Pessoa, M.S., Leal, I.R., Mariano-Neto, E., 2023. The breakdown of ecosystem functionality driven by deforestation in a global biodiversity hotspot. *Biol. Conserv.* 283, 110126. https://doi.org/10.1016/j.biocon.2023.110126

Ferreira, M.S., Fontes, M.P.F., Pacheco, A.A., Rodrigues, S.C., 2021. Health risks of potentially toxic trace elements in urban soils of Manaus city, Amazon, Brazil. *Environ. Geochem. Health* 43, 3407–3427. https://doi.org/10.1007/s10653-021-00834-0

Ferreira, M.A., Silva, F.M., Bispo, S.V., Azevedo, M., 2009. Estratégias na suplementação de vacas leiteiras no semi-árido do Brasil. *Rev. Bras. Zootec.* 38, 322–329. https://doi.org/10.1590/S1516-35982009001300032

Fletcher Jr., R.J., Reichert, B.E., Holmes, K., 2018. The negative effects of habitat fragmentation operate at the scale of dispersal. *Ecology* 99, 2176–2186. https://doi.org/10.1002/ecy.2467

Fonseca, W.J.L., Fonseca, W.L., Araújo Sousa, P.H.A., Sales, A.D., 2014. Ingestive behavior of cows in pastures Andropogon gayanus and Brachiaria decumbens in southern state of Piauí, Brazil. *J. Agric. Sci.* 6, 144. https://doi.org/10.5539/jas.v6n4p144

FUNCEME - Fundação Cearense de Meteorologia e Recursos Hídricos. Postos Pluviométricos, 2022. http://www.funceme.br/?page_id=2694 (Accessed 10 May 2024).

Gampe, D., Schwingshackl, C., Böhnisch, A., Sillmann, J., Fischer, E.M., 2024. Applying global warming levels of emergence to highlight the increasing population exposure to temperature and precipitation extremes. *Earth Syst. Dyn.* 15, 589–605. https://doi.org/10.5194/esd-15-589-2024

Gilbert, C.L., Dwyer, C.M., 2024. Sheep and goats. The UFAW Handbook on the Care and Management of Laboratory and Other Research Animals, 609-627. https://doi.org/10.1002/9781119555278.ch34

Giro, A., Pezzopane, J.R.M., Barioni Junior, W., Pedroso, A.F., Maia, A.S.C., Andrade, P., 2019. Behavior and body surface temperature of beef cattle in integrated crop-livestock systems with or without tree shading. *Sci. Total Environ.* 684, 587–596. https://doi.org/10.1016/j.scitotenv.2019.05.377

Godefroid, S., Koedam, N., 2003. How important are large vs. small forest remnants for the conservation of the woodland flora in an urban context? *Glob. Ecol. Biogeogr.* 12, 287–298. https://doi.org/10.1046/j.1466-822X.2003.00035.x

Grecchi, R., Gwyn, Q., Bénié, G., Formaggio, A., 2013. Assessing the spatio-temporal rates and patterns of land-use and land-cover changes in the Cerrados of southeastern Mato Grosso, Brazil. *Int. J. Remote Sens.* 34, 5369–5392. https://doi.org/10.1080/01431161.2013.788798

Han, L., Zhang, Q., Zhang, Z., Qin, W., Sun, B., 2021. Drought area, intensity and frequency changes in China under climate warming, 1961–2014. *J. Arid Environ.* 193, 104596. https://doi.org/10.1016/j.jaridenv.2021.104596

IBGE - Instituto Brasileiro de Geografia e Estatística. Produção Agrícola e Pecuária Municipal Iguatu, Ceará, 2022. https://sidra.ibge.gov.br/pesquisa/pam/tabelas. (Accessed 13 June 2024).

INMET - Instituto Nacional de Meteorologia. Banco de Dados Meteorológicos para Ensino e Pesquisa (INMET/BDMEP), 2024. https://portal.inmet.gov.br/servicos/bdmep-dados-hist%C3%B3ricos (Accessed 10 May 2024).

Jenkins, K., Warren, R., 2015. Quantifying the impact of climate change on drought regimes using the standardised precipitation index. *Theor. Appl. Climatol.* 120, 41–54. https://doi.org/10.1007/s00704-014-1143-x

Jimenez, J.C., Marengo, J.A., Alves, L.M., Souza, T.C.L., Cunha, A.P.M.A., 2021. The role of ENSO flavours and TNA on recent droughts over Amazon forests and the Northeast Brazil region. *Int. J. Climatol.* 41, 3761–3780. https://doi.org/10.1002/joc.6453

LaCanne, C.E., Lundgren, J.G., 2018. Regenerative agriculture: merging farming and natural resource conservation profitably. *PeerJ* 6, e4428. https://doi.org/10.7717/peerj.4428

Lemos, J.J.S., 2020. Vulnerabilidades induzidas no semiárido brasileiro. *Desenvolv. Reg. em Debate* 10, 245–268. https://doi.org/10.24302/drd.v10i0.2728

Lemos, J.D.J.S., Paiva, E.C.D., Costa Filho, J.D., Holanda, F.J.C.D., 2022. Interaction between spatial and temporal instabilities of rainfall on milk production in the Brazilian semi-arid region. Int. J. Energy Environ. Econ. 7, 67-74. DOI: 10.11648/j.ijeee.20220703.12

Liu, S., Yin, Y., Liu, X., Zhan, J., 2017. Ecosystem services and landscape change associated with plantation expansion in a tropical rainforest region of Southwest China. *Ecol. Model.* 353, 129–138. https://doi.org/10.1016/j.ecolmodel.2016.03.009

Lopes, F.B., Andrade, E.M.D., Meireles, A., Becker, H., Batista, A.A., 2014. Assessment of the water quality in a large reservoir in semiarid region of Brazil. *Rev. Bras. Eng. Agric. Ambient.* 18, 437-445. https://doi.org/10.1590/S1415-43662014000400012

Magalhães, A.R., Marengo, J.A., Torres, R.R., 2021. Drought in Northeast Brazil: A review of agricultural and policy adaptation options for coping with extreme climate events. *Climate Resilience and Sustainability* 1, e17. https://doi.org/10.1002/cli2.17

Marengo, J.A., Cunha, A.P.M., Nobre, C.A., Ribeiro Neto, G.G., Magalhaes, A.R., Torres, R.R., Sampaio, G., Alexandre, F., Alves, L.M., Cuartas, L.A., Deusdará, K.R.L., Álvala, R.C., 2020. Assessing drought in the drylands of northeast Brazil under regional warming exceeding 4 C. *Natural Hazards*. 103, 2589-2611.

Marengo, J.A., Alves, L.M., Alvala, R.C.S., Cunha, A.P.M.A., Brito, S., Moraes, O.L.L., 2018. Climatic characteristics of the 2010–2016 drought in the semiarid Northeast Brazil region. *An. Acad. Bras. Ciênc.* 90, 1973–1985. https://doi.org/10.1590/0001-3765201720170206

Marengo, J.A., Torres, R.R., Alves, L.M., 2017. Drought in Northeast Brazil—past, present, and future. *Theor. Appl. Climatol.* 129, 1189–1200. https://doi.org/10.1007/s00704-016-1840-8

Marinho, A.P.F., Nascimento, C.W.A., Cunha, K.P.V., 2022. Soil degradation and Cu, Cr, Ni, Pb and Zn contamination in dumpsites of humid and semiarid tropical regions in northeastern Brazil. *Environ. Monit. Assess.* 194, 459. https://doi.org/10.1007/s10661-022-10122-8

Mattos, L.C., Mattos, J.L.S.D., Blackburn, R., Nogueira, A.L.R., Silva, A.K.L., 2020. A saga do algodão no semiárido nordestino: histórico, declínio e as perspectivas de base agroecológica. *Desenvolv. Meio Ambient.* 55. https://doi.org/10.5380/dma.v55i0.72576

McKee, T.B., Doesken, N.J., Kleist, J., 1993. The relationship of drought frequency and duration to time scales. *Proceedings of the 8th Conference on Applied Climatology.* American Meteorological Society, Anaheim, pp. 179–183.

Mendes, C.B., Prevedello, J.A., 2020. Does habitat fragmentation affect landscape-level temperatures? A global analysis. *Landsc. Ecol.* 35, 1743–1756. https://doi.org/10.1007/s10980-020-01041-5

Metzger, J., Bustamante, M., Ferreira, J., Brancalion, P.H.S., 2019. Why Brazil needs its Legal Reserves. *Perspect. Ecol. Conserv.* 17, 91–99. https://doi.org/10.1016/j.pecon.2019.07.002

Montenegro, S., Ragab, R., 2012. Impact of possible climate and land use changes in the semi-arid regions: a case study from northeastern Brazil. *J. Hydrol.* 434–435, 55–68. https://doi.org/10.1016/j.jhydrol.2012.02.036

Morales-Barquero, L., Borrego, A., Skutsch, M., Lovett, J.C., 2015. Identification and quantification of drivers of forest degradation in tropical dry forests: a case study in Western Mexico. *Land Use Policy* 49, 296–309. https://doi.org/10.1016/j.landusepol.2015.07.006

Morton, D., DeFries, R., Shimabukuro, Y., Anderson, L., Arai, E., del Bon Espirito-Santo, F., Freitas, R., Morisette, J., 2006. Cropland expansion changes deforestation dynamics in the southern Brazilian Amazon. *Proc. Natl. Acad. Sci. U. S. A.* 103, 14637–14641. https://doi.org/10.1073/pnas.0606377103

Mota, N.S.O., Pereira Filho, J.M., Formiga, L.D.A.D.S., Santos, N.M., Silva, A.P., Santos, E.M., 2018. Comparison between lambs and goat kids meat production of animals fed Caatinga vegetation enriched with buffel (Cenchrus ciliaris L.) grass. *Semina Ciênc. Agrár.* 39, 2795. https://doi.org/10.5433/1679-0359.2018v39n6p2795

Novelli, T.I., Bium, B.F., Biffi, C.H.C., Gennari, R.F., Millen, D.D., Silva, S.L., 2022. Consumption, productivity and cost: three dimensions of water and their relationship with the supply of artificial shading for beef cattle in feedlots. *J. Clean. Prod.* 376, 134088. https://doi.org/10.1016/j.jclepro.2022.134088

Nunes, A.T., Cabral, D.L.V., Amorim, E.L.C., Albuquerque, U.P., 2016. Plants used to feed ruminants in semiarid Brazil: a study of nutritional composition guided by local ecological knowledge. *J. Arid Environ.* 135, 96–103. https://doi.org/10.1016/j.jaridenv.2016.08.015

Oliveira, T.K., Oliveira, A.J.A., 2022. Capitalismo e natureza no Brasil colonial: a pecuária bovina no Ceará e a continentalidade do jogo das trocas (ca. 1680–1750). *Tempo* 28, 198–219. https://doi.org/10.1590/TEM-1980-542X2022v2801011

Paiva, E.C.D., Lemos, J.D.J.S., Campos, R.T., 2022. Previsões para a produção de leite sob instabilidade pluviométrica no Ceará no período de 1974 a 2019. *Rev. Econ. Sociol. Rural* 60, e252091. https://doi.org/10.1590/1806-9479.2021.252091

Pereira, B., Medeiros, P., de Araújo, J., 2023. Seca no Ceará 2012–2017. https://www.researchgate.net/profile/Bruno-Pereira-86/publication/375890905_Seca_no_Ceara_2012-2017/links/656103f93fa26f66f4243573/Seca-no-Ceara-2012-2017.pdf. (Accessed 13 June 2024).

Pereira, E.C.B., Lopes, F.B., Almeida, A.M.M., Silva, E.F.F., Silva, C.R.M., 2021. Sediments and nutrients input to a small reservoir in the tropical semiarid region. *Rev. Ciênc. Agronômica* 52, e20196717. https://doi.org/10.5935/1806-6690.20210007

Pineda Suárez, D.F.; Sánchez Román, R.M., 2018. Consumo de água em arroz irrigado por inundação em sistema de multiplas entradas. *IRRIGA* 1, 78, DOI: 10.15809/irriga.2016v1n1p78-95.

Püttker, T., Crouzeilles, R., Almeida-Gomes, M., Schiesari, L., Benedito, E., Verdade, L.M., 2020. Indirect effects of habitat loss via habitat fragmentation: a cross-taxa analysis of forest-dependent species. *Biol. Conserv.* 241, 108368. https://doi.org/10.1016/j.biocon.2019.108368

Raiesi, F., Beheshti, A., 2022. Evaluating forest soil quality after deforestation and loss of ecosystem services using network analysis and factor analysis techniques. *Catena* 208, 105778. https://doi.org/10.1016/j.catena.2021.105778

Reis, A.P.L., Silva, M.A.F.D.S., Maia, A.L.V., Barbosa, J.F., Viana, M.C.M., 2021. Levantamento florístico das espécies nativas da caatinga do estado do Ceará/Floristic survey of native species of caatinga in the state of Ceará. *Braz. J. Anim. Environ. Res.* 4, 3060–3078. https://doi.org/10.34188/bjaerv4n3-023

Ribeiro, E.M.S., Arroyo-Rodríguez, V., Santos, B.A., Tabarelli, M., Leal, I.R., 2015. Chronic anthropogenic disturbance drives the biological impoverishment of the Brazilian Caatinga vegetation. *J. Appl. Ecol.* 52, 611–620. https://doi.org/10.1111/1365-2664.12420

Rybicki, J., Abrego, N., Ovaskainen, O., 2020. Habitat fragmentation and species diversity in competitive communities. *Ecol. Lett.* 23, 506–517. https://doi.org/10.1111/ele.13450

Sampaio, E.G., Almeida, F.A., Oliveira, A.M., Leite, M.L.T., Fonseca, W.L., Silva Xavier, L.M., 2022. Extrato pirolenhoso no manejo de *Meloidogyne enterolobii* em mudas de goiabeira, cv. paluma. *Rev. Ciênc. Agrár.*, 45, 136-143. https://doi.org/10.19084/rca.26524

Santana, A.S.D., Santos, G.R.D., 2020. Impactos da seca de 2012–2017 na região semiárida do Nordeste: notas sobre a abordagem de dados quantitativos e conclusões qualitativas. *Bol. Reg. Urbano Ambient.* 22, 119–129. https://doi.org/10.38116/brua22art9

Schulz, K., Guschal, M., Kowarik, I., Walz, U., 2019. Grazing reduces plant species diversity of Caatinga dry forests in northeastern Brazil. *Appl. Veg. Sci.* 22, 348–359. https://doi.org/10.1111/avsc.12434

Silva, M.I., Lima, M.T.V., Costa, C.T.F., Ribeiro, L.J., Guimarães, T.A., Souza, R.M., 2023a. Groundwater quality assessment in a peri-urban Brazilian semiarid microbasin. Environ. Earth Sci. 82, 73. https://doi.org/10.1007/s12665-023-10752-2

Silva, B.F., Rodrigues, R.Z.S., Heiskanen, J., Abera, T.A., Gasparetto, S.C., Biase, A.G., Ballester, M.V.R., Moura, Y.M., et al., 2023b. Evaluating the temporal patterns of land use and precipitation under desertification in the semi-arid region of Brazil. *Ecol. Inform. 77*, 102192. https://doi.org/10.1016/j.ecoinf.2023.102192

Silva, T.A., Ferreira, J., Calijuri, M.L., Domingos, R.N., 2021a. Efficiency of technologies to live with drought in agricultural development in Brazil's semiarid regions. *J. Arid Environ.* 192, 104538. https://doi.org/10.1016/j.jaridenv.2021.104538

Silva, T. A., Ferreira, J., Calijuri, M.L., Santos, V. J., Carmo Alves, S., Siqueira Castro, J., 2021b. Efficiency of technologies to live with drought in agricultural development in Brazil's semi-arid regions. *Journal of Arid Environments*, 192, 104538. https://doi.org/10.1016/j.jaridenv.2021.104538

Silva, R.F.B., Batistella, M., Moran, E.F., 2018. Regional socioeconomic changes affecting rural area livelihoods and Atlantic forest transitions. *Land* 7, 125. https://doi.org/10.3390/land7040125

Silva, J.M.C., Barbosa, L.C.F., Leal, I.R., Tabarelli, M., 2017. The Caatinga: Understanding the Challenges. In: Silva, J.M.C., Leal, I.R., Tabarelli, M. (Eds) Caatinga. Springer, Cham. https://doi.org/10.1007/978-3-319-68339-3_1

Skidmore, M.E., Sims, K.M., Rausch, L.L., Gibbs, H.K., 2022. Sustainable intensification in the Brazilian cattle industry: the role for reduced slaughter age. *Environ. Res. Lett.* 17, 064026. https://doi.org/10.1088/1748-9326/ac6f70

Sobrinho, M.S., Tabarelli, M., Machado, I.C., Lopes, A.V., 2016. Land use, fallow period and the recovery of a Caatinga forest. *Biotropica* 48, 586–597. https://doi.org/10.1111/btp.12334

Sousa, M.C., Veloso, G.V., Gomes, L.C., Paiva, R.S., 2021. Spatio-temporal dynamics of land use changes of an intense anthropized basin in the Brazilian semiarid region. *Remote Sens. Appl. Soc. Environ.* 24, 100646. https://doi.org/10.1016/j.rsase.2021.100646

Tripathy, K.P., Mukherjee, S., Mishra, A.K., Mishra, V., 2023. Climate change will accelerate the high-end risk of compound drought and heatwave events. *Proc. Natl. Acad. Sci. U.S.A.* 120, e2219825120. https://doi.org/10.1073/pnas.2219825120

Vieira-Alencar, J.P.S., Bolochio, B.E., Carmignotto, A.P., Passamani, M., 2023. How habitat loss and fragmentation are reducing conservation opportunities for vertebrates in the most threatened savanna of the world. *Perspect. Ecol. Conserv.* 21, 121–127. https://doi.org/10.1016/j.pecon.2023.02.004

Vieira, R.M.D.S.P., Tomasella, J., Cunha, A.P.M.D.A., Barbosa, A.A., Pompeu, J., Ferreira, Y., et al., (2023). Vulnerabilidade socioambiental à seca e à degradação do solo: uma avaliação em duas bacias hidrográficas do nordeste brasileiro. *Sustentabilidade*, 15, 8029. https://doi.org/10.3390/su15108029

Wang, Q., Zhang, R., Qi, J., Zhang, H., Wang, C., 2022. An improved daily standardized precipitation index dataset for mainland China from 1961 to 2018. *Sci. Data* 9, 124. https://doi.org/10.1038/s41597-022-01201-z

Wiegand, T., Revilla, E., Moloney, K.A., 2005. Effects of habitat loss and fragmentation on population dynamics. *Conserv. Biol.* 19, 108–121. https://doi.org/10.1111/j.1523-1739.2005.00208.x

Wijerathna-Yapa, A., Pathirana, R., 2022. Sistemas agroalimentares sustentáveis para enfrentar as mudanças climáticas e a segurança alimentar. *Agricultura* 12, 1554. https://doi.org/10.3390/agriculture12101554

Willmer, J.N.G., Püttker, T., Prevedello, J.A., 2022. Global impacts of edge effects on species richness. *Biol. Conserv.* 272, 109654. https://doi.org/10.1016/j.biocon.2022.109654

Wu, R., Tiessen, H., 2002. Effect of land use on soil degradation in alpine grassland soil, China. *Soil Sci. Soc. Am. J.* 66, 1648–1655. https://doi.org/10.2136/sssaj2002.1648

Yue, S., Wang, C., 2004. The Mann-Kendall test modified by effective sample size to detect trend in serially correlated hydrological series. *Water Resour. Manag.* 18, 201–218. https://doi.org/10.1023/B:WARM.0000043140.61082.60

Zhang, W., Zhou, T., Wu, P., 2024. Anthropogenic amplification of precipitation variability over the past century. *Science* 385, 427–432. https://doi.org/10.1126/science.adp0212

Zhao, T., Li, X., Li, Y., Sun, Q., Wang, J., 2024. Concurrent droughts across major river basins of the world modulated by El Niño–Southern Oscillation. *J. Hydrol*. 644, 132112. https://doi.org/10.1016/j.jhydrol.2024.132112

CHAPTER II: CHANGES IN SOIL ORGANIC MATTER FRACTIONS, ENZYMATIC ACTIVITY, SOIL FERTILITY, AND MICROSTRUCTURE UNDER INTENSIVE AGRICULTURAL AND LIVESTOCK LAND USE IN A SEMIARID REGION

ABSTRACT

Land-use intensification in semi-arid regions threatens soil quality. This study assessed the impacts of different land use systems on soil organic matter fractions, enzymatic activity, fertility attributes, and micromorphological structure in agricultural and livestock landscapes in municipality of Iguatu, state of Ceará, Brazil. Soil samples were collected at 0–10 and 10–20 cm depths under corn-bean consortium (CBC), corn monoculture (CORN), banana cultivation (BAN), guava-horticulture consortium (GHC), pasture with *Urochloa mosambicensis* under dairy cattle grazing (PB1 and PB2), and preserved native forest (NF) (Caatinga) as a reference. Chemical attributes, organic carbon pools, and enzymatic activities (β-glucosidase, arylsulfatase, and dehydrogenase) were quantified, complemented by multivariate approaches (Pearson's correlations, principal component analysis, and hierarchical clustering). Regardless of crop type, soil organic carbon (SOC) exhibited substantial declines of -47% and -39% at depths of 0–10 cm and 10–20 cm, respectively, compared to NF. Regardless of crop type, soil organic carbon (SOC) exhibited substantial declines of -47% and -39% at depths of 0–10 cm and 10–20 cm, respectively, compared to native forest. Severe reductions in labile carbon fractions under intensive agriculture, with CORN and GHC systems showing losses exceeding 80% for particulate organic carbon (POC) and 50% for microbial biomass carbon (MBC). Enzymatic activities were strongly suppressed, with average declines of 40–69% compared to NF, especially for arylsulfatase and dehydrogenase. In contrast, pasture soils maintained higher stability of labile pools and even exceeded NF in the Carbon Management Index (CMI) at 10–20 cm, PB1 (CMI=121), and PB2 (137). Microstructural analyses revealed greater aggregation and organic coatings in pasture and NF soils, whereas agricultural systems displayed disrupted structures with limited biological interactions. Overall, the study highlights that intensive fruit and grain systems accelerate soil degradation under conventional tillage, while pastures function as effective conservation practices in semi-arid environments.

Keywords: Carbon pools. Microbial biomass. Particulate organic carbon. Cropping systems. Pastures.

1 INTRODUCTION

Addressing the escalating challenges of global environmental change, particularly climate change mitigation and soil degradation, requires a deep and mechanistic understanding of soil dynamics and their interactions with land use and management. In arid and semi-arid regions, establishing key soil parameters for study is essential not only to sustain agricultural and livestock systems under climatic stress but also to enhance carbon sequestration, optimize nutrient cycling, and maintain soil structural integrity, thereby aligning with the targets of the United Nations Sustainable Development Goals (SDGs). Advancing the 2030 SDG agenda demands responsible land stewardship that explicitly incorporates these soil quality metrics to inform sustainable management strategies. In doing so, it becomes possible to directly contribute to SDG 1 and SDG 2 (poverty alleviation and food security through sustainable agriculture), SDG 8 (economic growth through increased rural productivity), SDG 13 (climate change mitigation via SOC stabilization), and SDG 15 (conservation of terrestrial ecosystems and biodiversity) (Abrar et al., 2025; Rathika et al., 2025; Lal et al., 2021).

Arid and semi-arid zones cover more than 40% of the Earth’s surface, hosting approximately 2.5 billion people and contributing around half of the world’s livestock and 45% of global food production (Dzvene et al., 2025; Kumar et al., 2022). The United Nations projects that by 2084 the global population will peak at 10.3 billion, and agricultural production will need to increase by approximately 30% to ensure food security (Nketsang et al., 2025). However, in semi-arid environments, agricultural practices often face severe water scarcity, low resilience, and inherently poor soil fertility (Ahmad et al., 2024). Under the pressure to boost productivity while maintaining ecosystem services, intensive farming and grazing have accelerated the depletion of native soil organic carbon and reduced microbial biomass and enzymatic activity, thereby compromising soil fertility and altering key biochemical processes (Garba et al., 2024; Ying et al., 2023; Nehrani et al., 2020). These changes are recognized as key indicators of soil degradation in semi-arid landscapes (Kooch et al., 2022), as degraded soils are physically and chemically altered and rapidly depleted of essential nutrients and carbon (Jin et al., 2022).

In Brazil’s semiarid region, especially in Ceará state, degradation has been particularly severe over the last four decades (Oliveira et al., 2025). Extensive deforestation of native Caatinga vegetation for annual and perennial crops, as well as pasture formation, has profoundly altered the physical, chemical, and biological properties of the soil. However, the extent and magnitude of these changes in the central-southern region of Ceará remain understudied. Achieving sustainable agricultural and livestock production in these soils depends on optimizing carbon storage and improving soil fertility assessments (Naorem et al., 2023). Given the complexity of organic carbon pools, it is essential to fractionate SOM to better understand its dynamics.

Soil organic carbon can be partitioned by physical or chemical fractionation. Physically, SOC can be divided into particulate organic carbon (POC), a coarse, light, and labile fraction vulnerable to land use disturbances, and mineral-associated organic carbon (MAOC), which is more stable and resistant to microbial decomposition (Haddix et al., 2020; Zhao et al., 2025; Poeplau et al., 2018). Chemically, SOC includes labile fractions such as permanganate-oxidizable carbon (POXC), representing soluble organic matter and microbial residues, which are strongly linked to enzymatic activity and nutrient cycling (Nn et al., 2025; Ahmad et al., 2024; Lasota et al., 2020).

In contrast, recalcitrant fractions, such as humic substances composed of fulvic acids, humic acids, and humin, are formed through humification and play a central role in long-term carbon stabilization and biogeochemical regulation (Nn et al., 2025; García et al., 2019). The Carbon Management Index (CMI) complements this approach by providing a synthetic indicator of soil management quality, with higher values (CMI>100) reflecting conservation effectiveness and lower values indicating degradation (CMI<100) (Yang et al., 2024). The current paradigm is shifting from isolated assessments of soil fertility to integrated evaluations of soil multifunctionality, highlighting the need for reliable and interpretable indicators. Despite progress, biological and organic indicators are still underrepresented in standard protocols (Fan et al., 2025).

Given the projected increase in global aridification of 13–23% by the end of the century (Naorem et al., 2023), and the broader applicability of our findings to ecosystems under similar climatic and management conditions, studies of this nature are imperative for the diagnosis and monitoring of land degradation. Therefore, the objective of this study was to evaluate the response of labile, biological, and recalcitrant organic matter fractions, as well as soil fertility, to intensive use of agricultural and livestock lands in the semiarid region of Ceará, Brazil.

2 MATERIALS AND METHODS

The study on intensive use of agricultural and livestock land was conducted in the municipality of Iguatu, located in the central-southern region of Ceará State, Brazil (6°21′34″ S, 39°17′55″ W; 218 m). The region's climate is classified as BSh, characterized by hot, semiarid conditions, with two distinct seasons: a protracted dry period and a brief, erratic rainy season. The mean annual temperature is 28°C, and the average annual precipitation is 996.6 mm, with rainfall concentrated between December and May (Dubreuil et al., 2018; INMET, 2024). The native vegetation is classified as hyperxerophilous Caatinga, a seasonally dry tropical forest dominated by deciduous and xerophytic species, including a wide range of spiny shrubs and trees (Reis et al., 2021; Andrade et al., 2018). At the time of sampling, the native vegetation, hereafter referred to as "native forest", exhibited structural variability and a mosaic of herbaceous and woody components (Oliveira et al., 2025).

Seven land use systems were selected, including one reference area under preserved native Caatinga vegetation. The cultivated areas included: (1) corn-bean consortium (CBC); (2) corn monoculture (CORN); (3) banana cultivation (BAN) (Musa spp.); (4) guava-horticulture consortium (GHC); (5) pasture with *Urochloa mosambicensis* under dairy cattle grazing (PB1); (6) pasture with *Urochloa mosambicensis* under dairy cattle grazing (PB2); and (7) native forest (Caatinga). The location of the experimental sites and sampling points is presented in Figure 1, and the land use history of each site is detailed in Table 1. The soil classification for all land uses was either Cambisol (Santos et al., 2018), Incepsol (Soil Taxonomy, 1999), or Cambisol (World Reference Base for Soil Resources, IUSS, 2022) (Figure 1), with texture varying depending on location (Table 2).

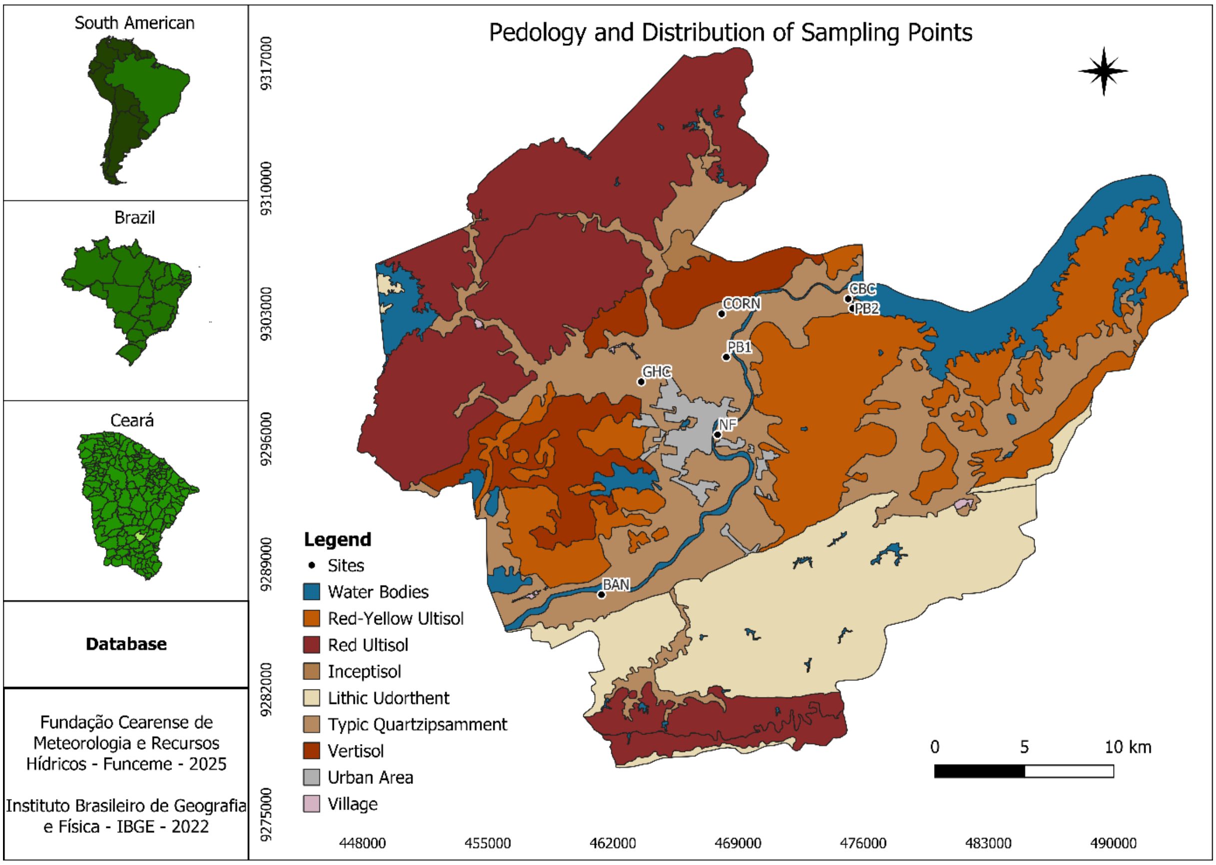

Figure 1. Location map of the areas with their respective land use in the municipality of Iguatu, Ceará state, Brazil. Sites: corn-bean consortium (CBC); corn monoculture (CORN); banana cultivation (BAN) (Musa spp.); guava-horticulture consortium (GHC); pasture with *Urochloa mosambicensis* under dairy cattle grazing (PB1 and PB2), and native forest (Caatinga). Source: Own authorship

Table 1. Land use history and cropping systems in the municipality of Iguatu, Ceará state, Brazil.

Land use	Land use history
Corn-bean consortium (CBC)	3.0 ha area cultivated with intercropped corn (*Zea mays* L.) and cowpea (*Vigna unguiculata* (L.) Walp.). No chemical fertilizers are applied, but after harvest, dairy cattle graze on crop residues. The area has been under conventional tillage (shallow plowing and harrowing) since 2010, although at a lower intensity compared to other systems. Irrigation is performed via furrow flooding from the nearby Orós Reservoir.
Corn monoculture (CORN)	8.0 ha area under continuous corn (*Zea mays* L.) cultivation. Only chemical fertilization is used, based on crop requirements.

	Conventional tillage (plowing and harrowing) has been applied since 2005. Maize is rotated with cucurbits (pumpkin and watermelon) and cowpea. Crop residues are often removed for silage production. Irrigation is via Sprinkler Irrigation.
Banana (*Musa* spp.) cultivation (BAN)	1.5 ha area cultivated with banana (*Musa* spp., Pacovan cultivar) since 2014. Fertilization includes both mineral fertilizers and cattle manure. Irrigated using micro-sprinklers.
Guava-horticulture consortium (GHC);	1.5 ha area with guava (*Psidium guajava* L.) planted in 2021 under conventional tillage. One year after planting, intercropped vegetable beds (lettuce, scallion, coriander, watermelon) were introduced and are rotated periodically. Irrigated using micro-sprinklers.
Pasture with *Urochloa mosambicensis* under dairy cattle grazing (PB1)	6.1 ha area cultivated with (*Urochloa mosambicensis* (Hanck) Dandy) since 2010, used for dairy cattle grazing. No mineral or organic fertilization is applied. is sprinkler-irrigated during the dry season.
Pasture with *Urochloa mosambicensis* under dairy cattle grazing (PB2)	6.1 ha area cultivated with (*Urochloa mosambicensis* (Hanck) Dandy) since 2010, used for dairy cattle grazing. No mineral or organic fertilization is applied. The area is naturally flooded during the rainy season due to its proximity to the Orós reservoir and is sprinkler-irrigated during the dry season.
Native forest (Caatinga) (NF)	Preserved native area used as a reference, dominated by deciduous and xerophytic herbaceous and woody species. Common species include *Combretum leprosum* (mofumbo), *Schinus terebinthifolius* (aroeira), *Cydonia oblonga* (marmeleiro), and *Mimosa hostilis* (jurema-preta).

Source: Own authorship

Soil sampling was conducted during the dry season, specifically in October 2022. Each land use area was subdivided into ten $100m^2$ plots, which served as experimental replicates. Within each plot, 10 subsamples were collected using a Dutch auger from two soil depths (0–10 cm and 10–20 cm). Environmental heterogeneity was incorporated by stratifying the area according to edaphic, topographic, and land use characteristics. This ensured that different environmental conditions were represented and facilitated the identification of true replicates.

The samples were stored in labeled plastic bags and transported to the Laboratory of Soil, Water, and Plant Analysis (LASAP) at the Federal Rural University of the Semi-Arid (UFERSA). In the laboratory, the samples were subjected to a series of procedures. Initially, they were air-dried. Then, they were gently crushed and sieved through a 2 mm mesh. This process yielded air-dried fine earth (ADFE), which was subsequently employed for standard physical and chemical analyses. To perform total and fractionated carbon analysis, subsamples of ADFE were meticulously ground and subsequently sieved through a 0.210 mm (60 mesh) screen.

The analyzed soil attributes included hydrogen potential (pH) and electrical conductivity (EC), both determined in a water saturated paste extract. Exchangeable calcium (Ca^{2+}) and magnesium (Mg^{2+}) were extracted using 1 mol L^{-1} potassium chloride and quantified by atomic absorption spectrophotometry. Phosphorus (P), sodium (Na^{+}), and potassium (K^{+}) were extracted using the Mehlich-1 solution. P was quantified via colorimetry, while Na^{+} and K^{+} were determined by flame photometry. Potential acidity ($H^{+}+Al^{3+}$) was extracted with calcium acetate and quantified by titration. Micronutrient contents copper (Cu), manganese (Mn), zinc (Zn) and iron (Fe) were extracted using Mehlich-1 and quantified by atomic absorption spectrophotometry. All chemical analyses were performed following the standardized procedures described by Teixeira et al. (2017).

Particle-size distribution was determined using the pipette method, employing sodium hexametaphosphate as a chemical dispersant in 20 g of ADFE. Sand content was measured by sieving, clay by sedimentation, and silt was calculated by difference (Teixeira et al., 2017). The results for sand, silt, and clay contents, as well as the soil textural classification for the 0–20 cm layer, are presented in Table 2.

Table 2. Granulometric analysis and textural classification of different land uses in the municipality of Iguatu, Ceará state, Brazil.

Land use	Coarse sand	Fine sand	Total sand	Silt	Clay	Textural classification
			dag kg^{-1}			
			0-10 cm			
CBC	3.6±0.29	15.7±0.64	19.2±0.38	45.8±1.73	35.0±0.61	Silty Clay Loam
CORN	2.4±0.09	28.2±0.35	30.6±0.04	40.3±0.45	29.1±1.91	Clay Loam
BAN	6.7±0.35	21.7±0.50	28.4±0.40	47.5±0.66	24.1±0.90	Loam
GHC	8.1±0.10	39.6±0.70	47.7±0.75	30.2±0.00	22.1±0.90	Loam
PB1	1.5±0.15	19.4±4.61	20.9±1.20	43.9±0.16	35.2±0.51	Clay Loam

PB2	2.2±0.10	21.0±0.70	23.2±0.80	45.4±1.05	31.4±0.45	Clay Loam
NF	13.4±0.25	30.7±0.70	44.1±1.95	30.5±0.50	25.4±0.55	Loam
			10-20 cm			
CBC	1.6±0.03	17.0±0.17	18.5±1.17	45.6±0.18	35.9±1.36	Silty Clay Loam
CORN	1.5±0.13	32.1±0.96	33.6±1.73	38.2±0.05	28.1±0.10	Clay Loam
BAN	5.2±0.15	27.4±0.90	32.6±0.71	43.2±0.50	24.2±1.85	Loam
GHC	9.1±0.25	39.8±0.80	48.9±0.16	27.0±0.85	24.1±1.88	Sandy Clay Loam
PB1	2.0±0.08	21.5±0.50	23.5±9.17	42.6±1.18	33.9±0.21	Clay Loam
PB2	3.5±0.25	22.1±0.90	25.6±1.15	43.3±0.96	31.1±0.21	Clay Loam
NF	14.2±0.15	31.2±0.35	45.4±0.41	29.8±1.30	24.8±0.25	Loam

Mean±standard error of the mean (n=4). CBC= corn/bean consortium, CORN= corn monoculture; BAN= banana; GHC= Guava-horticulture consortium; PB1 and PB2= pasture with *Urochloa mosambicensis* under dairy cattle grazing; NF= native forest (Caatinga preserved). Source: Own authorship

Soil organic carbon (SOC) was determined using the wet oxidation method with external heating, following the procedure described by Yeomans and Bremner (1988). Labile carbon (LC) was quantified through oxidation with potassium permanganate ($KMnO_4$ – 0.033 mol L^{-1}), according to the method proposed by Shang e Tiessen (1997). To calculate the Carbon Management Index (CMI), the native forest soil was used as the reference condition. Based on the changes in SOC and LC, the following indices were computed: carbon lability (L), lability index (LI), carbon pool index (CPI), and the carbon management index (CMI), as expressed in equations (1) through (4), respectively (Blair; Lefroy; Lisle, 1995):

$$\text{Lability (L)} = \frac{\text{LC}}{(\text{SOC} - \text{LC})} \quad (1)$$

$$\text{Lability Index (LI)} = \frac{\text{L}_{\text{soil use}}}{\text{L}_{\text{native forest}}} \quad (2)$$

$$\text{Carbon Pool Index (CPI)} = \frac{\text{SOC}_{\text{soil use}}}{\text{SOC}_{\text{native forest}}} \quad (3)$$

$$\text{Carbon Manegement Index (CMI)} = \text{CPI} \times \text{LI} \times 100 \quad (4)$$

Humified fractions (humin, humic acids, and fulvic acids) were obtained based on their differential solubility in alkaline and acidic solutions. The sum of these fractions represented the humic substances (Swift, 1996), and the carbon content of each fraction was quantified following the method of Yeomans and Bremner (1988). To physically fractionate the soil organic matter, the air-dried fine earth (ADFE) was separated according to its particle size into two distinct fractions: particulate organic carbon (POC, >53 μm) and mineral-associated organic carbon (MAOC, <53 μm). This procedure followed sodium hexametaphosphate dispersion and wet-sieving protocols as described by Cambardella and Elliott (1992) and Gao et al. (2024). To analyze soil microstructures under different land use, undisturbed ADFE samples from the 0–10 cm depth was examined using Scanning Electron Microscopy (SEM). The images were captured using a secondary electron (SE) detector on a VEGA 3 LMU SEM (Tescan, Czech Republic), which operated with an accelerating voltage of 20 kV (Fernandes, 2019).

Microbial biomass carbon (MBC) was determined using the irradiation–extraction method on 20 g of ADFE, as proposed by Islam e Weil (1998). Enzymatic assays focused on enzymes directly linked to biological soil activity and to carbon and sulfur cycling. The selected enzymes were β-glucosidase (Bglu), arylsulfatase (ARYL), and dehydrogenase (DHA) (Daunoras; Kačergius; Gudiukaitė, 2024). β-glucosidase activity was quantified by colorimetric detection of p-nitrophenol (pNP) released from p-nitrophenyl-β-D-glucoside, following the protocol of Eivazi and Tabatabai (1988). Arylsulfatase activity was determined by measuring pNP released after incubation with potassium p-nitrophenyl sulfate, as described by Tabatabai and Bremner (1970), and results were expressed in mg pNP g^{-1} soil h^{-1}. Dehydrogenase activity was measured using the reduction of triphenyl tetrazolium chloride (TTC) to triphenyl formazan (TPF), with incubation in a water bath at 37 °C for 24 h in the dark, followed by colorimetric analysis (Casida; Klein; Santoro, 1964; Elhaddad et al., 2024). DHA results were expressed as µg TPF g^{-1} soil h^{-1}. The calculation of the average specific enzymatic activity (ASEA) was performed by considering only Bglu and ARYL. Each enzyme activity was normalized by SOC, yielding S-GLU and S-ARYL values, and ASEA was calculated as the arithmetic mean of both indices (Chaer et al., 2023).

All data were expressed as mean ± standard error of the mean. Reductions in SOC and organic carbon fractions were calculated using the equation: Reductions SOC = $(C_{use\ soil} - C_{native\ forest})/C_{native\ forest}) \times 100$, where negative values indicate carbon loss. To verify that the data set followed a normal distribution and homogeneity of variance, the Shapiro-Wilk, and Bartlett tests were performed, respectively. Multivariate statistics were applied to identify sensitive attributes distinguishing land use types. Pearson correlation analyses ($p \leq 0.05$) were initially performed for data standardization, followed by Principal Component Analysis (PCA), and Clustering Analysis using the R software program (R Core Team, 2021). Univariate analysis used the Scott-Knott test ($p \leq 0.05$) to separate treatment means into homogeneous groups and avoid overlapping letters using the R software program (R Core Team, 2021).

3 RESULTS

3.1 Relationships between the chemical and organic attributes of different land uses

3.1.1 Pearson's correlation matrix

The Pearson's correlation matrix revealed consistent patterns across the studied depths, highlighting interactions among chemical attributes, soil organic carbon (SOC) and its fractions, humic substances, and biological indicators in soils under different land uses. In both soil layers (0–10 cm and 10–20 cm), robust positive correlations were observed between SOC and the carbon management index (CMI), as well as with labile fractions (LC, POC) and microbial biomass carbon (MBC), underscoring the interdependence between carbon stocks, high-turnover pools, and microbial activity. SOC also showed significant positive correlations with humic fractions (FA, HA, H), particularly humic substances (HS) and humic acids (HA), suggesting that carbon accumulation is closely linked to stabilization in recalcitrant forms (Figure 2 A; B).

At both depths, CMI exhibited a strong association with β-glucosidase and dehydrogenase, suggesting a direct link between carbon quality and enzymatic activities involved in carbohydrate degradation and microbial metabolism (Figures 2A, B). Arylsulfatase and β-glucosidase maintained positive correlations with LC, MBC, and CMI, reflecting the high sensitivity of these enzymes to variations in biologically active carbon. Conversely, attributes potentially related to degradation processes, such as electrical conductivity (EC) and exchangeable sodium, displayed negative correlations with MBC and humic fractions, particularly in the surface layer, suggesting that salinization and sodification are associated with qualitative losses in organic matter (Figure 2A, B). Clay and silt fractions were positively correlated with chemical attributes (Na, P, Ca^{2+}, Mg^{2+}, and Zn^{2+}), reflecting the role of finer particles in the dynamics of exchangeable bases and their potential to retain phosphorus. Regarding specific chemical attributes, copper (Cu) was positively correlated with calcium (Ca), while zinc (Zn) was positively associated with Ca, Mg, and Na. Soil pH, in turn, exhibited negative correlations with enzymatic activities, MBC, and the soluble fractions of SOC (HA and FA) (Figure 2A; B).

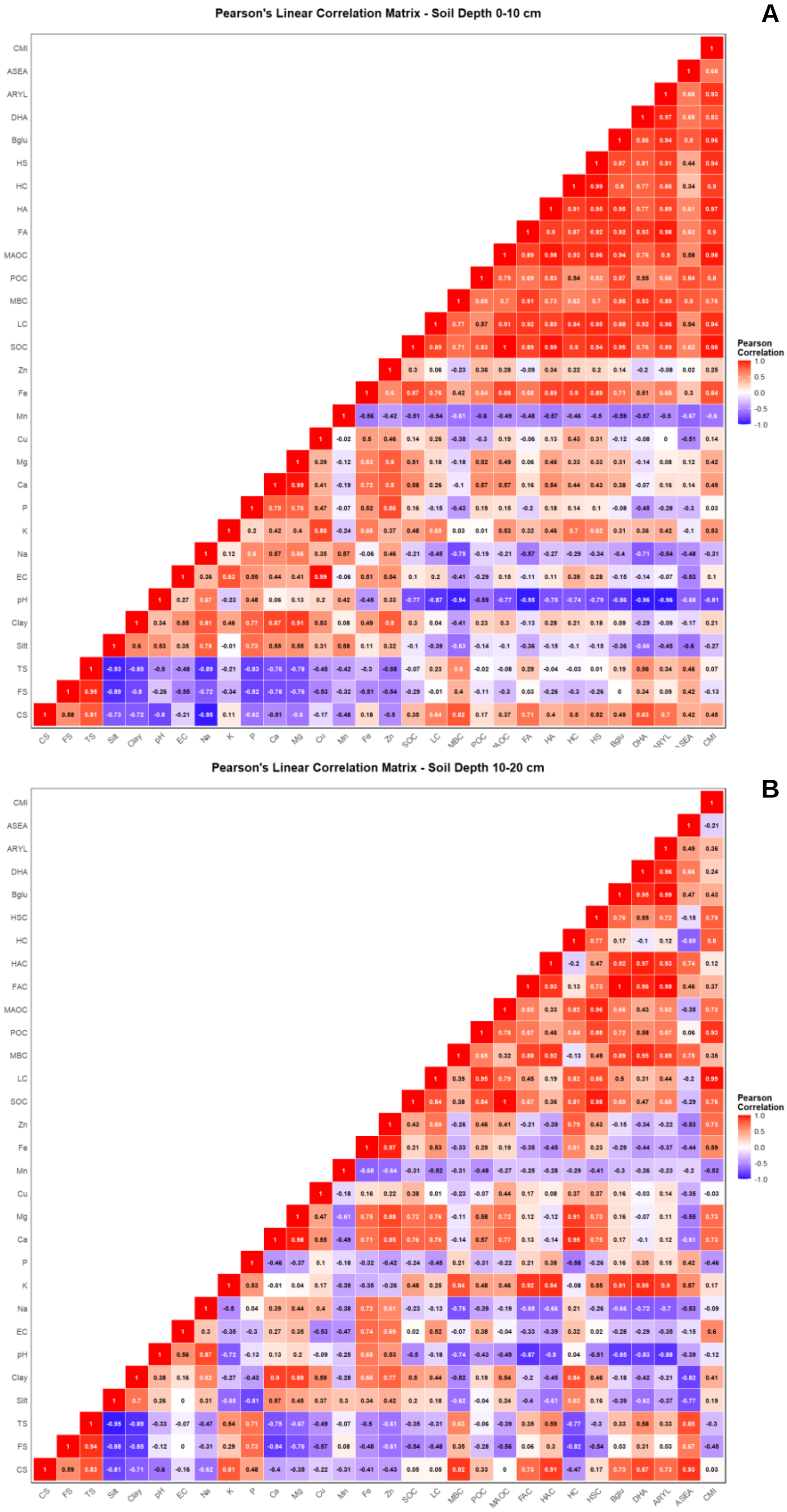

Figure 2. Pearson’s correlation matrix between the main chemical and organic soil attributes. indicating significant interactions under different land uses. Red indicates positive interactions and blue negative. Source: Own authorship

3.1.2 Principal Component Analysis

The principal component analysis (PCA) applied to soil attributes in the 0–10 cm layer explained 81.5% of the total variance through the first two axes (PC1 = 49.3%; PC2 = 32.2%), revealing clear association patterns among chemical, biological, and organic matter variables across different land-use systems (Figure 3A). Soil under native forest (NF) exhibited high clustering with variables linked to organic matter stability, microbial biomass carbon (MBC), and enzymatic activity. Similarly, the corn–bean consortium (CBC) and the pasture with bovine (PB1 and PB2) systems were in the upper-right quadrant of the biplot, highlighting a strong association with soil fertility indicators and carbon accumulation, including soil organic carbon (SOC). The presence of mineral-associated organic carbon (MAOC), particulate organic carbon (POC), and carbon management index (CMI) has been identified, in addition to nutrients including Ca, Mg, Zn, and Cu. In contrast, systems such as banana (BAN), guava–horticulture consortium (GHC), and corn monoculture (CORN) were positioned in the lower quadrants, exhibiting weaker associations with organic carbon pools and microbial activity, suggesting reduced soil biological functionality (Figure 3A).

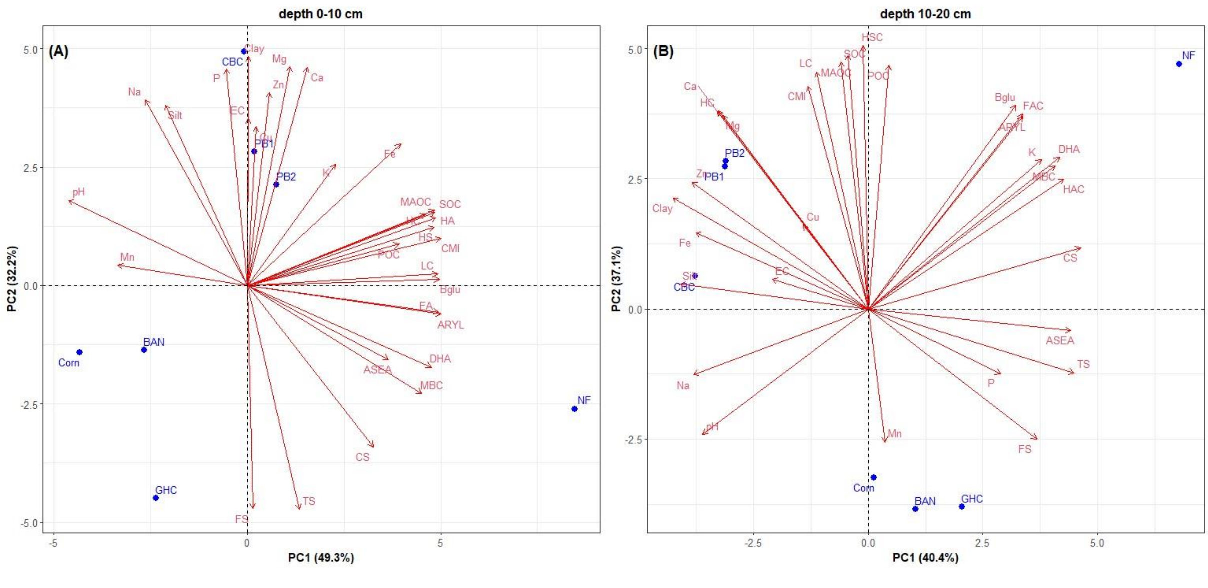

Figure 3. Principal component analysis (PCA) of the organic fractions and physical-chemical parameters of the under different land use types in the municipality of Iguatu, Ceará state, Brazil. A) Individual contribution of the variables to PC1 (0-10 cm); B) Individual contribution of the variables to PC2 (10-20 cm). Land use (blue): CBC= corn/bean consortium, CORN= corn monoculture; BAN= banana; GHC= guava-horticulture consortium; PB1 and PB2= pasture with *Urochloa mosambicensis* under dairy cattle grazing; NF= native forest (Caatinga preserved). Source: Own authorship

For the 10–20 cm layer, the first two components explained 77.5% of the total variance (PC1 = 40.4%; PC2 = 37.1%) (Figure 3B). As in the surface layer, NF clustered with SOC, LC, POC, MAOC, HS, and CMI, along with Bglu, ARYL, and fulvic and humic acids carbon (FAC and HAC), highlighting the persistence of organic matter quality and enzymatic activity at greater depths (Figure 3B).

The PB1 and PB2 systems showed a positive association with SOC, LC, CMI, Ca, Mg, and Cu, while CBC aligned with clay, Fe, and silt, reinforcing their role in nutrient storage, organic total and fractions, and soil structural stability. Conversely, higher values of Na and EC were distant from organic carbon fractions and microbial indicators, reflecting chemical constraints likely associated with salinization and sodification. Guava–horticulture consortium (GHC), corn monoculture (CORN), and banana (BAN) systems were positioned predominantly in the lower quadrants of the biplot (Figure 3B), showing weak associations with key indicators of soil organic matter quality. Their spatial distribution shows a reduced linkage with enzymatic activities (β-glucosidase, arylsulfatase, and dehydrogenase) and microbial biomass carbon (MBC), suggesting limited biological functionality in the subsurface layer.

3.1.3 Hierarchical cluster analysis

The hierarchical cluster analysis (HCA) based on Ward’s method revealed distinct groupings of land-use systems for both evaluated depths, highlighting clear patterns of similarity in soil attributes related to chemical fertility, organic matter fractions, and biological indicators (Figure 4). At the surface layer (0-10 cm), three main clusters were identified (Figure 4A). The first cluster, composed exclusively of native forest (NF), stood apart from all other systems, reflecting its unique profile characterized by high organic carbon content, stable humic fractions, and elevated enzymatic activity, which together sustain superior soil quality under natural vegetation.

In the second cluster, the systems GHC, CORN, and BAN were grouped according to the following characteristics: lower SOC levels and reduced contents of both labile and recalcitrant carbon fractions. These findings highlight the degradation of soil organic matter. The third cluster comprised the corn-bean consortium (CBC) and pasture systems (PB1 and PB2), which exhibited closer similarity, likely due to higher nutrient availability, similar clay and silt contents, and intermediate levels of soil carbon. This suggests that grass-legume consortia and managed pastures promote a gradual decline in organic matter compared to other systems.

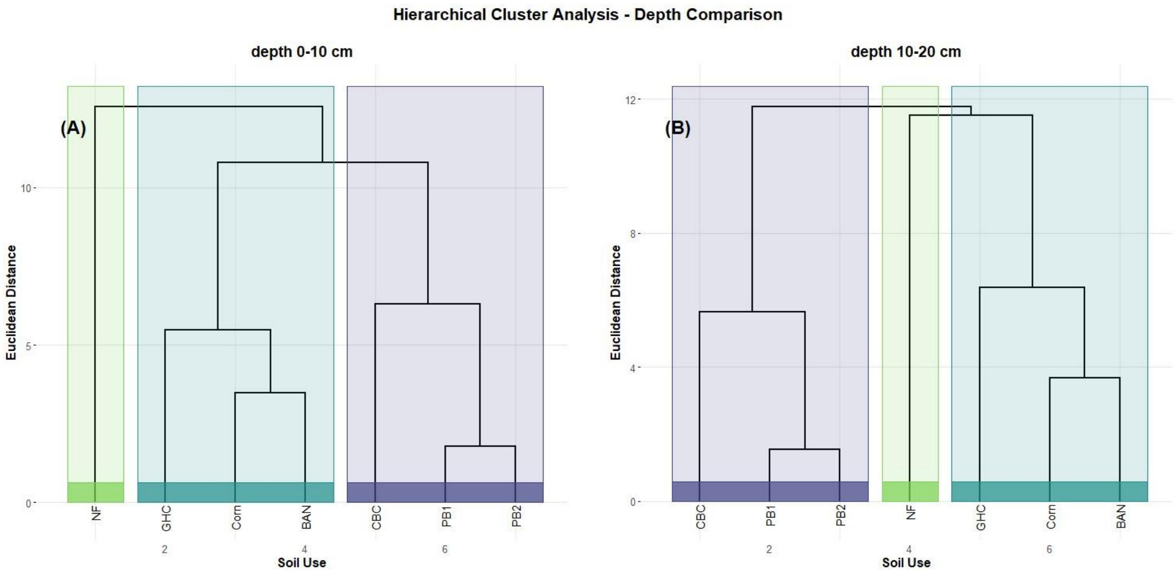

Figure 4. Hierarchical clustering dendrogram obtained using Ward's method for different land uses at depths of 0-10 cm (A) and 10-20 cm (B). Land use (blue): CBC= corn/bean consortium, CORN= corn monoculture; BAN= banana; GHC= guava-horticulture consortium; PB1 and PB2= pasture with *Urochloa mosambicensis* under dairy cattle grazing; NF= native forest (Caatinga preserved) in the municipality of Iguatu, Ceará state, Brazil. Source: Own authorship

At the 10-20 cm depth, although the arrangement of treatments across the three clusters shifted, the overall pattern remained consistent. The principal distinction observed pertained to a diminished Euclidean distance among PB1 and PB2, CBC, and NF, suggesting enhanced preservation of organic matter in deeper soil strata. This assertion is substantiated by elevated CMI values recorded under these management systems, especially pastures (Figure 4B). The third cluster included GHC, CORN, and BAN, mirroring their grouping in the surface layer and suggesting that these systems share similar subsurface constraints, such as reduced labile carbon fractions and lower microbial activity, which may limit long-term soil functionality.

3.2 Effects of land use on organic matter fractions, enzymatic activity, and soil fertility

The univariate analysis revealed significant differences ($p<0.05$) in chemical attributes across land-use systems and soil depths (Table 3). At the surface layer (0-10 cm), pH (mean=7.2) values were generally high and statistically similar among agricultural systems (CBC, CORN, BAN, GHC, PB1, PB2), all classified as slightly alkaline, whereas NF exhibited significantly lower pH (6.1), demonstrating more acidic conditions typical of preserved Caatinga soils. Electrical conductivity (EC) did not differ among systems, remaining at low levels, suggesting no immediate risk of salinity at this depth (Table 3).

Phosphorus (P) showed no statistical differences, but numerical means were higher in CBC and PB1 (22.6 mg dm^{-3}) compared to NF (15.2 mg dm^{-3}). Exchangeable sodium (Na) was significantly lower in NF and GHC, while CBC, CORN, and PB1 maintained the highest values. Potassium (K) was highest in CBC and NF (0.44 cmolc dm^{-3} and 0.31 cmolc dm^{-3}, respectively). Calcium (Ca) and magnesium (Mg) were markedly higher in CBC, PB1, and PB2, with values surpassing 13.0 cmolc dm^{-3} for Ca and 8.3 cmolc dm^{-3} for Mg, contrasting with the reduced contents in GHC and BAN. Micronutrient analysis revealed significantly higher copper (Cu) in CBC, while Mn and Fe were elevated in CORN, BAN, and NF. Zinc (Zn) was highest in CBC, PB1, and PB2, with NF and the fruit-based systems (BAN, GHC) showing lower concentrations (Table 3).

In the subsurface layer (10-20 cm), pH values remained statistically similar among most systems, except for NF, which was significantly more acidic (pH=6.1). EC was highest in CBC, PB1, and PB2, while NF maintained the lowest values, demonstrating minimal salt accumulation under natural vegetation. Phosphorus concentrations were generally lower than in the surface layer, with BAN, PB1, and PB2 presenting significantly reduced levels (<10 mg dm^{-3}). Sodium followed a similar pattern to the surface, with highest levels in CBC and GHC and lowest in NF and BAN. Potassium was significantly higher in NF, while Ca and Mg again reached maximum levels in CBC, PB1, and PB2, and minimum levels in BAN and GHC. For micronutrients, CBC maintained the highest Cu content, whereas CORN, BAN, and GHC showed reduced concentrations. Mn and Fe were elevated in CORN and BAN, while Zn remained highest in CBC, PB1, and PB2, consistent with the surface layer trend (Table 3).

Table 3. Analysis of the chemical attributes of soils under different types of use in the municipality of Iguatu, Ceará state, Brazil.

Soil use	pH	EC	P	Na	K	Ca	Mg	Cu	Mn	Fe	Zn
	H_2O	dS m^{-1}	mg dm³	cmolc dm³				mg dm³			
					0-10 cm						
CBC	7.3±0.04A	0.06±0.12A	22.6±2.3A	0.63±0.40A	0.44±0.04A	13.01±0.41A	8.36±0.55A	0.344±0.02A	1.487±0.05B	4.960±0.33A	0,65±0,05A
CORN	7.2±0.15A	0.06±0.00A	15.3±1.4A	0.66±0.08A	0.18±0.01B	8.25±0.78B	4.35±0.34B	0.110±0.01B	2.894±0.75A	1.660±0.05B	0,27±0,01B
BAN	7.1±0.02A	0.06±0.00A	18.9±1.8A	0.40±0.07B	0.12±0.03B	5.17±0.22C	2.99±0.11C	0.088±0.01B	2.488±0.62A	2.905±0.47B	0,27±0,01B
GHC	7.2±0.00A	0.04±0.02A	16.5±2.7A	0.20±0.04C	0.15±0.04B	3.78±0.26D	3.30±0.24C	0.075±0.01B	0.744±0.04B	2.355±0.63B	0.42±0.06B
PB1	7.2±0.04A	0.07±0.04A	22.6±3.5A	0.63±0.08A	0.17±0.02B	13.05±0.41A	8.66±0.55A	0.088±0.01B	1.379±0.11B	4.147±0.32A	0.69±0.014A
PB2	7.0±0.03A	0.08±0.03A	20,5±3.8A	0.60±0.05	0.20±0.04B	14.52±0.51A	9.02±0.69A	0.095±0.02B	1.396±0.23B	4.023±0.42A	0.526±0.10A
NF	6.1±0.11B	0.06±0.00A	15.2±2.7A	0.11±0.04C	0.31±0.83A	7.94±0.23B	4.93±0.55B	0.110±0.02B	0.765±0.07B	4.913±1.02A	0.34±0.04B
F	**32.1****	**20.0****	**15.6****	**20.8****	**33.2****	**25.6****	**30.1****	**92.2****	**8.1****	**6.2****	**9.2****
VC	**1.99**	**1.27**	**29.2**	**24.48**	**20.09**	**8.33**	**20.2**	**19.5**	**32.71**	**30.25**	**29.9**
					10-20 cm						
CBC	7.2±0.04A	0.17±0.02A	12.2±1.6A	0.62±0.09A	0.13±0.08B	12.93±0.29A	7.45±1.04A	0.328±0.01A	1.168±0.08B	3.403±0.21A	0.523±0.02A
CORN	6.8±0.06A	0.18±0.01A	15.0±2.2A	0.38±0.02B	0.14±0.01B	5.25±0.45B	3.08±0.57C	0.158±0.02B	3.357±0.19A	1.651±0.07B	0.176±0.01B
BAN	6.9±0.06A	0.18±0.05A	8.8±0.95B	0.25±0.03C	0.11±0.01B	3.52±0.02C	1.62±0.15D	0.089±0.01C	3.229±0.20A	1.733±0.24B	0.154±0.01B
GHC	7.4±0.00A	0.26±0.00A	16.5±1.16A	0.50±0.04A	0.15±0.04B	3.77±0.14C	2.08±0.17C	0.075±0.01C	0.744±0.04B	3.105±0.64A	0.366±0.09A
PB1	7.1±0.08A	0.28±0.02A	8.7±0.88B	0.40±0.09B	0.14±0.44B	12.31±0.83A	8.36±0.92A	0.088±0.01C	1.379±0.11B	3.397±0.89A	0.589±0.18A
PB2	7,0±0.05	0,29±0.03A	9.75±1.05B	0,42±0.02B	0.13±0.34B	12,58±0.96A	7,58±0.88A	0.161±0.01B	1.365±0.13B	3.952±0.91A	0.652±0.11A
NF	6.1±0.12B	0.06±0.00B	14.7±1.65A	0.11±0.04C	0.23±0.74A	7.70±0.62B	4.58±0.30B	0.177±0.01B	1.378±0.42B	1.577±0.43B	0.199±0.02B
F	**33.2****	**22.38****	**4.58***	**8.75****	**10.82****	**72.28***	**37.71***	**131.5****	**15.19****	**1.34***	**7.21****
VC	**1.88**	**24.14**	**29.2**	**39.75**	**21.02**	**13.2**	**20.8**	**13.2**	**26.78**	**62.5**	**50.6**

Mean±standard error of the mean. Means followed by the same letter do not differ by the Scott-Knott test (p<0.05). F= F test (significance ** and *, 1 and 5%, respectively). CV = coefficient of variation. pH = potential hydrogen, EC = electrical conductivity, P = phosphorus, Na = sodium, K = potassium, Ca = calcium, Mg = magnesium, Cu = copper, Fe = iron, Mn = manganese, Zn = zinc. CBC= corn/bean consortium, CORN= corn monoculture; BAN= banana; GHC= Guava-horticulture consortium; PB1 and PB2= pasture with *Urochloa mosambicensis* under dairy cattle grazing; NF= native forest (Caatinga preserved). Source: Own authorship

Soil organic carbon (SOC) content across land uses ranged from 22.6 to 11.0 g kg^{-1} at 0-10 cm and from 14.7 to 4.1 g kg^{-1} at 10-20 cm (Table 4). In the preserved Caatinga forest (NF), SOC contents were 31.3 and 16.1 g kg^{-1} in the respective layers. These results show that converting native vegetation to agricultural use in the semi-arid region of Ceará led to an average -47% (0-10 cm) and -39% (10-20 cm) reduction in SOC, regardless of the cropping system. The greatest losses of SOC occurred in soils under GHC (-68% and -75%), followed by CORN (-65% and -42%) and BAN (-56% and -68%). The smallest reductions were observed in soils under PB2 (28% and 9%), PB1 (-31% and -11%), CBC (-36% and -29%) for the 0–10 cm and 10–20 cm layers, respectively.

Intensive land use led to average reductions of -65%, -57%, and -55% in labile carbon (LC), microbial biomass carbon (MBC), and particulate organic carbon (POC) fractions, respectively, at the 0–10 cm depth, and reductions of -22%, -57%, and -58% at the 10–20 cm depth, relative to native forest. The CORN system exhibited the most severe depletion of labile carbon pools, with declines of -94%, -69%, and -75% at 0–10 cm, and -94%, -51%, and -70% at 10–20 cm for POC, LC, and MBC, respectively. Soils under BAN and GHC also showed substantial losses in labile fractions, highlighting marked degradation of organic matter quality within these systems. In contrast, the pasture systems demonstrated greater stability in labile carbon fractions.

Table 4. Soil organic carbon content and carbon labile and recalcitrant fractions of soil organic matter under different land use types in the municipality of Iguatu, Ceará state, Brazil.

Soil use	SOC	LC	MBC	POC	MAOC	FA	HA	H	HS	CMI
	g kg^{-1}		µg g^{-1} de C				g kg^{-1}			
					0-10 cm					
CBC	19.9±0.4B	1.47±0.04B	71.50±2.89C	0.46±0.03D	19.42±0.40B	1.70±0.09B	2.99±0.09B	18.57±1.24B	23.26±1.34B	55±3.7B
CORN	11.0±1.0C	0.66±0.02C	74.33±7.52C	0.13±0.01E	10.92±1.02C	0.89±0.09C	0.81±0.16D	7.24±0.24D	8.94±0.20E	23±0.6E
BAN	13.9±0.4C	0.68±0.00C	113.07±14.49B	0.46±0.02D	13.39±0.42C	1.91±0.23B	1.75±0.16C	11.94±0.22C	15.59±0.43D	25±1.1E
GHC	10.0±0.8C	0.67±0.04C	127.27±4.95B	0.59±0.07C	9.44±0.73C	1.11±0.17C	1.10±0.08D	7.71±0.23D	9.91±0.13E	26±2.1E
PB1	21.5±0.8B	0.95±0.04B	121.21±3.06B	1.86±0.04B	19.62±0.75B	1.96±0.22B	3.59±0.27B	12.94±0.97C	18.49±1.12C	53±2.4B
PB2	22.6±1.1B	1.12±0.06B	123.25±4.06B	1.96±0.05B	20.59±0.66B	1.98±0.21B	3.12±0.24B	13.54±0.88C	18.65±1.24C	62.8±2.8B
NF	31.3±2.2A	2.61±0.12A	241.77±8.34A	2.05±0.04A	29.21±2.26A	4.58±0.69A	5.40±0.41A	23.57±0.41A	33.55±0.72A	100.0A
F	**47.82****	**55.79****	**40.29****	**304.86****	**40.32****	**19.87****	**50.52****	**60.92****	**100.1****	**31.6****
VC	**11.86**	**15.38**	**12.95**	**9.11**	**10.56**	**31.17**	**16.82**	**13.63**	**10.01**	**29.51**
					10-20 cm					
CBC	11.4±0.5B	0.72±0.07C	53.45±4.13C	0.40±0.03C	11.03±0.53B	0.76±0.03B	1.00±0.09C	10.91±1.24B	12.67±1.21C	71±7.2C
CORN	9.4±0.9C	0.49±0.07D	57.34±6.27C	0.11±0.00C	9.26±0.85C	0.57±0.05C	0.27±0.03E	7.28±0.35C	8.12±0.32D	48±6.9D
BAN	5.1±0.6D	0.52±0.04D	91.14±6.56B	0.27±0.06C	4.84±0.60D	0.46±0.03C	1.09±0.08C	5.16±0.17D	6.71±0.11E	54±4.5D
GHC	4.1±0.1D	0.58±0.02D	103.50±5.83B	0.37±0.05C	3.72±0.34D	0.38±0.05C	1.54±0.13B	3.63±0.25D	5.56±0.36E	63±3.4C
PB1	14.3±1.3A	1.20±0.06A	93.28±2.09B	1.60±0.09B	12.73±1.27A	1.00±0.07B	0.61±0.11D	13.31±1.24A	14.92±1.29B	121±8.5A
PB2	14.7±1.8A	1.22±0.09A	95.24±1.88B	1.66±0.12B	12.99±1.07A	1.02±0.09B	0,62±0.09D	13.02±0.94A	14,67±1.34B	137±7.8A
NF	16.1±0.4A	1.01±0.02B	191.07±7.23A	1.78±0.09A	14.35±0.35A	3.53±0.22A	5.64±0.28A	8.09±0.54C	17.25±0.65A	100.0B
F	**39.3****	**32.4****	**39.9****	**113.2****	**30.07****	**108.95***	**180.26****	**19.01****	**33.66****	**29.2****
VC	**11.78**	**12.84**	**13.68**	**17.96**	**12.84**	**18.96**	**17.49**	**16.82**	**13.09**	**29.35**

Mean±standard error of the mean. Means followed by the same letter do not differ by the Scott-Knott test ($p<0.05$). F= F test (significance ** and *, 1 and 5%, respectively). CV = coefficient of variation. SOC= soil organic carbon, LC= labile carbon, MBC= microbial biomass carbon, POC= particulate organic carbon, FA= fulvic acid, HA= humic acid, H=Humin, HS=humic substances, CMI=carbon management index. CBC= corn/bean consortium, CORN= corn monoculture; BAN= banana; GHC= Guava-horticulture consortium; PB1 and PB2= pasture with *Urochloa mosambicensis* under dairy cattle grazing; NF= native forest (Caatinga preserved). Source: Own authorship

Soils under preserved native forest (NF) exhibited the highest enzymatic activity among all land-use systems. β-Glucosidase (BG) activity reached 286 and 246 mg pNP g^{-1} soil h^{-1}, arylsulfatase (ARS) activity reached 35 and 20 mg pNP g^{-1} soil h^{-1}, and dehydrogenase (DHA) activity reached 189 and 177 µg TPF g^{-1} soil h^{-1} at depths of 0–10 cm and 10–20 cm, respectively (Figures 5 and 6). Intensive land use markedly suppressed enzymatic activity, with the most pronounced reductions observed for ARS. On average, enzymatic activities decreased by 61%, 58%, and 74% at 0–10 cm, and by 69%, 58%, and 68% at 10–20 cm for BG, DHA, and ARS, respectively, regardless of cropping system. However, the magnitude of these reductions varied notably among land uses.

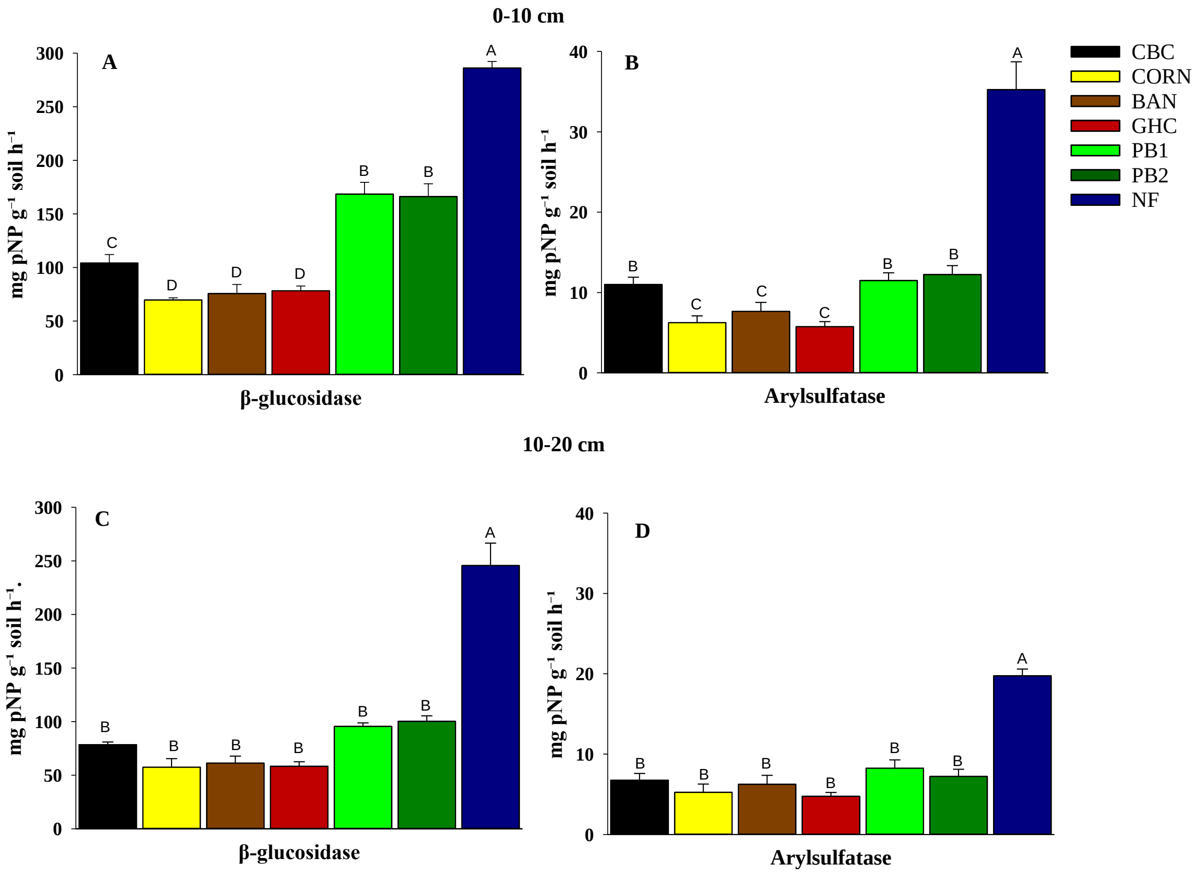

Figure 5. Enzymatic activity β-Glucosidase and arylsulfatase among all land uses at depths of 0-10 and 10-20 cm. Sites: corn-bean consortium (CBC); corn monoculture (CORN); banana cultivation (BAN) (*Musa* spp.); guava-horticulture consortium (GHC); pasture with *Urochloa mosambicensis* under dairy cattle grazing (PB1 and PB2); native forest (Caatinga). Source: Own authorship

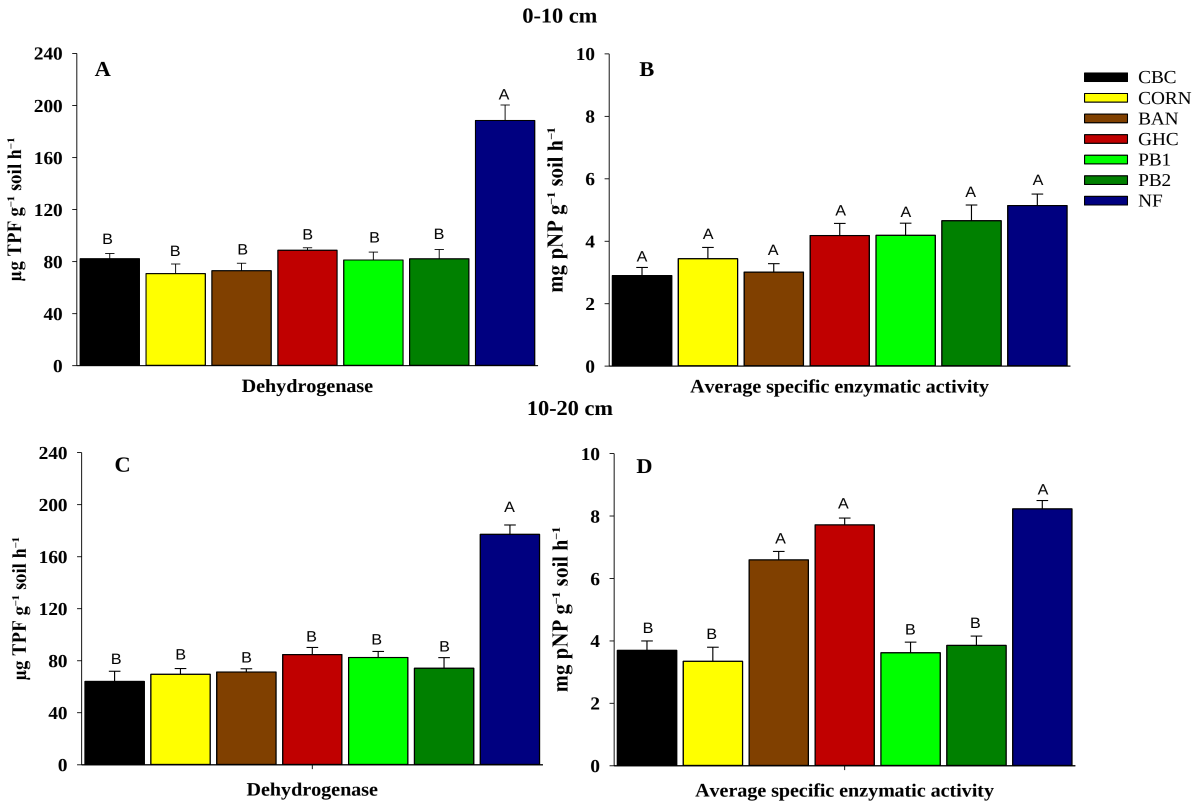

Figure 6. Enzymatic activity dehydrogenase and average specific enzymatic activity (ASEA) among all land uses at depths of 0-10 and 10-20 cm. Sites: corn-bean consortium (CBC); corn monoculture (CORN); banana cultivation (BAN) (*Musa* spp.); guava-horticulture consortium (GHC); pasture with *Urochloa mosambicensis* under dairy cattle grazing (PB1 and PB2); native forest (Caatinga). Source: Own authorship

Declines greater than 70% in BG activity were recorded under CORN, BAN, and GHC systems at both depths. DHA activity dropped by more than 60% in soils under CORN and BAN cultivation. The most substantial ARS losses, exceeding 80% at 0–10 cm and 70% at 10–20 cm, were observed under CORN and GHC, demonstrating severe disruption to sulfur cycling processes. Regarding average specific enzymatic activity (ASEA), the greatest reductions at 0–10 cm occurred under CBC and BAN, with declines of 44% and 41%, respectively. At 10–20 cm, the largest decreases were recorded in CBC and CORN, with reductions of 55% and 59%, respectively (Figure 6 B, D).

The highest carbon contents in the recalcitrant fractions of soil organic matter (SOM) were consistently observed in soils under native forest (NF). In the 0–10 cm layer, mineral-associated organic carbon (MAOC) and carbon associated with humic substances (HS) reached 29.2 g kg^{-1} and 33.5 g kg^{-1}, respectively, while in the 10–20 cm layer, they reached 14.4 g kg^{-1} and 17.4 g kg^{-1} (Table 4). When the humified SOM fractions were analyzed separately, Caatinga soils contained 4.6 and 3.7 g kg^{-1} of fulvic acid carbon (FA) and 5.4 and

5.6 g kg^{-1} of humic acid carbon (HA) at the 0–10 cm depth, as well as 23.6 and 8.1 g kg^{-1} of humin carbon (H) at the 10–20 cm depth (Table 4).

As with the labile fractions, MAOC and HS decreased sharply under intensive cropping systems such as GHC and CORN, with carbon losses exceeding 60%, particularly in the surface layer. The most pronounced declines among the humified fractions occurred in the soluble components (FA and HA), with reductions greater than 80% in soils under CORN and GHC. The humin fraction, representing the most stable organic carbon pool, also experienced substantial depletion, with losses of 68% and 67% under CORN and GHC, respectively, at 0–10 cm.

Assessing the degradation of both the quantity and quality of SOC in the native forest system (NF) revealed that all land-use systems, except for deep-layer pastures, exhibited Carbon Management Index (CMI) values below 100, highlighting varying degrees of organic matter degradation. The most degraded systems in the 0–10 cm layer were CORN (23), BAN (25), and GHC (26), reflecting substantial declines in both labile and recalcitrant carbon pools. In contrast, at 10–20 cm, pasture soils (PB1 and PB2) achieved a CMI of 121 and 137, surpassing the reference threshold, suggesting that these systems can enhance carbon quality in deeper horizons under semi-arid conditions. All other cropping systems, however, remained below 100 at this depth, with the lowest values observed under CORN (48) and BAN (54) (Table 4).

3.3 Soil Micromorphology

The microstructure analysis of soils using scanning electron microscopy (SEM) revealed distinct structural features across the different land-use systems. In soil under CBC, silt particles appeared as both rounded and angular structures, whereas clay particles displayed predominantly lamellar forms. Fine capillary roots from corn and beans were observed penetrating the soil matrix, with organic matter particles adhering to their surfaces. Fungal structures, visible as thin hyphal filaments, were also detected around the roots and between soil particles, contributing together with the root system to the stabilization and aggregation of soil particles (Figure 7 – CBC).

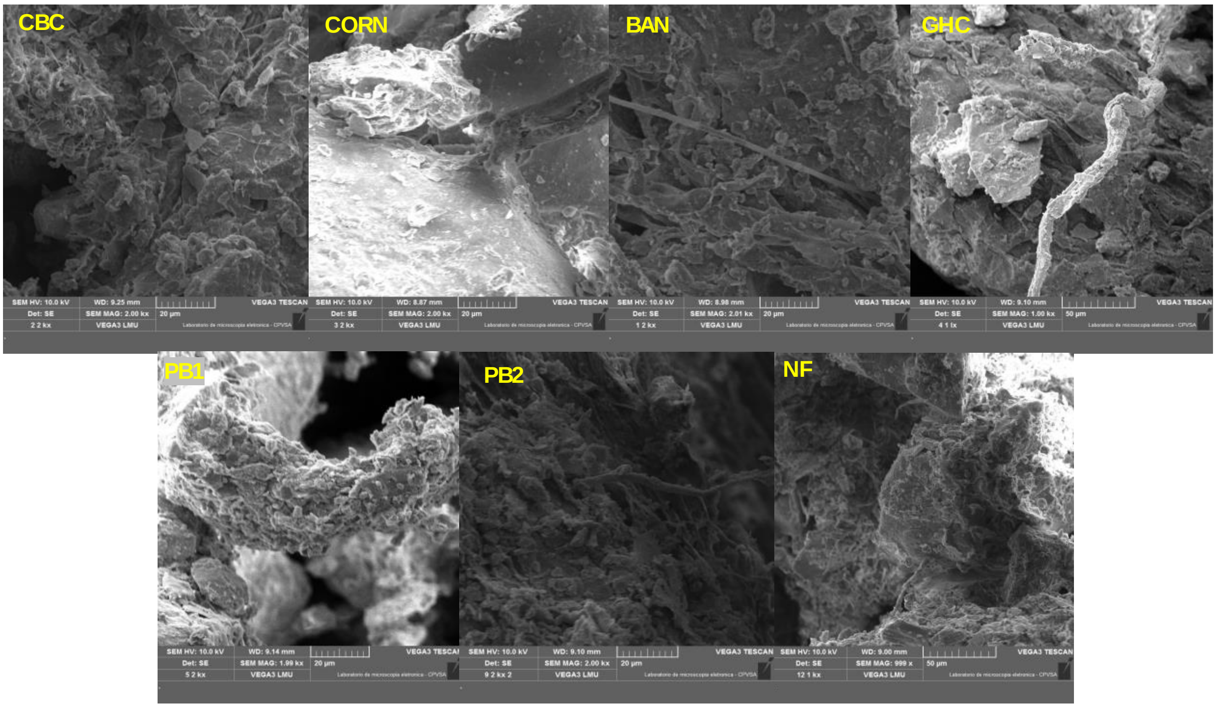

Figure 7. Scanning electron microscopy (SEM) micrographs under different land use types in the municipality of Iguatu, Ceará state, Brazil. CBC= corn/bean consortium, CORN= corn monoculture; BAN= banana; GHC= guava-horticulture consortium; PB1 and PB2= pasture with *Urochloa mosambicensis* under dairy cattle grazing; NF= native forest (Caatinga preserved). Source: Own authorship

In soil under CORN, sand particles appeared as large to medium structures with irregular and porous surfaces embedded within the soil matrix. A lack of cohesion among particles was evident, and only a few fine roots were observed interspersed within the matrix (Figure 7 – CORN). In soils under BAN, large irregular sand particles were also present; however, smaller and irregular silt particles were additionally observed, along with a sparse distribution of fine root hairs (Figure 7 – BAN). In soils under GHC, a more uniform distribution of sand particles was noted, with smaller particle sizes favoring improved arrangement and connectivity with thicker roots (Figure 7 – GHC).

In soils under PB1 and PB2, SEM micrographs revealed smaller, denser, and more compact aggregates, attributable to the higher proportion of fine particles (silt and clay). The images showed laminar and granular structures that may represent secondary aggregates, distinguished by the presence of organic material (e.g., root hairs and fungal hyphae) forming coatings around aggregates (Figure 7 – PB1; PB2).

In soils under NF, fragmented structures were dominated by coarse particles, primarily fine to medium sand with irregular or faceted surfaces. Notably, interactions between organic matter (root hairs, roots, and fungi) and the mineral components of the soil were evident.

Organic particles adhered to mineral surfaces, either forming coatings or directly interacting with aggregates. The presence of fungal hyphae and rounded structures resembling bacterial colonies was also observed, highlighting an active biological presence in these systems (Figure 7 – NF).

4 DISCUSSIONS

The present study demonstrates that land-use change in the semi-arid region of Ceará profoundly alters soil organic matter (SOM) dynamics, enzymatic activity, and fertility attributes, with cascading implications for soil quality and ecosystem functioning. By integrating univariate and multivariate approaches with micromorphological evidence, the findings reveal that native forest systems maintain higher stability of carbon pools, greater enzymatic activity, and more favorable structural arrangements than agricultural systems. These results provide new insights into how intensive land use compromises carbon stabilization and nutrient cycling under fragile semi-arid environments.

Soils under native vegetation (Caatinga) exhibited higher levels of total and recalcitrant carbon fractions, as well as elevated enzymatic activity, reflecting the role of natural vegetation in promoting organic matter accumulation and stabilization. The strong association between SOC, microbial biomass, and humic fractions highlights the synergistic effect of organic inputs, microbial activity, and organo-mineral interactions in sustaining soil quality (Soares et al., 2025; Fernandes et al., 2025; Lehmann & Kleber, 2015). Similar findings have been reported in other semi-arid ecosystems, where undisturbed soils showed greater stocks of stable carbon and microbial functionality compared to agricultural soils (Soares et al., 2025; Fernandes et al., 2025; Medeiros et al., 2025). The micromorphological evidence further confirmed that root residues, fungal hyphae, and mineral particles act as binding agents in forest soils, supporting aggregate stability and long-term carbon protection (Fernandes et al., 2025).

Regardless of crop type, soil organic carbon (SOC) exhibited substantial declines of -47% and -39% at depths of 0–10 cm and 10–20 cm, respectively. These findings underscore the pronounced vulnerability of SOC stocks in managed semiarid soils, where cultivation practices accelerate organic matter depletion. Medeiros et al. (2020) demonstrated that conventional annual cropping systems can reduce SOC by 13–26%, depending on land-use duration and soil depth. Similarly, Soares et al. (2025) reported SOC losses ranging from 36% to 56% following the conversion of native vegetation to cultivated areas at 0–30 cm.

Furthermore, a meta-analysis by Medeiros et al. (2025) across semiarid regions of Brazil confirmed that conversion of native ecosystems to conventional agriculture resulted in an average SOC decline of 10.96%. Collectively, these studies reinforce that land-use intensification significantly undermines soil carbon storage, with potential consequences for soil fertility, ecosystem resilience, and carbon sequestration capacity under semiarid conditions.

In contrast, soils managed under intensive systems such as corn monoculture (CORN), guava-horticulture consortium (GHC), and banana (BAN) cultivation, exhibited substantial depletion of both labile (POC, LC, MBC) and recalcitrant fractions (HA, FA, H). The marked reductions in enzymatic activities, particularly arylsulfatase and β-glucosidase, suggest functional suppression of microbial communities, likely driven by reduced litter input, soil disturbance, and lower soil fertility associated with lower clay content. These factors accelerate organic matter mineralization and destabilization, affecting soil health, as reported in semi-arid agroecosystems (Maia et al., 2025; Vasconcelos et al., 2025; Okolo et al., 2020). Such degradation is critical since enzymatic activity directly regulates nutrient turnover and soil resilience under climatic stressors (Liang et al., 2025; Mahalingam et al., 2025; Khan et al., 2025). The coarse texture and low specific surface area, especially in GHC, impede the adsorption of organic matter to soil colloids and microbial decomposition products. Greater SOC losses in more sandy soils under agriculture have also been documented in other semiarid regions of Brazil (Gava *et al.*, 2022; Medeiros; Soares; Maia, 2022; Medeiros *et al.*, 2023).

The findings were corroborated by PCA and cluster analysis, which demonstrated that intensive systems (CORN, BAN, GHC, and PC) exhibited lower levels of carbon fractions and enzymatic activity, while native forest, CBC, PB1, and PB2 systems formed distinct groups with higher quality attributes.

The functional proximity of CBC and PB2 to native vegetation suggests a greater capacity to protect organic matter from decomposition and to sustain higher soil fertility, due to organic inputs, active root systems, and the flood irrigation management system. Being located near the margins of the Orós Reservoir and subjected to flood irrigation, the accumulation of soil organic matter (SOM) tends to be enhanced by hydrological and biogeochemical processes that simultaneously promote the deposition of organic residues and reduce their decomposition. Periodic flooding facilitates the deposition of fine sediments enriched with plant residues and nutrients, creating conditions in which fresh litter and root exudates are continuously incorporated into the soil matrix (Wu et al., 2023; Fan et al., 2024).

At the same time, water saturation limits oxygen availability, constraining microbial activity and slowing the mineralization of organic compounds (Li et al., 2024). This dual mechanism, constant organic matter inputs coupled with reduced decomposition, results in greater carbon stabilization in these soils. Moreover, sediment deposition during flood events acts as a protective layer, physically occluding organic particles within aggregates and thereby enhancing long-term carbon persistence (Li et al., 2024; Sun et al., 2024). Supporting this evidence, Sun et al. (2024) reported a 15% increase in SOC stocks under flood irrigation compared to sprinkler and drip irrigation systems.

Pasture systems (PB1 and PB2) were consistently associated with higher levels of both labile and recalcitrant carbon fractions, greater enzymatic activity (DHA, ARYL, and β-glu), and superior carbon management index (CMI) values compared to fruit and grain monocultures. At 10–20 cm depth, CMI values reached 121 and 137 for PB1 and PB2, respectively, likely reflecting the contribution of increased belowground biomass. This relative resilience can be attributed to continuous root inputs, organic exudates, and the reduced soil disturbance inherent to grazing management, all of which stimulate microbial activity and promote aggregate formation. Moreover, scanning electron microscopy (SEM) imaging revealed a strong correlation between soil microstructure and the presence of roots and fungal hyphae, which play a critical role in aggregate formation and physical stabilization. Both consortium and pasture systems exhibited a higher frequency of aggregated particles with organic matter adhered to mineral matrices, providing evidence of biologically driven physical aggregation (Li, Chen & Leung, 2024; Ren et al., 2022; Kihara et al., 2012).

Jiang *et al*. (2020), in a meta-analysis of 122 studies, reported that pasture soils often show a shift in carbon input allocation, promoting subsoil C accumulation and compensating for surface C losses due to grazing. In northeastern Brazil, intensive grazing by cattle and goats has been shown to significantly reduce SOC in the top 5 cm, while having negligible effects in deeper layers (Schulz *et al.*, 2016). The SOC reduction in the 0–10 cm layer may be related to decreased aboveground net primary productivity, reduced biomass, and lower soil moisture levels (Bagchi; Ritchie, 2010; Jiang *et al.*, 2020; Yan *et al.*, 2018).

The observed reduction in enzymatic activity in cultivated areas (CORN, BAN, and GHC), particularly arylsulfatase and β-glucosidase, reflects a loss of biological functionality and nutrient cycling capacity. β-glucosidase is a rate-limiting enzyme in microbial cellulose degradation, critical for converting cellulose into glucose, a key carbon source for soil microorganisms (Adetunji *et al.*, 2017; Daunoras; Kačergius; Gudiukaitė, 2024). Arylsulfatases catalyze the release of SO_4^{2-} from sulfate esters (Kunito et al., 2022), and their activity is largely governed by the availability of carbon sources and SOC decomposition (Meena; Rao, 2021). These enzymes exhibit sensitivity to practices of residue removal, thereby underscoring their function in the decomposition of organic matter and the release of essential nutrients, including sulfur and glucose (Adetunji et al., 2017; Daunoras; Kačergius; Gudiukaitė, 2024; Meena; Rao, 2021). The strong positive correlations between enzymatic activity and labile organic fractions (LC, POC, and MBC) reaffirm the essential role of microbial communities and organic residue in sustaining soil health.

Furthermore, the association of SOC with both labile (LC, POC, MBC) and recalcitrant (MAOC and HS) fractions suggests that soil carbon quality depends not only on total quantity but also on the biochemical stability of its compartments (Lehmann et al., 2020; Sainepo; Gachene; Karuma, 2018). Considering projected global aridification trends (Naorem et al., 2023), the findings of this study provide robust evidence for the urgent need to adopt soil management practices centered on plant diversity, organic residue return, and structural conservation. Such strategies not only mitigate degradation but also promote soil multifunctionality and contribute to achieving several Sustainable Development Goals (SDGs 2, 13, and 15).

5 CONCLUSIONS

This study demonstrated that intensive land use in the Brazilian semiarid region, particularly under conventional agricultural systems with low crop diversity and residue removal, significantly compromises soil organic carbon (SOC) stocks, enzymatic activity, and the stability of organic matter fractions. SOC losses of up to 75%, especially within labile and recalcitrant fractions, combined with declines in the activity of key enzymes such as β-glucosidase and arylsulfatase, reveal severe functional soil degradation resulting from simplified and mechanized agricultural practices. In contrast, grass-legume consortium systems and managed pastures with organic residue return exhibited greater edaphic resilience, as evidenced by higher carbon management index (CMI) values, increased biological activity, and improved micro aggregate structure.

Integrating multivariate analyses, micromorphological observations, and assessments of chemical and organic fractions provided a comprehensive understanding of soil multifunctionality. This approach also highlighted the critical role of interactions between soils and agricultural systems. In more diversified systems, the contributions of fine roots, fungal hyphae, and stable aggregates reinforce the biological mechanisms underlying carbon protection and soil quality maintenance. These findings suggest that increasing agricultural productivity without considering organic matter management and soil biodiversity conservation can result in irreversible losses in ecosystem functionality, especially in sandy soils.

In the context of accelerating global aridification, the implications of this study extend beyond the Brazilian semiarid region to other areas vulnerable to desertification. The adoption of management systems based on plant diversity, organic residue retention, and reduced soil disturbance is imperative to mitigate degradation, promote edaphic resilience, and advance progress toward Sustainable Development Goals (SDGs 2, 13, and 15). It is recommended that future research place a premium on long-term temporal assessments and incorporate functional microbial indicators with a view to validating the stability of carbon stocks and their adaptive capacity under changing climate conditions.

REFERENCES

ABRAR, M. M. *et al.* Organic carbon sequestration in global croplands: evidenced through a bibliometric approach. **Frontiers in Environmental Science**, [*s. l.*], v. 13, p. 1495991, 2025. Disponível em: https://www.frontiersin.org/journals/environmental-science/articles/10.3389/fenvs.2025.1495991/full. Acesso em: 15 maio 2025.

ADETUNJI, A. T. *et al.* The biological activities of β-glucosidase, phosphatase and urease as soil quality indicators: a review. **Journal of Soil Science and Plant Nutrition**, [*s. l.*], v. 17, n. 3, p. 794–807, 2017. Disponível em: http://www.scielo.cl/scielo.php?script=sci_abstract&pid=S0718-95162017000300018&lng=es&nrm=iso&tlng=en. Acesso em: 18 maio 2025.

AHMAD, A. *et al.* Long-term raw crop residue but not burned residue incorporation improved soil multifunctionality in semi-arid agroecosystems. **Soil and Tillage Research**, [*s. l.*], v. 240, p. 106073, 2024. Disponível em: https://www.sciencedirect.com/science/article/pii/S0167198724000746. Acesso em: 15 maio 2025.

ANDRADE, E. M. D. *et al.* Hydrological responses of a watershed to vegetation changes in a Tropical Semiarid Region. **Revista Caatinga**, [*s. l.*], v. 31, p. 161–170, 2018. Disponível em: https://www.scielo.br/j/rcaat/a/3Q5zg5VFRhLYknGtnrxfVyM/?lang=en. Acesso em: 16 maio 2025.

BAGCHI, S.; RITCHIE, M. E. Introduced grazers can restrict potential soil carbon sequestration through impacts on plant community composition. **Ecology Letters**, [*s. l.*], v. 13, n. 8, p. 959–968, 2010. Disponível em: https://onlinelibrary.wiley.com/doi/abs/10.1111/j.1461-0248.2010.01486.x. Acesso em: 18 maio 2025.

BLAIR, G. J.; LEFROY, R. D. B.; LISLE, L. Soil carbon fractions based on their degree of oxidation, and the development of a carbon management index for agricultural systems. **Australian Journal of Agricultural Research**, [*s. l.*], v. 46, n. 7, p. 1459–1466, 1995. Disponível em: https://eurekamag.com/research/002/959/002959232.php. Acesso em: 24 jun. 2024.

CAMBARDELLA, C. A.; ELLIOTT, E. T. Particulate Soil Organic-Matter Changes across a Grassland Cultivation Sequence. **Soil Science Society of America Journal**, [*s. l.*], v. 56, n. 3, p. 777–783, 1992. Disponível em: https://onlinelibrary.wiley.com/doi/abs/10.2136/sssaj1992.03615995005600030017x. Acesso em: 24 jun. 2024.

CASIDA, L. E., Jr.; KLEIN, D. A.; SANTORO, T. Soil Dehydrogenase Activity. **Soil Science**, [*s. l.*], v. 98, p. 371–376, 1964. Disponível em: https://ui.adsabs.harvard.edu/abs/1964SoilS..98..371C. Acesso em: 16 maio 2025.

CHAER, G. M. *et al.* Evaluating C trends in clayey Cerrado Oxisols using a four-quadrant model based on specific arylsulfatase and β-glucosidase activities. **Applied Soil Ecology**, [*s. l.*], v. 183, p. 104742, 2023. Disponível em: https://www.sciencedirect.com/science/article/pii/S0929139322003584. Acesso em: 16 maio 2025.

DAUNORAS, J.; KAČERGIUS, A.; GUDIUKAITĖ, R. Role of Soil Microbiota Enzymes in Soil Health and Activity Changes Depending on Climate Change and the Type of Soil Ecosystem. **Biology**, [*s. l.*], v. 13, n. 2, p. 85, 2024. Disponível em: https://www.mdpi.com/2079-7737/13/2/85. Acesso em: 16 maio 2025.

Dubreuil, V., Fante, K. P., Planchon, O., & Sant'anna Neto, J. L. (2019). Climate change evidence in Brazil from Köppen's climate annual types frequency. International Journal of Climatology, 39(3), 1446-1456. https://doi.org/10.1002/joc.5893

Dzvene, A. R. *et al.* A scoping review on challenges and measures for climate change in arid and semi-arid agri-food systems. **Discover Sustainability** v. 6, p.151, 2025. Disponível em: https://doi.org/10.1007/s43621-025-00945-z

EIVAZI, F.; TABATABAI, M. A. Glucosidases and galactosidases in soils. **Soil Biology and Biochemistry**, [*s. l.*], v. 20, n. 5, p. 601–606, 1988. Disponível em: https://www.sciencedirect.com/science/article/pii/0038071788901411. Acesso em: 16 maio 2025.

ELHADDAD, F. *et al.* Alternative Cover Crops and Soil Management Practices Modified the Macronutrients, Enzymes Activities, and Soil Microbial Diversity of Rainfed Olive Orchards (cv. Chetoui) under Mediterranean Conditions in Tunisia. **Sustainability**, [*s. l.*], v. 16, n. 13, p. 5329, 2024. Disponível em: https://www.mdpi.com/2071-1050/16/13/5329. Acesso em: 16 maio 2025.

FAN, Y. *et al.* Development of soil quality assessment framework: A comprehensive review of indicators, functions, and approaches. **Ecological Indicators**, [*s. l.*], v. 172, p. 113272, 2025. Disponível em: https://www.sciencedirect.com/science/article/pii/S1470160X25002018. Acesso em: 19 maio 2025.

FAN, Y., *et al*. Assessing flood-depth effects on water quality, nutrient uptake, carbon sequestration, and rice yield cultivated on Histosols. **Climate Smart Agriculture**, v. 1, n. 1, 2024. 100005. Disponível em:https://doi.org/10.1016/j.csag.2024.100005

FERNANDES, B. C. C. **Characterization of eucalyptus wood-derived biochar and its effects on hexazinone behavior in soil**. 2019. 70 f. - Universidade Federal Rural do Semi-Árido, Mossoró/RN, 2019. Disponível em: https://repositorio.ufersa.edu.br/items/edc322fc-115a-44bb-acf9-b0d3fc390837. Acesso em: 16 maio 2025.

FERNANDES, J. E. G. *et al*. Soil functioning and interrelations with hydrophysical attributes and organic and microstructural fractions in soils under land uses in the Brazilian Semiarid. **Environmental Monitoring and**

Assessment, v. 197, n. 7, p. 730, 2025. Disponível em: https://doi.org/10.1007/s10661-025-14151-x

GAO, Y. *et al.* Achieving accurate regional carbon-sink accounting and its significance for “missing” carbon sinks. **The Innovation**, [*s. l.*], v. 5, p. 100552, 2024.

GARBA, I. I. *et al.* Optimizing ecosystem function multifunctionality with cover crops for improved agronomic and environmental outcomes in dryland cropping systems. **Agricultural Systems**, [*s. l.*], v. 214, p. 103821, 2024. Disponível em: https://www.sciencedirect.com/science/article/pii/S0308521X23002263. Acesso em: 15 maio 2025.

GARCÍA, A. C. *et al.* Structure–Property–Function Relationship of Humic Substances in Modulating the Root Growth of Plants: A Review. **Journal of Environmental Quality**, [*s. l.*], v. 48, n. 6, p. 1622–1632, 2019. Disponível em: https://onlinelibrary.wiley.com/doi/abs/10.2134/jeq2019.01.0027. Acesso em: 16 maio 2025.

GAVA, C. A. T. *et al.* Land-use change alters the stocks of carbon, nitrogen, and phosphorus in a Haplic Cambisol in the Brazilian semi-arid region. **Soil Use and Management**, [*s. l.*], v. 38, n. 1, p. 953–963, 2022. Disponível em: https://onlinelibrary.wiley.com/doi/abs/10.1111/sum.12716. Acesso em: 16 maio 2025.

HADDIX, M. L. *et al.* Climate, carbon content, and soil texture control the independent formation and persistence of particulate and mineral-associated organic matter in soil. **Geoderma**, [*s. l.*], v. 363, p. 114160, 2020. Disponível em: https://www.sciencedirect.com/science/article/pii/S0016706119323778. Acesso em: 15 maio 2025.

INMET. **Instituto Nacional de Meteorologia. Banco de Dados Meteorológicos para Ensino e Pesquisa (INMET/BDMEP). Dados históricos de precipitação**. [*S. l.*], 2024. Disponível em: https://portal.inmet.gov.br/servicos/bdmep-dados-hist%C3%B3ricos. Acesso em: 10 jun. 2024.

ISLAM, K. R.; WEIL, R. R. Microwave irradiation of soil for routine measurement of microbial biomass carbon. **Biology and Fertility of Soils**, [*s. l.*], v. 27, n. 4, p. 408–416, 1998. Disponível em: https://doi.org/10.1007/s003740050451. Acesso em: 16 maio 2025.

IUSS. **World reference base for soil resources 2022: International soil classification system for naming soils and creating legends for soil maps**. 4th edition. Vienna, Austria: International Union of Soil Sciences, 2022.

JIANG, Z.-Y. *et al.* Light grazing facilitates carbon accumulation in subsoil in Chinese grasslands: A meta-analysis. **Global Change Biology**, [*s. l.*], v. 26, n. 12, p. 7186–7197, 2020. Disponível em: https://onlinelibrary.wiley.com/doi/abs/10.1111/gcb.15326. Acesso em: 18 maio 2025.

JIN, Q. *et al.* Effect of soil degradation on the carbon concentration and retention of nitrogen and phosphorus across Chinese rice paddy fields. **CATENA**, [*s. l.*], v. 209, p. 105810, 2022. Disponível em: https://www.sciencedirect.com/science/article/pii/S0341816221006688. Acesso em: 15 maio 2025.

KHAN, M. T., *et al*. Climate, Soil, and Microbes: Interactions Shaping Organic Matter Decomposition in Croplands. **Agronomy,** v. 15, n. 8, p. 1928, 2025. Disponível em:https://doi.org/10.3390/agronomy15081928

KIHARA, J. *et al.* Soil aggregation and total diversity of bacteria and fungi in various tillage systems of sub-humid and semi-arid Kenya. **Applied Soil Ecology**, [*s. l.*], v. 58, p. 12–20, 2012. Disponível em: https://www.sciencedirect.com/science/article/pii/S0929139312000716. Acesso em: 18 maio 2025.

KOOCH, Y. *et al.* Investigation of the effects of the conversion of forests and rangeland to cropland on fertility and soil functions in mountainous semi-arid landscape. **CATENA**, [*s. l.*], v. 210, p. 105951, 2022. Disponível em: https://www.sciencedirect.com/science/article/pii/S0341816221008092. Acesso em: 15 maio 2025.

Kumar, L. *et al*. Climate change and future of agri-food production. In: Future foods. Cambridge, **Academic Press**, p. 49–79, 2022.

KUNITO, T. *et al.* **Microbial Synthesis of Arylsulfatase Depends on the Soluble and Adsorbed Sulfate Concentration in Soils**. Rochester, NY: Social Science Research Network, 2022. SSRN Scholarly Paper. Disponível em: https://papers.ssrn.com/abstract=4035157. Acesso em: 18 maio 2025.

LAL, R. *et al.* Soils and sustainable development goals of the United Nations: An International Union of Soil Sciences perspective. **Geoderma Regional**, [*s. l.*], v. 25, p. e00398, 2021. Disponível em: https://www.sciencedirect.com/science/article/pii/S2352009421000432. Acesso em: 15 maio 2025.

LASOTA, J. *et al.* Forest Humus Type Governs Heavy Metal Accumulation in Specific Organic Matter Fractions. **Water, Air, & Soil Pollution**, [*s. l.*], v. 231, n. 2, p. 80, 2020. Disponível em: https://doi.org/10.1007/s11270-020-4450-0. Acesso em: 15 maio 2025.

LEHMANN, J. *et al.* Persistence of soil organic carbon caused by functional complexity. **Nature Geoscience**, [*s. l.*], v. 13, n. 8, p. 529–534, 2020. Disponível em: https://www.nature.com/articles/s41561-020-0612-3. Acesso em: 19 maio 2025.

LEHMANN, J., KLEBER, M. The contentious nature of soil organic matter. **Nature**, v. 528, p. 60–68, 2015. Disponível em: https://doi.org/10.1038/nature16069.

LI, M.; CHEN, X. W.; LEUNG, A. K. Grass species and mycorrhizal fungi improved aggregate stability of compacted and vegetated soils. **Plant and Soil**, [*s. l.*], 2024. Disponível em: https://doi.org/10.1007/s11104-024-07038-2. Acesso em: 18 maio 2025.

LI, C.; HAN, W.; PENG, M. Effects of drip and flood irrigation on carbon dioxide exchange and crop growth in the maize ecosystem in the Hetao Irrigation District, China. J. **Arid Land,** v. 16, p. 282–297, 2024. Disponível em: https://doi.org/10.1007/s40333-024-0093-0

LIANG, X., *et al*. Integrated management practices foster soil health, productivity, and agroecosystem resilience. **Agronomy**, v. 15, n. 8, p. 1816, 2025. Disponível em: https://doi.org/10.3390/agronomy15081816

MAIA, S. M. F., *et al*. Deforestation and conventional agriculture's impact on soil quality in five Brazilian semi-arid soils. **Experimental Agriculture**, v. 61, p. e6, 2025. Disponível em: https://doi.org/10.1017/S0014479725000055.

MAHALINGAM, M., *et al*. Microbial-Mediated Carbon Processes in Soil Ecosystems: A Review on Climate Change Interactions. **Geomicrobiology Journal**, p. 1-21, 2025.

MEENA, A.; RAO, K. S. Assessment of soil microbial and enzyme activity in the rhizosphere zone under different land use/cover of a semiarid region, India. **Ecological Processes**, [*s. l.*], v. 10, n. 1, p. 16, 2021. Disponível em: https://doi.org/10.1186/s13717-021-00288-3. Acesso em: 18 maio 2025.

MEDEIROS, A. D. S.; SOARES, A. A. S.; MAIA, S. M. F. Soil carbon stocks and compartments of organic matter under conventional systems in brazilian semi-arid region. **Revista Caatinga**, [*s. l.*], v. 35, p. 697–710, 2022. Disponível em: https://www.scielo.br/j/rcaat/a/PfzsCwpL5zXBCvs3jTGsX8p/?lang=en. Acesso em: 16 maio 2025.

MEDEIROS, A. S. *et al.* Changes in soil organic carbon and soil aggregation due to deforestation for smallholder management in the Brazilian semi-arid region. **Geoderma Regional**, [*s. l.*], v. 33, p. e00647, 2023. Disponível em: https://www.sciencedirect.com/science/article/pii/S2352009423000433. Acesso em: 16 maio 2025.

MEDEIROS, A. S., *et al*. Differences in the storage of soil organic carbon in Brazil's agricultural land: A meta-analysis. **Catena**, v. 249, p.108680, 2025. Disponível em: https://doi.org/10.1016/j.catena.2024.108680

MEDEIROS, S. *et al.* Soil carbon losses in conventional farming systems due to land-use change in the Brazilian semi-arid region. **Agriculture, Ecosystems & Environment**, [*s. l.*], v. 287, p. 106690, 2020. Disponível em: https://www.sciencedirect.com/science/article/pii/S0167880919303068. Acesso em: 16 maio 2025.

NAOREM, A. *et al.* Soil Constraints in an Arid Environment—Challenges, Prospects, and Implications. **Agronomy**, [*s. l.*], v. 13, n. 1, p. 220, 2023. Disponível em: https://www.mdpi.com/2073-4395/13/1/220. Acesso em: 15 maio 2025.

NEHRANI, S. H. *et al.* Quantification of soil quality under semi-arid agriculture in the northwest of Iran. **Ecological Indicators**, [*s. l.*], v. 108, p. 105770, 2020. Disponível em: https://www.sciencedirect.com/science/article/pii/S1470160X19307642. Acesso em: 15 maio 2025.

Nketsang, T. S. *et al.* Understanding the Impacts of Rainfall Variability on Natural Forage–Livestock Dynamics in Arid and Semi-Arid Environments. **Applied Sciences**, v. 15, n. 7, p. 3918, 2025.

NN, A. *et al.* Understanding soil organic carbon dynamics in dryland ecosystems: A comprehensive review. **International Journal of Advanced Biochemistry Research**, [*s. l.*], v. 9, n. 1, p. 623–630, 2025. Disponível em: https://www.biochemjournal.com/archives/2025.v9.i1.3572/understanding-soil-organic-carbon-dynamics-in-dryland-ecosystems-a-comprehensive-review. Acesso em: 15 maio 2025.

OKOLO, C. C., *et al*. Assessing the sustainability of land use management of northern Ethiopian drylands by various indicators for soil health. **Ecological Indicators**, v. 112, p. 106092, 2020.

OLIVEIRA, F. É. R., *et al.* Droughts, livestock expansion, and Forest degradation: A 37-year assessment of landscape change in a semiarid municipality of Brazil. Science of The Total Environment, 986, 179733, 2025.

POEPLAU, C. *et al.* Isolating organic carbon fractions with varying turnover rates in temperate agricultural soils – A comprehensive method comparison. **Soil Biology and Biochemistry**, [*s. l.*], v. 125, p. 10–26, 2018. Disponível em: https://www.sciencedirect.com/science/article/pii/S0038071718302232. Acesso em: 15 maio 2025.

R CORE TEAM. **R: The R Project for Statistical Computing**. Versão 4.5.1. Vienna, Austria: R Foundation for Statistical Computing, 2021. Disponível em: https://www.r-project.org/. Acesso em: 24 jun. 2025.

RATHIKA, S. *et al.* Conservation agriculture: A pathway to achieving sustainable development goals. **Plant Science Today**, [*s. l.*], v. 12, n. sp1, p. 1–12, 2025. Disponível em: https://horizonepublishing.com/journals/index.php/PST/article/view/6268. Acesso em: 15 maio 2025.

REIS, A. P. L. *et al.* Levantamento florístico das espécies nativas da caatinga do estado do Ceará / Floristic survey of native species of caatinga in the state of Ceará. **Brazilian Journal of Animal and Environmental Research**, [*s. l.*], v. 4, n. 3, p. 3060–3078, 2021. Disponível em: https://ojs.brazilianjournals.com.br/ojs/index.php/BJAER/article/view/33146. Acesso em: 16 maio 2025.

REN, C. *et al.* The Changes in Soil Microorganisms and Soil Chemical Properties Affect the Heterogeneity and Stability of Soil Aggregates before and after Grassland Conversion.

Agriculture, [*s. l.*], v. 12, n. 2, p. 307, 2022. Disponível em: https://www.mdpi.com/2077-0472/12/2/307. Acesso em: 18 maio 2025.

SAINEPO, B. M.; GACHENE, C. K.; KARUMA, A. Assessment of soil organic carbon fractions and carbon management index under different land use types in Olesharo Catchment, Narok County, Kenya. **Carbon Balance and Management**, [*s. l.*], v. 13, n. 1, p. 4, 2018. Disponível em: https://doi.org/10.1186/s13021-018-0091-7. Acesso em: 19 maio 2025.

SANTOS, H. G. *et al.* **Sistema brasileiro de classificação de solos**. 5. ed. [*S. l.*]: Embrapa, 2018.

SCHULZ, K. *et al.* Grazing deteriorates the soil carbon stocks of Caatinga forest ecosystems in Brazil. **Forest Ecology and Management**, [*s. l.*], v. 367, p. 62–70, 2016. Disponível em: https://www.sciencedirect.com/science/article/pii/S0378112716300305. Acesso em: 18 maio 2025.

SHANG, C.; TIESSEN, H. Organic matter lability in a tropical oxisol: evidence from shifting cultivation, chemical oxidation, particle size, density, and magnetic fractionations:. **Soil Science**, [*s. l.*], v. 162, n. 11, p. 795–807, 1997. Disponível em: http://journals.lww.com/00010694-199711000-00004. Acesso em: 24 jun. 2024.

SOARES, S. D. C. *et al*. Soil organic matter fractions in the topsoil and subsoil of woody crop systems: Impact of reduced tillage plus cover crops under rainfed semi-arid Mediterranean conditions. **Agriculture, Ecosystems & Environment,** v. 393, p.109821, 2025. Disponível em: https://doi.org/10.1016/j.agee.2025.109821.

SOIL TAXONOMY, N. C. S. S. (NCSS). **Soil Taxonomy: A Basic System of Soil Classification for Making and Interpreting Soil Surveys**. 2. ed. [*S. l.*]: Soil Survey Staff, 1999. Disponível em: https://www.nrcs.usda.gov/sites/default/files/2022-06/Soil%20Taxonomy.pdf. Acesso em: 16 maio 2025.

SUN, W., *et al*. Response of soil carbon and nitrogen stocks to irrigation-A global meta-analysis. **Science of The Total Environment**, v. 957, p. 177641, 2024. Disponível em: https://doi.org/10.1016/j.scitotenv.2024.177641

SWIFT, R. S. Organic Matter Characterization. *In*: METHODS OF SOIL ANALYSIS. [*S. l.*]: John Wiley & Sons, Ltd, 1996. p. 1011–1069. Disponível em: https://onlinelibrary.wiley.com/doi/abs/10.2136/sssabookser5.3.c35. Acesso em: 16 maio 2025.

TABATABAI, M. A.; BREMNER, J. M. Arylsulfatase Activity of Soils. **Soil Science Society of America Journal**, [*s. l.*], v. 34, n. 2, p. 225–229, 1970. Disponível em: https://onlinelibrary.wiley.com/doi/abs/10.2136/sssaj1970.03615995003400020016x. Acesso em: 16 maio 2025.

TEXEIRA, P. C. *et al.* **Manual de métodos de análise de solos**. 3. ed. [*S. l.*]: Embrapa, 2017.

VASCONCELOS, G. X. D. M., *et al*. Organic fractions, microbial biomass carbon, and their interrelationships with structural attributes in different land uses. **Engenharia Agrícola**, v.

45,p. e20240189. Disponível em: http://dx.doi.org/10.1590/1809-4430-Eng.Agric.v45nespe120240189/2025

WU, Z., *et al*. Mapping soil organic carbon in floodplain farmland: Implications of effective range of environmental variables. **Land,** v. 12, n. 6, p. 1198, 2023. Disponível em: https://doi.org/10.3390/land12061198

YAN, Y. *et al.* Grazing modulates soil temperature and moisture in a Eurasian steppe. **Agricultural and Forest Meteorology**, [*s. l.*], v. 262, p. 157–165, 2018. Disponível em: https://www.sciencedirect.com/science/article/pii/S0168192318302326. Acesso em: 18 maio 2025.

YANG, J. *et al.* Can soil organic carbon sequestration and the carbon management index be improved by changing the film mulching methods in the semiarid region?. **Journal of Integrative Agriculture**, [*s. l.*], v. 23, n. 5, p. 1541–1556, 2024. Disponível em: https://www.sciencedirect.com/science/article/pii/S2095311923001363. Acesso em: 16 maio 2025.

YEOMANS, J. C.; BREMNER, J. M. A rapid and precise method for routine determination of organic carbon in soil. **Communications in Soil Science and Plant Analysis**, [*s. l.*], v. 19, n. 13, p. 1467–1476, 1988. Disponível em: https://doi.org/10.1080/00103628809368027. Acesso em: 16 maio 2025.

YING, D. *et al.* Soil properties and microbial functional attributes drive the response of soil multifunctionality to long-term fertilization management. **Applied Soil Ecology**, [*s. l.*], v. 192, p. 105095, 2023. Disponível em: https://www.sciencedirect.com/science/article/pii/S0929139323002937. Acesso em: 15 maio 2025.

ZHAO, Y. *et al.* A Global Meta-Analysis of Land Use Change on Soil Mineral-Associated and Particulate Organic Carbon. **Global Change Biology**, [*s. l.*], v. 31, n. 3, p. e70111, 2025. Disponível em: https://onlinelibrary.wiley.com/doi/abs/10.1111/gcb.70111. Acesso em: 15 maio 2025.

CHAPTER III: IRRIGATION IN SEMI-ARID REGIONS: PHYSICAL, CHEMICAL, AND MICROBIOLOGICAL QUALITY OF GROUNDWATER AND SURFACE WATER AS A CRITICAL FACTOR FOR SUSTAINABLE AGRICULTURE

ABSTRACT

Increasing anthropogenic pressures and climate change are exacerbating the risks of water quality degradation in semi-arid regions, particularly where surface and groundwater resources are heavily exploited for irrigation. This study assessed water quality across multiple sources in the semi-arid region of Ceará, Brazil, including wells tapping sedimentary basin and crystalline shield aquifers (G1–G4, G6, G8–G10), stretches of the Jaguaribe River (R7, R11–R13), and the Orós Reservoir (OR5). We performed a comprehensive characterization with physicochemical and microbiological analyses, supported by multivariate statistical techniques and irrigation suitability indices to elucidate seasonal hydrogeochemical processes. Parameters measured included electrical conductivity, total dissolved solids, major ions, heavy metals, *Escherichia coli*, and total coliforms. Statistical approaches included principal component analysis (PCA), hierarchical cluster analysis (HCA), Pearson correlation, and standard water quality indices for irrigation. Results revealed pronounced seasonal variability, with higher salinity, sodium (Na^+), chloride (Cl^-), and sodium adsorption ratio (SAR) levels during the dry season, reflecting the influence of evapoconcentration and lithology. PCA indicated SAR, Na^+, Mg^{2+}, Ca^{2+}, Cl^-, and HCO_3^- as the primary multivariate discriminants. Groundwater sources exhibited potential irrigation constraints due to salt accumulation and elevated concentrations of Fe and Mn. The rainy season led to dilution of dissolved constituents but an increase in microbial loads, with critical detection of coliforms and *Escherichia coli* in specific stretches of the Jaguaribe River. By integrating physicochemical, microbiological, statistical, and classification approaches, this study delivers robust scientific insights for water monitoring and sustainable resource use in semi-arid settings. The findings are crucial to enhancing water and agricultural security in the face of intensified land use and regional climate variability.

Keywords: Irrigation suitability indices; Semi-arid water management; Jaguaribe River; Orós Reservoir; salinity and sodicity risk; *Escherichia coli*.

1 INTRODUCTION

Irrigation represents a strategic pillar for agricultural production and food security in regions where low and irregular rainfall severely limits rainfed crop cultivation. In semi-arid regions worldwide, irrigation enables multiple production cycles throughout the year, mitigates climatic risks, stabilizes yields, and increases farmers' income. Moreover, irrigation plays a crucial role in promoting the productive inclusion of smallholders and sustaining the export capacity of large-scale producers, thereby fostering regional socio-economic development and supporting rural livelihoods (Zhang et al., 2024). However, its use must be guided by rigorous technical criteria and the rational management of water resources, incorporating robust monitoring methodologies to assess the quality of irrigation water sources (Javadi et al., 2025; Mitroi et al., 2025; Santos et al., 2025; Macedo et al., 2024; Vale et al., 2024).

Assessing water quality for irrigation is critical in semi-arid environments, where water scarcity constitutes one of the main constraints to agricultural sustainability. Global projections indicate that, by 2050, water demand could increase by 50% to 55%, while by 2030, nearly half of the world's population may face severe water scarcity (Alharbi et al., 2024; Abd-Elhamid et al., 2021; He et al., 2021). In the Brazilian semi-arid region, rainfall is projected to decrease by 10–20% by 2040, exacerbating water deficits, intensifying aridification and desertification processes, and increasing irrigation demand (Marengo et al., 2021; Gonçalves et al., 2022).

According to climate projections from the Intergovernmental Panel on Climate Change (IPCC), there is a consistent trend toward more frequent and intense droughts across different parts of the globe, particularly in areas already vulnerable to water scarcity (Allan et al., 2023). In this context, ensuring the quality of water sources used for irrigation is not only a technical requirement but also a strategic necessity to secure water resources and align agricultural systems with the United Nations 2030 Agenda for Sustainable Development Goals (SDG). Scientific evidence underscores that water security drives not only food security (SDG 2) and human health (SDG 3) but also strengthens water governance (SDG 6), biodiversity conservation (SDG 15), and climate change mitigation (SDG 13) (Alum et al., 2024; Ishaque et al., 2024).

In the northern portion of the Brazilian semi-arid region lies the state of Ceará, where approximately 92% of the territory is subject to arid conditions, extreme rainfall variability, prolonged and intense droughts, and high temperatures (Oliveira et al., 2025; Seigerman et al., 2024). Despite the adoption of water management strategies and hydraulic infrastructure, most municipalities in this state have not experienced significant reductions of climate vulnerability (Mitroi et al., 2025). One such municipality is Iguatu, where intensifying droughts have reduced water bodies and consequently increased irrigation demand to sustain agricultural production (Oliveira et al., 2025). Irrigation water demand in this area is met by groundwater, tributaries of the Jaguaribe River, and the Trussu and Orós Reservoirs, which are extensively exploited for local agriculture. Under these conditions, evaluating irrigation water quality becomes essential, as water scarcity imposes severe challenges to agricultural sustainability.

The presence of soluble salts, potentially toxic elements, and compounds that alter pH and electrical conductivity directly compromises the soil's physicochemical structure, restricts nutrient uptake by plants and interferes with their physiological development. Moreover, indices such as the Sodium Adsorption Ratio (SAR), Magnesium Adsorption Ratio (MAR), Magnesium Hazard (MH), Residual Sodium Carbonate (RSC), Soluble Sodium Percentage (SSP), Kelly's Index (KI), Permeability Index (PI), and total hardness can serve as effective indicators of water quality (Damiba et al., 2025; Mokhtar et al., 2022; Thapa et al., 2017; El Behairy et al., 2021). In this context, systematic monitoring of physicochemical parameters, water quality indices, and microbiological analyses becomes an indispensable strategy to ensure the rational and safe use of water resources, as well as to mitigate the risks of soil salinization and sodification.

As irrigated agriculture continues to expand as an alternative to overcome the climatic constraints of semi-arid regions, the use of low-quality water sources without adequate technical control may intensify irreversible degradation processes, jeopardizing agricultural productivity, food security, and the socio-economic resilience of rural communities. In addition, the alternation between dry and rainy seasons can exert a direct and significant influence on the quality of both surface and groundwater in semi-arid environments. Therefore, the objective of this study is to analyze the physical, chemical, and microbiological parameters of groundwater and surface water sources, as well as to assess irrigation-related indices, during both dry and rainy seasons in the municipality of Iguatu, Ceará, located in the Brazilian semi-arid region.

2 MATERIALS AND METHODS

2.1 Study area description

This study was conducted using surface and groundwater sources in the municipality of Iguatu, located in the south-central region of Ceará State, Brazil, at 6º 21′ 34″ S and 39º 17′ 55″ W, with an altitude of 218 m. According to the Köppen climate classification, the region is hot semi-arid (BSh), with mean annual temperatures of approximately 28 °C and an average total annual precipitation of 996.6 mm. Most rainfall occurs between December and May, while the highest evapotranspiration rates—reaching 1,902.5 ± 117.8 mm yr^{-1} are concentrated from August to January (Oliveira et al., 2025; INMET, 2024; Dubreuil et al., 2018).

The Caatinga vegetation is typically described as a xerophytic savanna steppe, dominated by small, thorny trees with twisted trunks, highly branched shrubs, and numerous spiny annual herbs. This biome is predominantly deciduous and displays remarkable adaptations to prolonged drought periods. Its physiognomy is characterized by a dense shrubland with thorny and branched vegetation, frequently interspersed with bromeliads, euphorbias, and cacti (Costa et al., 2024; Nóbrega et al., 2024). Representative species include *Piptadenia stipulacea* (jurema branca), *Mimosa tenuiflora* (jurema preta), *Desmanthus virgatus* (jureminha), and *Mimosa caesalpiniifolia* (sabiá), which together form a deciduous thorny scrub typical of this semiarid landscape (Nóbrega et al., 2024).

The geomorphology of the area consists of erosional surfaces bordered by crystalline massifs and the margins of sedimentary basins (Silva and Maia, 2017). The crystalline basement features rocky outcrops, while the sedimentary basin includes floodplains. Most agricultural and irrigated semi-intensive and extensive livestock areas are in the sedimentary basin (Oliveira et al., 2025). Geologically, part of the municipality lies within the Iguatu sedimentary basin, covering a total area of 715 km², which also encompasses smaller basins such as Malhada Vermelha and Lima Campos. Lithology is dominated by sedimentary rocks, largely associated with the Mesozoic basin and overlain by more recent sediments, which consist mainly of rhythmites, siltstones, shales, and fine sandstones – predominantly red and green, with interbedded limestones and marls, especially in the Moura Formation and alluvial deposits (FUNCEME et al., 2024; Pinéo et al., 2020; Lima et al., 2019). Another portion of the municipality lies within the Precambrian crystalline basement, most prominent in the upper Jaguaribe River basin, where metamorphic and igneous rocks, particularly granites and gneisses, occur within the Ceará Central, Jaguaribeano, and Granjeiro geological domains (FUNCEME, 2024; Silva and Maia, 2017).

Hydrologically, Iguatu is part of the Upper Jaguaribe River sub-basin, whose drainage is dominated by the Jaguaribe River and its main tributaries, including the Trussu River and local streams such as Carnaúba and Antônico (Oliveira et al., 2016; Oliveira et al., 2025). The Orós Reservoir, located downstream of Iguatu and with a storage capacity of approximately 1.94×10^9 m³, regulates surface water flow and plays a crucial role in water supply and irrigation across the region. The smaller Trussu Reservoir, with a capacity of approximately 3.01×10^8 m³, supplements the local water supply, storing water for urban and agricultural use in Iguatu (Dantas et al., 2011). These reservoirs contribute to the regulation of hydrological regimes, mitigate extreme events such as floods and droughts, and support water security, particularly under conditions of high rainfall variability. Groundwater supply is complemented by tubular wells, highlighting the importance of subsurface water to Iguatu. Notably, some wells yield over 80 $m^3\ h^{-1}$ of high-quality water, underscoring the resilience of alluvial and fissured aquifer systems as strategic water sources during dry periods, and serving as a key pillar for integrated water resource management in the municipality (Cavalcante et al., 2007).

2.2 Selection of sampling sites and water collection

The selection of water sampling sites was based on their use for irrigating annual and perennial crops (fruit orchards) and pastures, ensuring representativeness of the municipality. Some sampling points were also used for livestock watering, recreational activities, and domestic purposes. Surface and groundwater samples were collected during the rainy season (May 2023) and the dry season (August 2023). Thirteen sampling locations were established, including eight sites for groundwater analysis from tubular wells and five sites for surface water analysis (one point in the Orós Reservoir and four locations along the Jaguaribe River) (Figure 1) (Figure 1). At each site, six replicates were collected. Groundwater sampling depths ranged from 25 to 70 m, corresponding to shallow wells. Historical land use and geological characteristics of the sampling sites are presented in Table 1.

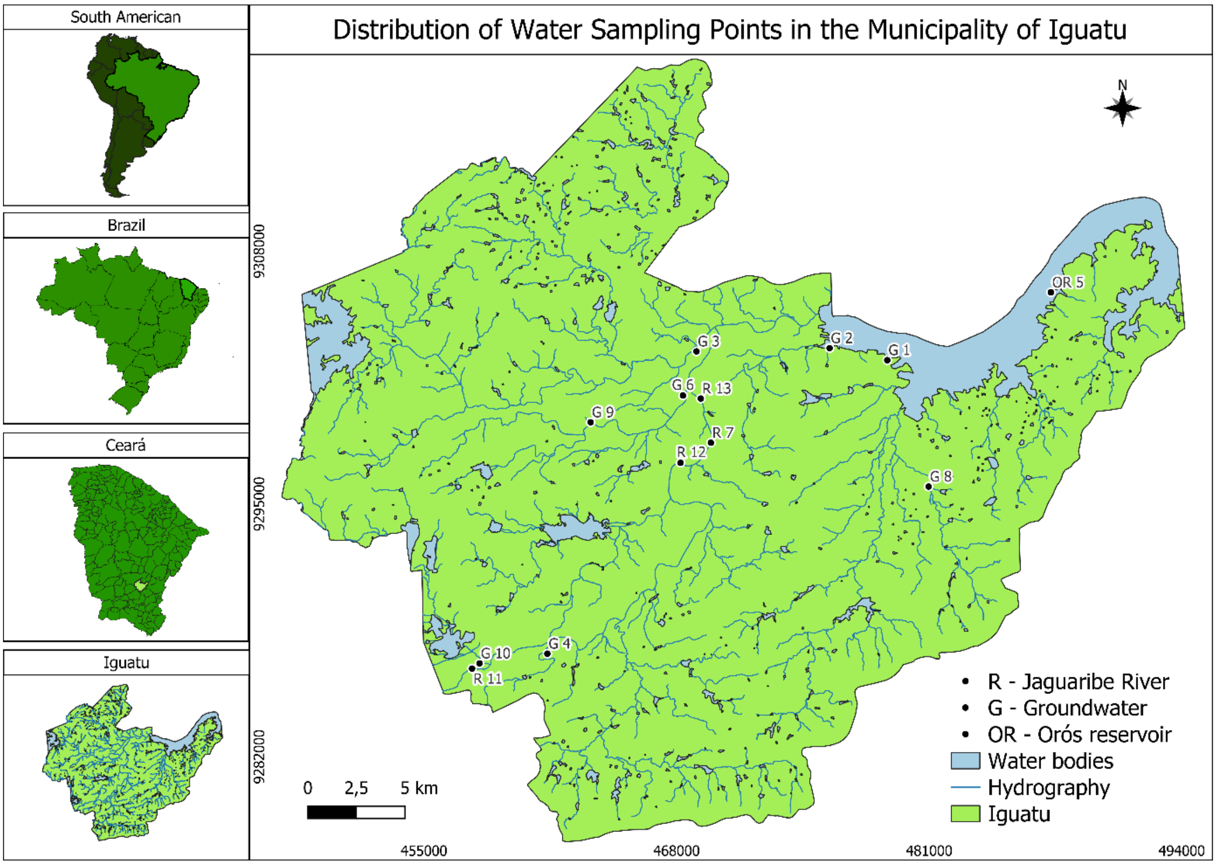

Figure 1. Location map of groundwater and surface water sampling points in the municipality of Iguatu, Ceará, Brazil. Source: Own authorship

Table 1. Sampling sites, geological structure, and historical use of surface and groundwater in the municipality of Iguatu, Ceará, Brazil.

Site	Water type	Geological structure	Historical use
G1*	Groundwater	Sedimentary basin	Agricultural use (pasture irrigation) and livestock watering
G2	Groundwater	Sedimentary basin	Agricultural use (irrigation of annual crops – Poaceae and Fabaceae). During drought, this well serves as an alternative source for domestic human consumption.
G3	Groundwater	Sedimentary basin	Agricultural use (irrigation of annual crops – Poaceae, Fabaceae, and Cucurbitaceae)
G4	Groundwater	Sedimentary basin	Agricultural use (irrigation of fruit crop – banana)
OR5	Surface water	Crystalline basement	Five collection points in the Orós Reservoir were composited into a single sample for analysis with six replicates. These waters are used for irrigating various crops and livestock watering. Also used for human water supply.
G6	Groundwater	Sedimentary basin	Agricultural use (irrigation of pastures and annual crops – Poaceae and Fabaceae)
R7	Surface water	Sedimentary basin	Jaguaribe River (irrigation of various crops, including agroforestry systems, near a Permanent Preservation Area –

Site	Water type	Geological structure	Historical use
			PPA).
G8	Groundwater	Crystalline basement	Agricultural use (pasture irrigation)
G9	Groundwater	Crystalline basement	Agricultural use (irrigation of sugarcane, fruit crops – guava, and vegetables)
G10	Groundwater	Sedimentary basin	Agricultural use (irrigation of fruit crop – banana)
R11	Surface water	Sedimentary basin	Jaguaribe River (irrigation of various crops and recreational human use). Upstream from the municipality of Iguatu.
R12	Surface water	Sedimentary basin	Jaguaribe River (irrigation of various crops and recreational human use). Within the urban area of Iguatu.
R13	Surface water	Sedimentary basin	Jaguaribe River (irrigation of various crops and recreational human use). Downstream from the municipality of Iguatu.

*These numbers indicate the order in which the water samples were collected. Source: Own authorship

Water samples for physicochemical analyses were collected in 500 mL polyethylene bottles, which were triple rinsed with water from the respective sampling source to ensure container homogenization. Groundwater samples from tubular wells were collected after opening the outlet and allowing the water to flow for three minutes. Surface water samples from the river or reservoir were collected 2–3 meters from the banks of the water bodies. For microbiological analyses, surface and groundwater samples were collected in sterilized 70 mL plastic containers, stored in insulated coolers with ice, and kept under refrigeration until analysis.

2.3 Physical, chemical, and microbiological analyses of water, and calculated indices

The parameters analyzed included pH, electrical conductivity (EC), and turbidity, measured using a benchtop pH meter, conductivity meter, and turbidimeter, respectively. Potassium and sodium concentrations were determined by flame photometry. Calcium, magnesium, chloride, carbonate, and bicarbonate were analyzed by titrimetry, and sulfate by turbidimetry. All physicochemical analyses were conducted at the Laboratory of Soil, Water, and Plant Analysis (LASAP/UFERSA) following the Standard Methods for the Examination of Water and Wastewater (APHA, 2005).

For metal determination, water samples underwent pre-treatment by adding 3 mL of nitric acid (HNO_3) to each 100 mL of sample. The mixture was heated on a hot plate until the volume was reduced to approximately 50 mL, then brought back to 100 mL in a volumetric flask, following APHA (2005) recommendations. Concentrations of copper (Cu), manganese (Mn), iron (Fe), zinc (Zn), chromium (Cr), cadmium (Cd), and lead (Pb) were quantified using atomic absorption spectrophotometry.

Microbiological analyses were performed at the Laboratory of Inspection of Products of Animal Origin (LIPOA/UFERSA) according to the methodology established by Normative Instruction No. 30/2018 of the Ministry of Agriculture, Livestock, and Food Supply (MAPA) (Brazil, 2018). The presence of total coliforms, thermotolerant coliforms, and *Escherichia coli* was determined following ISO 9308-1, and thermotolerant coliforms were analyzed according to ISO 6222.

For the calculation of irrigation water quality indices, the following chemical elements were considered: calcium (Ca^{2+}), magnesium (Mg^{2+}), sodium (Na^{+}), potassium (K^{+}), chloride (Cl^{-}), bicarbonate (HCO_3^{-}), and carbonate (CO_3^{2-}), all expressed in $mmol_c L^{-1}$. The calculated indices included: Sodium Absorption Ratio (SAR), Magnesium Adsorption Ratio (MAR), Magnesium Hazard (MH), Residual Sodium Carbonate (RSC), Soluble Sodium Percentage (SSP), Kelly's Index (KI), and Permeability Index (PI), as described in Equations 1 through 7, respectively.

$$\mathrm{SAR} = \frac{\mathrm{Na}^{+}}{\sqrt{\frac{\mathrm{Ca}^{2+} + \mathrm{Mg}^{2+}}{2}}} \quad (1)$$

$$\mathrm{MAR} = \frac{\mathrm{Mg}^{+2}}{\sqrt{\frac{\mathrm{Ca}^{2+} + \mathrm{Mg}^{2+} + Na^{+}}{2}}} \quad (2)$$

$$MH = \frac{Mg^{+2}}{Ca^{+2} + Mg^{+2}} x\ 100$$

(3)

$$\mathrm{RSC} = (\mathrm{CO}_3^{2-} + \mathrm{HCO}^{3-}) - (\mathrm{Ca}^{2+} + \mathrm{Mg}^{2+})$$

(4)

$$\mathrm{SSP} = \frac{\mathrm{Na}^{+} + \mathrm{K}^{+}}{\mathrm{Ca}^{2+} + \mathrm{Mg}^{2+} + \mathrm{Na}^{+} + \mathrm{K}^{+}} \mathrm{x}\ 100 \quad (5)$$

$$\mathrm{KI} = \frac{\mathrm{Na}^{+}}{\mathrm{Ca}^{2+} + \mathrm{Mg}^{2+}} \mathrm{x}\ 100 \quad (6)$$

$$PI = \frac{Na^{+} + \sqrt{HCO_3^{-}} x100}{Ca^{+2} + Mg^{+2} + Na^{+}}$$

(7)

2.4 Statistical analysis

Multivariate statistical methods were employed to distinguish between seasons and water sources. To build a robust analytical matrix, Pearson's correlation and linear regression analyses ($p \leq 0.05$) were first applied to identify interdependent variables of relevance to the dataset. Subsequently, Principal Component Analysis (PCA) and cluster analyses were performed using the R statistical environment. Salinity and sodicity risks were evaluated using the U.S. Salinity Laboratory Diagram (Richards et al., 1954), while ionic water classification was conducted with the Piper Diagram. Both diagrams were generated using Qualigraf software, version 1.17 (FUNCEME, 2023).

3 RESULTS

3.1 Pearson's correlation, principal component analysis, nutrient and metal contents

Pearson's linear correlation matrix for the rainy and dry seasons revealed a significant dynamic in the interactions among water chemical variables, reflecting the impact of seasonality. In the dry season, statistically significant correlations were observed between major cations and anions: Mg^{2+} and HCO_3^- (r = 0.81*), Ca^{2+} and HCO_3^- (r = 0.80***), Fe^{2+} and SO_4^{2-} (r = 0.79**), as well as Na^+ and Cl^- (r = 0.85*) and Na^+ and HCO_3^- (r = 0.66*), suggesting a strong influence of carbonate mineral dissolution and soluble salts (Figure 2A). Total hardness showed a robust positive correlation with Mg^{2+} (r = 0.86*), Ca^{2+} (r = 0.90***), and HCO_3^- (r = 0.90***), while SAR correlated with Cl^- (r = 0.90*) in addition to sodium, reinforcing the role of Na^+ as a key driver of sodicity risk. Turbidity correlated significantly with Fe^{2+} (r = 0.98***) and SO_4^{2-} (r = 0.79**), demonstrating the influence of suspended particles associated with reduced hydrological activity during the dry season (Figure 2A).

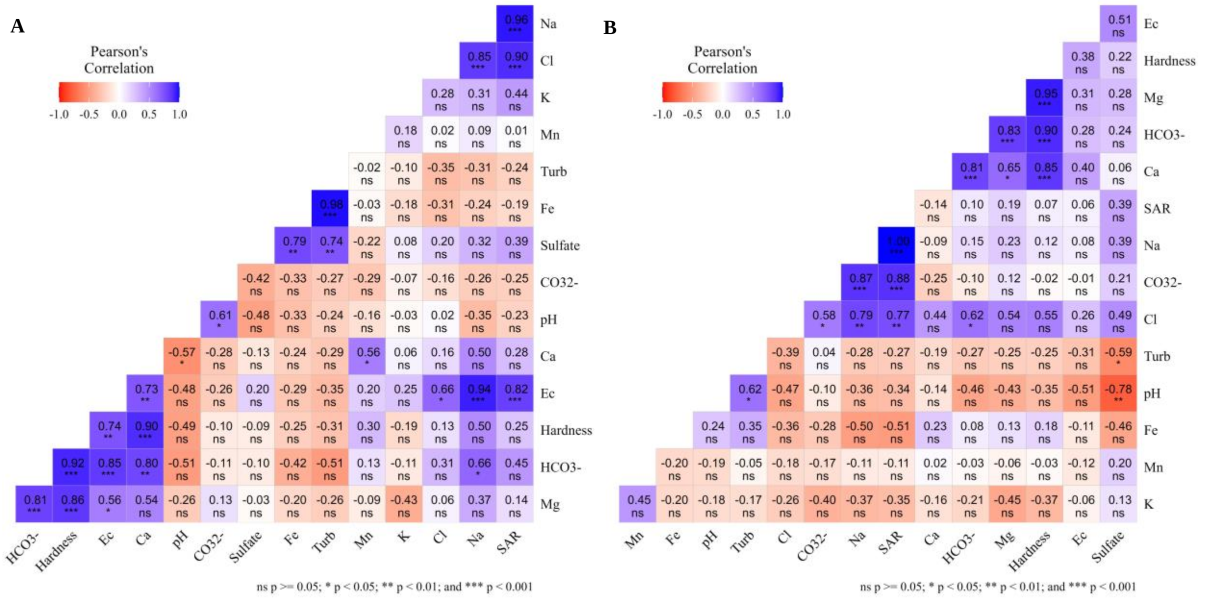

Figure 2. Pearson's linear correlation matrix between the physical and chemical parameters of water from groundwater wells (G1–G4, G6, G8, G9, G10), surface reservoir (OR5 – Orós Reservoir), and stretches of the Jaguaribe River (R7, R11, R12, R13). A) Dry season; B) Rainy season. Significant correlations r ≥ 0.70 (***, **, and * denote significance at 0.1%, 1%, and 5%, respectively). Source: Own authorship

In the rainy season, similar correlation patterns were maintained, confirming the consistency and reliability of these relationships even under greater hydrological dilution. Associations between Mg^{2+} and HCO_3^- (r = 0.83*), Mg^{2+} and Ca^{2+} (r = 0.65*), and Ca^{2+} and HCO_3^- (r = 0.81***) persisted, suggesting that carbonate dissolution processes remain active during aquifer recharge. Correlations between Na^+ and Cl^- (r = 0.79) and Na^+ and HCO_3^- (r = 0.87***) reinforced the same trend observed in the dry season, suggesting a dominant ionic control of these chemical species. Hardness remained strongly associated with Mg^{2+}, Ca^{2+}, and HCO_3^-, with even higher coefficients (r ≥ 0.85***). SAR also correlated significantly with Cl^- (r = 0.77*) and HCO_3^- (r = 0.88***), in addition to sodium, maintaining the sodicity risk pattern (Figure 2B).

For the Principal Component Analysis (PCA), data were normalized in advance and analyzed based on the first two principal components (PC1 and PC2). PCA clearly distinguished sample groups according to water source type and seasonality. In the dry season, PC1 (39.6%) and PC2 (21.5%) together explained 61.1% of the total variance. Wells G9 and G6 showed a strong negative association with PC1, demonstrating salinization (Figure 3A). In contrast, samples R11, R12, and R13 consistently clustered in the positive quadrant of PC1, reinforcing that surface waters maintain lower salt concentrations and fewer adverse chemical parameters even during drought. EC, HCO_3^-, hardness, and Mg^{2+} remained determinant in PC2, contributing to the differentiation of harder groundwater, such as G8.

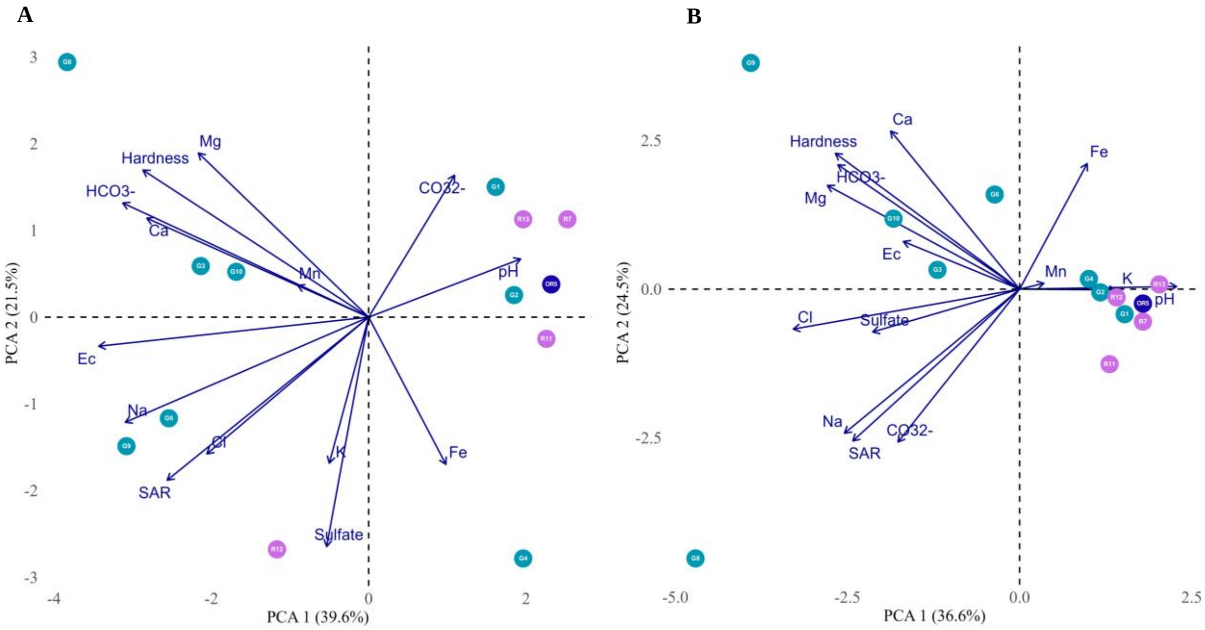

Figure 3. Principal component analysis (PCA) and distribution of zones in the multivariate space of physical and chemical parameters of water from groundwater wells (G1–G4, G6, G8, G9, G10 – green), surface reservoir (OR5 – Orós Reservoir – blue), and stretches of the Jaguaribe River (R7, R11, R12, R13 – purple). A) Dry season; B) Rainy season. Source: Own authorship

In the rainy season, PC1 (36.6%) and PC2 (24.5%) jointly explained 61.1% of the total variance, like the dry season. PC1 was strongly positively correlated with pH, K, Mn, and Fe, and negatively correlated with Na^+, CO_3^{2-}, SAR, Cl^-, SO_4^{2-}, and TDS. PC2 was more closely associated with hardness, Ca^{2+}, Mg^{2+}, and HCO_3^-, demonstrating local geochemical (likely lithological) influence. Samples R7, R11–R13, OR5, and G1, G2, and G4 clustered in the positive quadrant of PC1, highlighting better water quality conditions associated with higher pH, K, and Mn—typical of more oxygenated, less saline surface waters. Conversely, G9 samples were strongly associated with the negative quadrant of PC1, suggesting salinity, and G8 showed high salt content linked to hardness (Na^+, CO_3^{2-}, SAR, Cl^-), differing from the dry season (Figure 3B).

Chemical element concentrations for the different water sources in the dry and rainy seasons are presented in Supplementary Table S1. Overall, in the dry season, mean EC, Na^+, Ca^{2+}, Mg^{2+}, Cl^-, SO_4^{2-}, and alkalinity (HCO_3^-) values were higher in several samples (notably G6, G8, and G9), reflecting increased salinity due to evapoconcentration typical of the season (Table S1). In the rainy season, although some sites, especially G8, G9, and G10, still maintained elevated concentrations, precipitation-driven dilution reduced salinity levels in most samples, particularly for Na^{+}, Cl^{-}, and SO_4^{2-}. pH values ranged from 6.6 (G4) to 9.6 (R7) in the dry season and from 6.6 (G10) to 8.8 (R13) in the rainy season. Turbidity showed greater variation in the dry season at sites such as G4 and R12, suggesting increased suspended solids linked to anthropogenic activity or erosive processes. TDS concentrations followed the EC pattern, with maximum values of ~0.34 g L^{-1} (R12) in the dry season and 0.70 g L^{-1} (G10) in the rainy season. Supplementary Tables S2 and S3 present nutrient comparison parameters according to World Health Organization guidelines and irrigation reference values (Ayers and Westcot, 1985), highlighting sites that exceeded recommended thresholds.

Supplementary Table S4 presents micronutrient and metal concentrations (Cu, Mn, Fe, Zn, Cr, Ni, Cd, Pb). During the dry season, Fe levels exceeded the WHO (2019) limit of 0.3 mg L^{-1} in several locations, most notably in well G4, which showed an extreme value of 5.738 ± 0.221 mg L^{-1}, suggesting localized contamination. Wells G2 (0.788 mg L^{-1}) and G10 (0.405 mg L^{-1}) also exceeded this threshold, potentially posing risks of irrigation system clogging due to ferric precipitation. For Mn, with a WHO (2019) limit of 0.4 mg L^{-1}, exceptionally high concentrations were observed in G3 (1.650 ± 0.043 mg L^{-1}) and, to a lesser extent, in G4 (0.052 mg L^{-1}) and G10 (0.071 mg L^{-1}). Although Cu was detected at all sites, concentrations remained below the limit of 2.0 mg L^{-1}; the same applied to Zn, which was detected only in trace amounts and within the safe range (<3 mg L^{-1}). Cd, Pb, Ni, and Cr were not detected in most samples, except for traces of Ni and Cr in R12, both below critical thresholds (Cr: 0.05 mg L^{-1}; Ni: 0.07 mg L^{-1}).

In the rainy season, a general dilution trend for metals was observed, with significant reductions of Fe and Mn concentrations at most sites. However, wells G3 and G4 continued to present elevated Mn levels (1.167 and 1.210 mg L^{-1}, respectively), again exceeding WHO limits and possibly related to metal mobilization due to changes in the water table (Supplementary Table S4). Although Fe levels decreased, they remained high in G1 (0.200 mg L^{-1}) and R7 (0.213 mg L^{-1}), close to the WHO threshold. Cu remained stable and below critical values (Supplementary Table S4). Ni and Cr reappeared in low concentrations (e.g., OR5 and G4), but always within international standards. No Pb or Cd was detected in any sample, indicating a low probability of direct anthropogenic contamination by these elements during the study period.

3.2 Irrigation water quality indices

An integrated analysis of irrigation water quality indices revealed that water quality varied among the different sources and between sampling periods; however, some indices were more sensitive than others. For the Sodium Adsorption Ratio (SAR) and Residual Sodium Carbonate (RSC), all sites in both periods remained well below the critical thresholds for irrigation (SAR < 10 and RSC < 2.5), suggesting low risk of sodification and carbonation (Table 2). The only exception was R11 during the rainy season, with RSC = 1.23, which is at the marginal threshold. For the Soluble Sodium Percentage (SSP), values were generally higher during the dry season compared to the rainy season, particularly for R12 (54.3%) and G9 (48.1%), both near the threshold (SSP < 50 – acceptable). In the rainy season, all sites recorded SSP < 50%, suggesting improved irrigation suitability (Table 2).

Table 2. Water quality indices for irrigation of groundwater (G) and surface water (R-river and OR- Orós Reservoir) sources in the municipality of Iguatu-CE, Brazil.

Sites	Dry period						
	SAR	RSC	SSP	MH	MAR	KI	PI
G1	1.01	0.29	30.6%	56.2%	1.27	0.38	65.8%
G2	1.00	-0.27	28.5%	60.3%	1.48	0.35	60.1%
G3	1.59	-0.42	36.2%	43.4%	1.13	0.50	61.1%
G4	1.23	-0.83	34.0%	63.3%	1.32	0.48	64.0%
OR5	0.57	-0.13	21.7%	65.4%	1.58	0.22	59.4%
G6	2.26	0.37	45.4%	51.6%	1.18	0.75	70.1%
R7	1.58	0.62	41.0%	71.5%	1.40	0.63	67.8%
G8	1.70	0.72	32.2%	60.9%	1.81	0.47	59.5%
G9	2.64	1.11	48.1%	60.3%	1.28	0.90	75.6%
G10	1.49	-0.17	33.7%	50.8%	1.33	0.47	61.3%
R11	1.05	0.22	31.9%	63.3%	1.33	0.42	69.9%
R12	2.55	0.55	54.3%	57.0%	1.06	0.97	77.9%
R13	1.40	0.15	37.5%	60.2%	1.24	0.55	70.6%
Sites	**Rainy period**						
	SAR	RSC	SSP	MH	MAR	KI	PI
G1	0.13	-0.07	6.2%	31.1%	0.69	0.06	63.6%
G2	0.12	1.01	5.6%	45.8%	1.07	0.05	70.5%
G3	0.19	0.21	6.5%	42.6%	1.23	0.06	51.6%
G4	0.12	0.40	6.5%	46.5%	0.97	0.06	73.0%
OR5	0.11	0.74	5.7%	53.2%	1.12	0.05	76.8%
G6	0.27	0.80	9.5%	45.3%	1.19	0.10	60.3%
R7	0.12	-0.36	5.3%	47.8%	1.15	0.05	56.3%
G8	0.19	-0.47	4.9%	58.1%	2.11	0.05	39.7%
G9	2.00	0.35	43.2%	56.6%	1.13	0.76	75.0%
G10	0.12	-0.18	4.6%	45.2%	1.28	0.04	50.0%
R11	0.15	1.23	6.9%	19.1%	0.42	0.07	77.3%
R12	0.09	-0.29	3.9%	42.9%	1.07	0.03	54.9%

R13	0.10	0.58	5.1%	40.5%	0.91	0.05	69.7%

*SAR: Sodium Absorption Ratio; RSC: Residual Sodium Carbonate; SSP: Soluble Sodium Porcentage; MH: Magnesium Hazard; MAR: Magnesium Adsorption Ratio; KI: Kelly's Index; PI: Permeability Index. G = Groundwater; OR= Oros reservoir; R = River. Source: Own authorship

For Magnesium Hazard (MH), most groundwater and surface water sites exceeded 50% during the dry season, except for G3, suggesting potential risks of compaction and reduced infiltration in clayey soils. In the rainy season, most MH values were < 50% (acceptable), except for G8, G9, and OR5. During the dry season, all sites exhibited Magnesium Adsorption Ratio (MAR) > 1, demonstrating Mg^{2+} dominance over Ca^{2+}, which can exacerbate soil dispersion under continuous irrigation; during the rainy season, dilution effects were observed only at G1, G4, R11, and R13. For Kelly's Index (KI), in the dry season, only G9 (0.90) and R12 (0.97) approached the threshold (KI < 1, good quality). In the rainy season, all points showed very low KI values (< 0.76), demonstrating good water quality. Finally, for the Permeability Index (PI), all sites in both seasons remained within the moderate (PI = 25–75%) to excellent (PI > 75%) range for irrigation water quality (Table 2).

3.3 Piper diagram, conama, u.s.s.l classifications, and hierarchical cluster analysis (HCA)

The combined analysis of hydrochemical data using Piper Diagram for the dry and rainy seasons characterized the dominant typologies of water sources in the municipality of Iguatu. The distribution of samples in the cation and anion triangles of the Piper diagram revealed marked differences between water source types and the significant influence of climatic seasonality on ionic composition. Groundwater (G) was generally characterized during the dry season by mixed types dominated by Na^{+}, K^{+}, Ca^{2+}, and Mg^{2+} as major cations, with Cl^{-} and HCO_3^{-} as predominant anions, classifying them as mixed chloride or mixed bicarbonate waters, typical of environments subject to intense evapoconcentration, low recharge rates, and ion-exchange processes (Figure 4A). In the rainy season, partial dilution of dissolved salts shifted the samples toward the left side of the diagram, reflecting mixed bicarbonate types with varying proportions of Ca^{2+} and Mg^{2+} (Figure 4B). This seasonal transition indicates a relative reduction in salinity and changes in ionic regimes associated with rainfall recharge and the influence of varied geological materials in the aquifer.

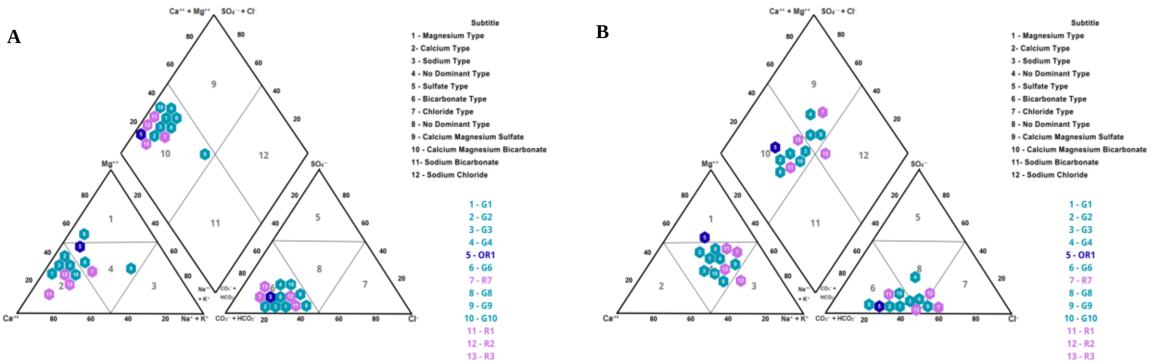

Figure 4. Water samples collected at points distributed among groundwater wells (G1–G4, G6, G8, G9, G10 – green), surface reservoir (OR5 – Orós Reservoir – blue), and stretches of the Jaguaribe River (R7, R11, R12, R13 – purple), during the dry (A) and rainy (B) periods, in the municipality of Iguatu, Ceará, Brazil, plotted on Piper's trilinear diagram. Source: Own authorship

Orós Reservoir exhibited intermediate characteristics between groundwater and river water. In the dry season, its composition was slightly more saline, with moderate proportions of magnesium and bicarbonate, reflecting concentration effects from evaporation and possible upstream ionic contributions (Figure 4A). In the rainy season, the composition shifted toward mixed bicarbonate waters, indicative of more diluted conditions and direct influence from surface runoff (Figure 4B). This pattern reinforces the reservoir's role as an accumulation and mixing zone, with quality strongly modulated by seasonality and the origin of inflowing waters.

Water from the Jaguaribe River showed varying classifications depending on the season and sampling location. In the dry season, most points were mixed-type for cations, except for R7, which was sodic, yielding mixed bicarbonate types (R13 and R11), mixed chloride (R7), and sodic mixed (R12) waters (Figure 4A). In the rainy season, dilution was evident, with predominance of calcium bicarbonate types, except for R7, which was classified as mixed bicarbonate (Figure 4B).

Physicochemical quality assessment based on electrical conductivity (EC) and total dissolved solids (TDS) allowed salinity classification following CONAMA Resolution No. 357/2005 (Table 3). In the dry season, five of the eight wells (G3, G6, G8, G9, and G10) exceeded 500 mg L^{-1} TDS, thus classified as brackish (Table 3). Conversely, G1, G2, and G4 remained freshwater despite high EC. In the rainy season, significant dilution occurred in six wells, shifting most to freshwater classification, including G3 and G6, previously brackish. Only G8 and G9 remained brackish, with TDS > 600 mg L^{-1}, suggesting persistent salinity from geological sources. The Orós Reservoir maintained freshwater status in both seasons, with TDS of 201.5 mg L^{-1} (dry) and 169.0 mg L^{-1} (rainy). Jaguaribe River waters were generally freshwater in both seasons, except R13 in the dry period (TDS = 546 mg L^{-1}, brackish). In the rainy season, all river sites became freshwater, reflecting dilution by rainfall and efficient hydrological renewal.

Table 3. Salinity classification of water from different water sources during dry and rainy periods based on total dissolved solids (TDS) and electrical conductivity (EC) in the municipality of Iguatu-CE, Brazil.

	Dry			Rainy		
	EC	TDS	Classification	EC	TDS	Classification
Unit	µS cm^{-1}	mg L^{-1}		µS/cm	mg L^{-1}	
G1	400,0	260,0	Fresh water	360,0	234,0	Fresh water
G2	450,0	292,5	Fresh water	380,0	247,0	Fresh water
G3	790,0	513,5	**Brackish water**	700,0	455,0	Fresh water
G4	400,0	260,0	Fresh water	250,0	162,5	Fresh water
OR5	310,0	201,5	Fresh water	260,0	169,0	Fresh water
G6	870,0	565,5	**Brackish water**	720,0	468,0	Fresh water
R7	430,0	279,5	Fresh water	330,0	214,5	Fresh water
G8	980,0	637,0	**Brackish water**	940,0	611,0	**Brackish water**
G9	930,0	604,5	**Brackish water**	930,0	604,5	**Brackish water**
G10	740,0	481,0	Fresh water	392,0	254,8	Fresh water
R11	370,0	240,5	Fresh water	340,0	221,0	Fresh water
R12	460,0	299,0	Fresh water	350,0	227,5	Fresh water
R13	840,0	546,0	**Brackish water**	340,0	221,0	Fresh water

*****G: Groundwater; OR: Oros reservoir; R: Jaguaribe River; EC: electrical conductivity; TDS = total dissolved solids. Source: Own authorship

The U.S. Salinity Laboratory (USSL) diagram classified sites according to salinity (C1–C4) and sodicity (S1–S4) hazards. In the dry season, six of eight wells fell into C2-S1 or C3-S1 classes, with G6, G8, and G9 showing EC > 870 µS cm^{-1} and SAR between 1.5–2.66 (C3-S1: high salinity, low sodicity hazard) (Figure 5A). In the rainy season, EC and SAR decreased across all wells, shifting to lower salinity classes (C2-S1) and, for G4, to C1-S1, demonstrating recharge response. G8 and G9 remained C3-S1 due to persistent mineralization (Figure 5B). The Orós Reservoir remained stable (C2-S1) in both seasons (EC = 260–310 µS cm^{-1}, SAR < 0.6). Most river sites were C2-S1 in the dry season, except R13 (C3-S1, EC = 840 µS cm^{-1}). In the rainy season, all river sites shifted to C2-S1 with reduced SAR and salinity.

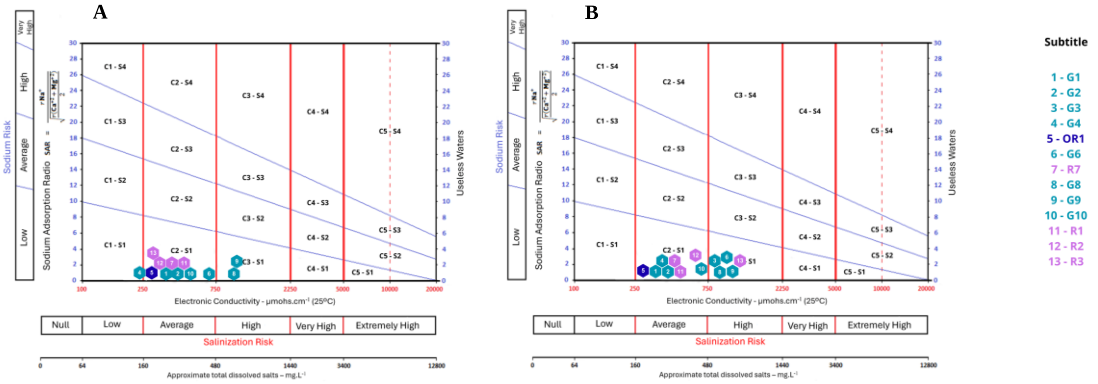

Figure 5. Water samples collected at points distributed among groundwater wells (G1–G4, G6, G8, G9, G10 – green), surface reservoir (OR5 – Orós Reservoir – blue), and stretches of the Jaguaribe River (R7, R11, R12, R13 – purple), during the dry (A) and rainy (B) periods, in the municipality of Iguatu, Ceará, Brazil, plotted on U.S.S.L. Diagram. Source: Own authorship

Hierarchical Cluster Analysis (HCA) using Euclidean distance and Ward's linkage identified four distinct clusters in both seasons, reflecting seasonal and hydrogeochemical variability among water sources (Figure 6). In the dry season, Cluster 1 isolated G8 due to high Na^{+}, Cl^{-}, SAR, and EC (indicative of salinization). Cluster 2 grouped G3, R12, G10, G6, and G9, characterized by high hardness, Mg^{2+}, HCO_3^{-}, and EC (except R12). Cluster 3 isolated G4 due to intermediate hardness and Mg^{2+}. Cluster 4 grouped river and reservoir waters with G1 and G2, reflecting dilution and stable pH, K^{+}, and Mn levels (Figure 6A). In the rainy season, Cluster 1 isolated G9 for persistent high hardness and alkaline salts. Cluster 2 grouped OR5, R7, R12, R13, G2, G1, and R11, demonstrating seasonal homogenization from aquifer recharge and mixing. Cluster 3 again isolated G8, albeit with less divergence, suggesting lithological control of salinity. Cluster 4 grouped G4, G3, G6, and G10, showing similar geochemical composition with moderate hardness, Ca^{2+}, HCO_3^{-}, and EC (Figure 6B).

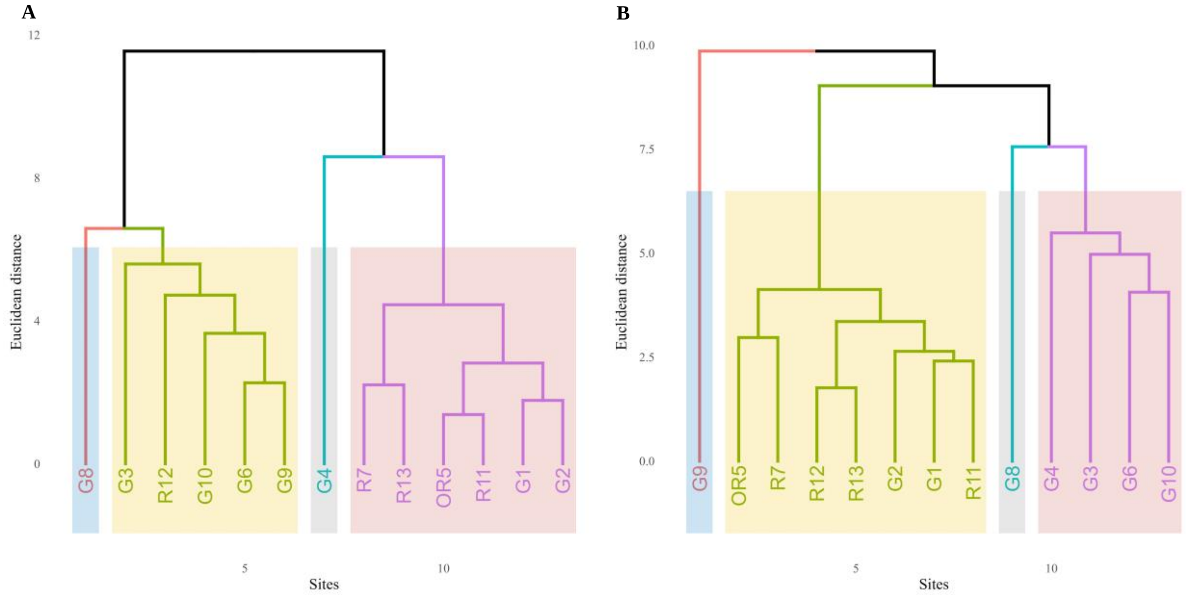

Figure 6. Hierarchical cluster dendrogram based on Euclidean distance and Ward's linkage method for different water sources: groundwater wells (sites G1 to G4, G6, G8, G9, and G10), surface reservoir (OR5 – Orós Reservoir), and stretches of the Jaguaribe River(sites R7, R11, R12, and R13), during the dry (A) and rainy (B) seasons in the municipality of Iguatu, Ceará, Brazil. Source: Own authorship

The microbiological assessment revealed the presence of total coliforms at varying population level across all sampling points in both the dry and rainy seasons. Notably, sites G3, G4, G8, R7, and R12 recorded the highest counts, ranging from 24 to 46 MPN/mL. Regarding thermotolerant coliforms – an indicator more specifically associated with recent fecal contamination – sites G3 and R7 also stood out, with values reaching up to 36 MPN/mL during the dry season, demonstrating a high risk of enteric pathogen presence (Table 4).

Table 4. Total and thermotolerant coliforms and Escherichia coli from different water sources (groundwater (G), Orós Reservoir (OR) and Jaguaribe River (R) during the dry and rainy seasons in the municipality of Iguatu, Ceará, Brazil.

Sites	Total coliform (MPN mL $^{-1}$)		Thermotolerant coliform (MPN mL $^{-1}$)		E. coli (CFU)	
	Dry	Rainy	Dry	Rainy	Dry	Rainy
G1	15	10	<3.0	<3.0	Absent	3.0
G2	9.3	10.3	<3.0	<3.0	15	Absent
G3	46	36	36	24	Absent	9.3
G4	24	19	<3.0	<3.0	3.0	3.0
OR5	9.3	9.9	<3.0	<3.0	Absent	Absent
G6	<3.0	<3.0	Absent	Absent	Absent	Absent
R7	46	48	36	24	Absent	9.3
G8	46	47	Absent	Absent	Absent	Absent
G9	12	15	<3.0	<3.0	Absent	3.0
G10	4.3	4.9	<3.0	<3.0	Absent	3.0
R11	<3.0	<3.0	Absent	Absent	Absent	Absent
R12	24	22	<3.0	<3.0	9.3	9.3
R13	<3.0	<3.0	6.3	4.3	Absent	0.9

*MPN = most probable number; CFU= colony forming unit. Source: Own authorship

For *Escherichia coli* (*E. coli*), a direct indicator of fecal contamination and microbiological risk, most samples showed absence (not detected or <3.0 CFU/mL). However, concerning levels were detected in G2 (15 CFU during the dry season), G3 (9.3 CFU during the rainy season), and in R7 and R12 (9.3 CFU) (Table 4). These findings are critical, as any detection of *E. coli* in water intended for human consumption, recreational activities, or irrigation of raw vegetables is deemed unacceptable according to WHO (2019). Seasonality had a marginal influence on total and thermotolerant coliform levels, with slight reductions observed during the rainy season at most groundwater sampling points.

4 DISCUSSIONS

This study integrated the assessment of groundwater, river, and reservoir water quality in the Iguatu, Ceará, in the Brazilian semiarid region. Physical, chemical, and microbiological parameters were evaluated during dry and rainy seasons, focusing on irrigation suitability and compliance with World Health Organization standards. Multivariate analysis and seasonal comparisons revealed substantial changes in water composition, underscoring the critical role of seasonality in driving hydrogeochemical processes. The distinction between groundwater and surface water was reinforced by differences in salinity, ionic relationships, and potential risks for irrigation use.

During the dry season, higher concentrations of ions such as Mg^{2+}, Ca^{2+}, Na^{+}, Cl^{-}, SO_4^{2-}, and HCO_3^{-} were observed, particularly in wells G8 and G9. Similar conditions were reported by Rojas et al. (2021) in northeastern Brazil. This pattern is likely linked to the crystalline basement geology, composed of igneous and metamorphic rocks (granites and gneisses) rich in primary minerals (feldspars, micas), which release Na^{+}, K^{+}, Ca^{2+}, Mg^{2+}, and silica during weathering, thereby increasing salinity (Gaaloul et al., 2022; Teramoto et al., 2023; Jalali et al., 2007). Furthermore, due to low porosity and permeability, water flows mainly through fractures and faults, resulting in prolonged residence times and increased contact with minerals (Wadi et al., 2022; Lachassagne et al., 2021). This promotes intense dissolution and chemical alteration, leading to salt accumulation, particularly chlorides and sulfates (Egbueri et al., 2025). The low permeability of these rocks' limits salt dilution, concentrating them in fractured aquifers (Egbueri et al., 2025). Human activities such as groundwater overexploitation and improper irrigation management may further contribute to salinization (Almeida et al., 2025; Faraj et al., 2020).

The formation of two well-defined multivariate groups, one axis associated with sodium and chlorides, influencing SAR and EC, and another linked to carbonates and alkaline earth cations, suggests chemical dissolution processes of minerals in rock–water contact zones. In addition to dissolution from crystalline basement rocks, the presence of carbonates and alkaline earth cations is likely influenced by fracture sealing due to calcite precipitation, which reduces available permeability with depth, as observed by Abiye et al. (2011) in crystalline rock aquifers in South Africa. Correlation analyses revealed stable hydrodynamic interactions throughout the year, such as the strong relationship between Mg^{2+}, Ca^{2+}, and HCO_3^{-}, and between SAR and Cl^{-}, suggesting that sodification is still a persistent risk, particularly in waters with high Na^{+} content and low relative hardness (Ayers & Westcot, 1985; WHO, 2019). These patterns suggest that even during the rainy season, groundwater quality may not fully recover from the saline concentration accumulated during the dry season, highlighting the need for more stringent water management, as demonstrated in this study.

Another critical aspect concerns the high pH values (9.6 at R7 and 8.8 at R13) recorded during the dry season, which exceed the thresholds established by FAO guidelines for irrigation water (Ayers and Westcot, 1985) and the Brazilian resolution CONAMA 357/2005 (BRASIL, 2005). These alkaline conditions were observed under peak solar radiation, suggesting a strong influence of eutrophication processes linked to nitrogen and phosphorus enrichment. Excessive algal and macrophyte growth under such nutrient availability enhances photosynthetic activity, leading to intense CO_2 assimilation and the consequent conversion of bicarbonates (HCO_3^-) into hydroxyl ions (OH^-), thereby elevating pH (Omokaro et al., 2025; Sitote and Gebremedhine, 2024; Devlin and Brodie, 2023; Beer et al., 2021; Dolui et al., 2021). Elevated pH in eutrophic waters has been widely reported in tropical reservoirs, where seasonal nutrient pulses and high irradiance act synergistically to increase primary productivity and shift carbonate equilibria (Omokaro et al., 2025; Dolui et al., 2021). This dynamic not only compromises water quality for irrigation but also alters trace metal solubility and the ecological balance of aquatic systems.

The metal contents were also relevant for assessing water potability and its suitability for agricultural use. Iron (Fe) exceeded the World Health Organization limit (0.3 mg L^{-1}) in several wells during the dry season, particularly G4, G2, and G10, compromising water use due to encrustation and clogging in irrigation systems (Cabrera-Garcia et al., 2024; Pavithran et al., 2022; WHO, 2019). Manganese (Mn) also surpassed acceptable limits in G3 and G4, possibly due to leaching from mafic rocks or fluctuations in the water table (Latif et al., 2025; Pattnaik & Majhi, 2024; WHO, 2019). Although Cu, Zn, Ni, and Cr levels remained below international thresholds, their presence demonstrates the need for continuous monitoring, particularly in urban and agricultural areas that may be subject to anthropogenic influence.

According to the calculated indices, most sampling points showed a low risk of sodification (SAR < 10) and carbonation (RSC < 2.5) in both periods, confirming the overall suitability of the water for irrigation based on the criteria of Ayers & Westcot (1985). However, marginal RSC values observed at point R11 (1.23 in the rainy season) and SSP values exceeding or close to 50% at R12 (54.3%) and G9 (48.1%) during the dry season warrant special attention, as they may lead to soil structure degradation over time (Mokhtar et al., 2022; Kundu et al., 2018). The high magnesium adsorption ratio (MAR > 1) at all points during the dry period, and partially in the rainy period, suggests dominance of Mg^{2+} over Ca^{2+}, which can promote colloid dispersion and compaction in clay soils, as discussed by Damiba et al. (2025). Most points also exceeded 50% in the magnesium hazard index (MH) during the dry season, especially G6, G8, OR5, and R7, implying a potential risk to the permeability of irrigated soils (Damiba et al., 2025; Kundu et al., 2018). Despite this, the Kelly's Index (KI < 1) and permeability index (PI > 60%) remained at satisfactory levels, suggesting a favorable ionic balance for infiltration and agricultural use, as highlighted by Ibrahim et al. (2023).

The Piper diagram indicated a strong influence of seasonality on the ionic composition of the water. In the dry period, the "mixed chloride" type predominated in groundwater, reflecting evapoconcentration, low recharge, and contact with geological materials rich in soluble salts (Aditya et al., 2024; Wu et al., 2021). During the rainy period, there was a transition to mixed bicarbonate waters, with dilution of ions and increased influence of recharge, as demonstrated by Aditya et al. (2024) and Matos et al. (2018). It is noteworthy that the Orós Reservoir presented an intermediate composition between aquifers and the river, shifting from bicarbonate–magnesian (dry) to mixed bicarbonate (rainy), evidencing its role as a mixing and hydrological stabilization reservoir. The waters of the Jaguaribe River showed variable typologies between points and periods, ranging from mixed sodium (R12 in the dry season) to calcium bicarbonate in the rainy season, reflecting greater river renewal and dilution of ionic loads. Analyzing the Jaguaribe River, Trussu Reservoir, and groundwater also in the municipality of Iguatu-CE, Souza et al. (2016) classified the waters as chloride–calcium, bicarbonate–calcium, and bicarbonate–sodium for surface and groundwater, and chloride–sodium for groundwater. Regarding irrigation classification, their results showed that surface waters had a low risk of salinity problems, whereas groundwater showed a medium to high risk of causing salinity.

According to the parameters of CONAMA Resolution No. 357/2005, during the dry season, five of the eight wells (G3, G6, G8, G9, and G10) were classified as brackish water – a typical effect of intense evaporation and mineralization in shallow crystalline aquifers (Teramoto et al., 2023). During the rainy season, six wells showed significant dilution, leading to reclassification as freshwater, except for G8 and G9, whose salinity remained high. The Orós Reservoir demonstrated excellent hydrological stability, which can likely be attributed to its large storage volume, continuous renewal from river inflows, and the intrinsic dilution capacity of the water body. The waters of the Jaguaribe River also exhibited good quality in both seasons, with a predominance of freshwater classification, except at point R13 during the dry season (classified as brackish water). This localized increase may be related to concentrated discharges, saline surface runoff, or longer local residence times, particularly in stretches with reduced flow velocity or impoundment.

The assessment using the U.S. Salinity Laboratory diagram revealed that, although many points fell into the C3-S1 class (high salinity and low sodicity hazard), after the rainy season there was a migration to C2-S1 or even C1-S1, highlighting the crucial role of rainfall in reducing salinity and improving water suitability for irrigation (Liberoff et al., 2023; Perri et al., 2022; Richards, 1954). Even so, G8 and G9 remained in the C3-S1 class, requiring restrictions on agricultural use or the adoption of specific management practices (e.g., gypsum application or cultivation of salt-tolerant crops).

The hierarchical cluster analysis (HCA) confirmed the influence of water source origin and seasonality on the distribution of chemical patterns. In the dry season, G8 stood out as an isolated point due to its high EC, Na^+, and Cl^- levels, representing a typical case of localized salinization. In the rainy season, G8 and G9 were isolated, the latter associated with higher hardness and alkaline earth cations. Distinct clusters grouped wells with similar composition (G3, G6, G10) and clustered surface waters (river and reservoir) with lower-salinity wells (G1 and G2), demonstrating strong compositional similarity. During the rainy season, greater homogeneity between groundwater and surface water was observed, with the grouping of points (OR5, R11, R13, G1, G2) into a single cluster, reinforcing the role of recharge and mixing of water masses in attenuating chemical contrasts (Perri et al., 2022; Carvalho et al., 2021; Tinôco et al., 2018).

The microbiological analysis revealed widespread contamination by total coliforms in all water samples, both surface and groundwater, during the dry and rainy seasons. Although values varied between sampling points, the consistent presence of these microorganisms is alarming, particularly in wells G3, G4, and G8, and in river waters at R7 and R12, where total coliform levels reached up to 46 MPN mL^{-1}, evidencing potential risk to human health. Shallow groundwater sources are more susceptible to contamination, as the short vertical distance facilitates the transport of pathogenic microorganisms. The effectiveness of reducing these contaminants along the subsurface flow depends on their retention and microbiological inactivation during the transit (van Geen et al., 2011).

According to the World Health Organization (WHO, 2019), total coliforms in any type of water intended for human consumption, irrigation of crops eaten raw, or recreational use represent non-compliance with potability and microbiological safety standards, requiring immediate corrective measures. Even more concerning was the detection of thermotolerant coliforms (Silva et al., 2024), classical indicators of recent fecal contamination, especially at G3 and R7, both with 36 MPN mL^{-1} in the dry season, reinforcing the hypothesis of domestic sewage infiltration or the presence of diffuse pollution sources.

The detection of *Escherichia coli* (E. coli) at sites such as G2 (15 CFU), G3 (9.3 CFU), and R12 (9.3 CFU) is particularly critical, as this bacterium is a direct marker of microbiological risk, associated with enteric pathogens such as Salmonella spp., Shigella spp., and pathogenic strains of *E. coli* (Dzodzomenyo et al., 2022). According to WHO (2019), any detectable concentration of *E. coli* in 100 mL of sample renders the water unsuitable for human consumption and also unfit for irrigating crops eaten raw, due to the high risk of transmitting diseases such as colibacillosis, hepatitis A, giardiasis, diarrhea, cholera, typhoid fever, salmonellosis, and poliomyelitis (Silva et al., 2024; Bagordo et al., 2024; WHO, 2019).

Seasonality had a differentiated impact on microorganisms. A slight reduction of total coliforms was observed during the rainy season, possibly due to dilution from higher precipitation volumes. However, the presence of *E. coli* worsened at some points during this same period, such as in wells G3 and G9 and river points R7 and R12, suggesting that surface runoff and recharge of contaminated aquifers may have transported fecal matter to water sources (Dzodzomenyo et al., 2022; Tagar et al., 2025). From a practical standpoint, these results indicate a high risk to public health, especially in areas where these waters are used for irrigating vegetables eaten raw, such as lettuce, coriander, and scallions, and where recreational activities take place, as in the Jaguaribe River. Consumption of food irrigated with contaminated water can lead to outbreaks of waterborne diseases, with direct impacts on food safety, the healthcare system, and the local economy.

5 CONCLUSIONS

This study provided a comprehensive assessment of the quality of surface and groundwater in the municipality of Iguatu, located in the semi-arid region of Ceará, using an integrated multivariate approach. The results revealed marked seasonal variations in the physicochemical and microbiological composition of the water, with higher salinity and concentrations of dissolved ions during the dry season, particularly in groundwater. This pattern reflects the influence of local geology, evapoconcentration processes, and limited recharge. The presence of total coliforms, thermotolerant coliforms, and *Escherichia coli* in some riverine sites, especially during the rainy season, denotes diffuse fecal contamination, representing a significant public health risk.

The application of irrigation water quality indices (SAR, RSC, SSP, MH, KI, MAR, PI) and technical diagrams (USSL, Piper) showed that some samples, particularly from wells of Crystalline basement, present restrictions for agricultural use, requiring management practices such as agricultural gypsum application, drainage systems, and the selection of salinity-tolerant cultivars. Principal Component Analysis (PCA) and Hierarchical Cluster Analysis (HCA) highlighted the spatial and seasonal distinctions between water sources, underscoring the hydrogeochemical heterogeneity of the basin. The convergence of these results confirms the urgency of integrated water management strategies aimed at ensuring water security, preventing soil salinization, and protecting human health.

Given the environmental and climatic vulnerability of the semi-arid region, this study recommends strengthening continuous water monitoring, expanding basic sanitation, and adopting social technologies that promote sustainable water use, such as treated water reuse and rainwater harvesting, in alignment with the principles of SDG 6 (Clean Water and Sanitation) and SDG 12 (Responsible Consumption and Production). Future research should incorporate eco-hydrological approaches, health risk assessments, and climate scenario modeling to support public policies for climate change adaptation, directly contributing to SDG 13 (Climate Action) and SDG 15 (Life on Land). Furthermore, by identifying hotspots of fecal coliform contamination and the risks associated with irrigating with low-quality water, this study reinforces the importance of SDG 3 (Good Health and Well-being), particularly in vulnerable rural communities. Therefore, the findings of this research are essential for guiding technical, environmental, and social decisions, fostering water security and agricultural resilience in contexts of scarcity and anthropogenic pressure in the Brazilian semi-arid region.

REFERENCES

ABD-ELHAMID, H. F. *et al.* Investigating and Managing the Impact of Using Untreated Wastewater for Irrigation on the Groundwater Quality in Arid and Semi-Arid Regions. **International Journal of Environmental Research and Public Health**, v. 18, n. 14, p. 7485, 2021.

ABIYE, T. A.; MENGISTU, H.; DEMLIE, M. B. Groundwater Resource in the Crystalline Rocks of the Johannesburg Area, South Africa. **Journal of Water Resource and Protection**, v. 3, n. 4, p. 199–212, 2011.

ADITYA, S. K.; KRISHNAKUMAR, A.; ANOOPKRISHNAN, K. Analysis of seasonal spatio-temporal variations in river water quality and its influencing factors in the Periyar River Basin, Southern Western Ghats, India. **Journal of Water and Climate Change**, v. 15, n. 9, p. 4434–4456, 2024.

ALHARBI, S. *et al.* Agricultural and Technology-Based Strategies to Improve Water-Use Efficiency in Arid and Semiarid Areas. **Water**, v. 16, n. 13, p. 1842, 2024.

ALLAN, R. P. *et al.* **Climate Change 2021 – The Physical Science Basis: Working Group I Contribution to the Sixth Assessment Report of the Intergovernmental Panel on Climate Change**. 1. ed: Cambridge University Press, 2023.

ALLISON, L. E. *et al.* United States Salinity Laboratory Staff, 1954.

ALMEIDA, T. A. B. *et al.* Spatiotemporal Variability of Groundwater Quality for Irrigation: A Case Study in Mimoso Alluvial Valley, Semiarid Region of Brazil. **Water**, v. 17, n. 3, p. 410, 2025.

ALUM, E. U.; OBEAGU, E. I.; UGWU, O. P.-C. Enhancing quality water, good sanitation, and proper hygiene is the panacea to diarrhea control and the attainment of some related sustainable development goals: A review. **Medicine**, v. 103, n. 38, p. e39578, 2024.

APHA. American Public Health Association. **Standard methods for the examination ofwater and watwater.** 21 ed. Washington, 2005.

Ayers, R. & Westcott, D. *Water quality for agriculture. FAO irrigation and drainage paper 29 Rev. 1, Food and Agricultural Organisation of the United Nations*. (1994).

BAGORDO, F. *et al.* Factors Influencing Microbial Contamination of Groundwater: A Systematic Review of Field-Scale Studies. **Microorganisms**, v. 12, n. 5, p. 913, 2024.

Beer, S., Björk, M., Beardall, J. (2021). Carbon Dioxide vs. Bicarbonate Utilisation. In: Gao, K., Hutchins, D.A., Beardall, J. (eds) Research Methods of Environmental Physiology in Aquatic Sciences. Springer, Singapore. https://doi.org/10.1007/978-981-15-5354-7_18

BRASIL. Resolução CONAMA nº 357/2005, de 17 de março de 2005. Dispõe sobre a classificação dos corpos de água e diretrizes ambientais para o seu enquadramento, bem como estabelece as condições e padrões de lançamento de efluentes, e dá outras providências.

Brazil, 2018. GM/MAPA Normative Instruction N.º 30/2018. Federal Official Gazette, Brasília-DF.

CABRERA-GARCIA, J. C.; TORO-HERRERA, M. A.; RAUDALES, R. E. Assessing micro-irrigation clogging risk through water quality classification systems. **Water Practice and Technology**, v. 19, p. 3237–3250, 2024.

CARVALHO, A. A. D. *et al.* Coupling Water Resources and Agricultural Practices for Sorghum in a Semiarid Environment. **Water**, v. 13, n. 16, p. 2288, 2021.

CAVALCANTE, I. N. *et al.* As águas subterrâneas de Iguatu e Quixelô - Ceará. **Águas Subterrâneas**, 2007.

Costa, D. P., Lentini, C. A., Cunha Lima, A. T., Duverger, S. G., Vasconcelos, R. N., Herrmann, S. M., ... & Franca Rocha, W. J. (2024). All deforestation matters: deforestation alert system for the Caatinga biome in South America’s tropical dry forest. *Sustainability*, *16*(20), 9006. **https://doi.org/10.3390/su16209006**

DAMIBA, W. A. F. *et al.* An optimized irrigation water quality index for evaluating surface water sustainability status of an agricultural watershed. **Water Environment Research: A Research Publication of the Water Environment Federation**, v. 97, n. 1, p. e70003, 2025.

DANTAS, S. P.; BRANCO, K. G. C.; BARRETO, L. L. Análise da distribuição dos recursos hídricos do Açude Orós: Bacia Hidrográfica do Jaguaribe/CE - Brasil. **Revista Geográfica de América Central**, 2011.

Devlin, M., Brodie, J. (2023). Nutrients and Eutrophication. In: Reichelt-Brushett, A. (eds) Marine Pollution – Monitoring, Management and Mitigation. Springer Textbooks in Earth Sciences, Geography and Environment. Springer, Cham. https://doi.org/10.1007/978-3-031-10127-4_4

Dolui, D., Saha, I., Sarkar, B., Ghosh, A., Adak, M.K. (2021). Bicarbonate Toxicity and Elevated pH in Plants: Metabolism, Regulation and Tolerance. In: Hasanuzzaman, M. (eds) Approaches to the Remediation of Inorganic Pollutants. Springer, Singapore. https://doi.org/10.1007/978-981-15-6221-1_5

Dubreuil, V., Fante, K. P., Planchon, O., & Sant'anna Neto, J. L. (2019). Climate change evidence in Brazil from Köppen's climate annual types frequency. International Journal of Climatology, 39(3), 1446-1456. **https://doi.org/10.1002/joc.5893**

DZODZOMENYO, M. *et al.* Impact of flooding on microbiological contamination of domestic water sources: a longitudinal study in northern Ghana. **Applied Water Science**, v. 12, n. 10, p. 235, 2022.

EGBUERI, J. C. *et al.* Groundwater Development Within the Nigerian Crystalline and Sedimentary Aquifers: Challenges and Opportunities. *In*: ALI, S.; NEGM, A. (org.). **Groundwater in Developing Countries**. Cham: Springer Nature Switzerland, 2025. (Springer Water). p. 297–325.

EL BEHAIRY, R. A. *et al.* Modelling and Assessment of Irrigation Water Quality Index Using GIS in Semi-arid Region for Sustainable Agriculture. **Water, Air, & Soil Pollution**, v. 232, n. 9, p. 352, 2021.

FARAJ, T.; RAGAB, A.; EL ALFY, M. Geochemical and hydrogeological factors influencing high levels of radium contamination in groundwater in arid regions. **Environmental Research**, v. 184, p. 109303, 2020.

FUNCEME, 2023. Qualigraf [WWW Document]. URL https://qualigraf.funceme.br/ (accessed 3.6.25).

FUNCEME. **Geosolos: Levantamento de reconhecimento de média intensidade dos solos do Estado do Ceará**. fortaleza, CE: Coletivo Duas Catitas, 2024.

GAALOUL, N.; ESLAMIAN, S. Groundwater Quality in Arid Environments. *In*: LEAL FILHO, W. *et al.* (org.). **Clean Water and Sanitation**. Cham: Springer International Publishing, 2022. (Encyclopedia of the UN Sustainable Development Goals). p. 260–272.

GONÇALVES, J. A. C.; DIAS, D. A. F. Índice de Qualidade da Água-IQA no médio curso rio Piracicaba (MG) para os anos de 2011 e 2020. **Revista Brasileira de Geografia Física**, v. 17, n. 6, p. 4575–4595, 2024.

HE, C. *et al.* Future global urban water scarcity and potential solutions. **Nature Communications**, v. 12, n. 1, p. 4667, 2021.

IBRAHIM, H. *et al.* Evaluation and Prediction of Groundwater Quality for Irrigation Using an Integrated Water Quality Indices, Machine Learning Models and GIS Approaches: A Representative Case Study. **Water**, v. 15, n. 4, p. 694, 2023.

INMET. **Instituto Nacional de Meteorologia. Banco de Dados Meteorológicos para Ensino e Pesquisa (INMET/BDMEP). Dados históricos de precipitação**. [*S. l.*], 2024. Disponível em: https://portal.inmet.gov.br/servicos/bdmep-dados-hist%C3%B3ricos. Acesso em: 10 jun. 2024.

ISHAQUE, W.; SULTAN, K.; UR REHMAN, Z. Water management and sustainable development in Pakistan: environmental and health impacts of water quality on achieving the UNSDGs by 2030. **Frontiers in Water**, v. 6, p. 1267164, 2024.

JALALI, M. Salinization of groundwater in arid and semi-arid zones: an example from Tajarak, western Iran. **Environmental Geology**, v. 52, n. 6, p. 1133–1149, 2007.

JAVADI, M.; HADDAD MOGHADDAM, H.; GHASEMZADEH, H. Investigating the role and impact of modern irrigation in preserving the country’s water resources. **School education in the third millennium**, v. 3, n. 4, p. 27–30, 2025.

KUNDU, A.; NAG, S. K. Assessment of groundwater quality in Kashipur Block, Purulia district, West Bengal. **Applied Water Science**, v. 8, n. 1, p. 33, 2018.

LACHASSAGNE, P.; DEWANDEL, B.; WYNS, R. Review: Hydrogeology of weathered crystalline/hard-rock aquifers—guidelines for the operational survey and management of their groundwater resources. **Hydrogeology Journal**, v. 29, n. 8, p. 2561–2594, 2021.

LATIF, D. *et al.* Zardahal banded manganese mineralization: Implications for hydrothermal processes and late diagenetic overprinting in the Qulqula Radiolarian Formation, Halabja Province, Iraq. **Journal of the Geological Society**, p. jgs2025-060, 2025.

LIBEROFF, A. L.; POCA, M. Groundwater-surface water interactions in a semi-arid irrigated agricultural valley: A hydrometric and tracer-aided approach. **Science of The Total Environment**, v. 903, p. 166625, 2023.

LIMA, L.; MOURA-FÉ, M.; PINHEIRO, M. Caracterização Geológica do Município de Iguatu, Ceará, 2019. p. 313–318.

MACEDO, R. S. *et al.* Assessment of Soil Quality of Smallholder Agroecosystems in the Semiarid Region of Northeastern Brazil. **Land**, v. 13, n. 3, p. 304, 2024.

MARENGO, J. A. *et al.* Climatic characteristics of the 2010-2016 drought in the semiarid Northeast Brazil region. **Anais da Academia Brasileira de Ciências**, v. 90, n. 2 suppl 1, p. 1973–1985, 2018.

MATTOS, J. B. *et al.* Spatio-seasonal changes in the hydrogeochemistry of groundwaters in a highland tropical zone. **Journal of South American Earth Sciences**, v. 88, p. 275–286, 2018.

MITROI, V. *et al.* Grounded perspectives on water infrastructures and drought imaginaries in the semi-arid Northeast of Brazil. **Journal of Hydrology**, v. 662, p. 133894, 2025.

MOKHTAR, A. *et al.* Prediction of irrigation water quality indices based on machine learning and regression models. **Applied Water Science**, v. 12, n. 4, p. 76, 2022.

Nóbrega, J. S., de Lucena Alcântara Bruno, R., Gleide da Silva, L., Lima, L. K. S., Nunes de Medeiros, A., Pereira de Andrade, A., ... & Rufino de Lima, C. (2024). Seed recovery of native plant species of the Caatinga biome ingested by goats and its effect on seed germination, in Brazilian semiarid region. *Arid Land Research and Management*, *38*(1), 109-121. https://doi.org/10.1080/15324982.2023.2235316

OLIVEIRA, F. É. R. *et al*. Diagnóstico da gestão participativa e a atuação do comitê da Sub-Bacia do Alto Jaguaribe, Ceará. **Revista geonorte**, v. 26, n.7, p. 106-121, 2016.

OLIVEIRA, F. É. R., *et al.* Droughts, livestock expansion, and Forest degradation: A 37-year assessment of landscape change in a semiarid municipality of Brazil. Science of The Total Environment, 986, 179733, 2025.

Omokaro, G. O., Nafula, Z. S., Iloabuchi, N. E., Chikukula, A. A., Osayogie, O. G., & Nnoli, E. C. (2025). Microalgae as Biofactories for Sustainable Applications: Advancing Carbon Sequestration, Bioenergy, and Environmental Remediation. *Sustainable Chemistry for Climate Action*, 100098.
PATTNAIK, S.; MAJHI, S. Mineralogy, geochemistry and genesis of low-grade manganese ores of Anujurhi area, Eastern Ghats, India. **Geologija**, v. 67, n. 2, p. 285–300, 2024.

PAVITHRAN, R. *et al.* Study on reduction of scale formation in drip irrigation nozzle using natural coagulation. **Materials Today: Proceedings**, v. 66, International Conference on Thermal Analysis and Energy Systems 2021, p. 1337–1342, 2022.

PERRI, S. *et al.* Contrasting effects of aridity and seasonality on global salinization. **Nature Geoscience**, v. 15, n. 5, p. 375–381, 2022.

PINÉO, T. R. G.; *et al.* Mapa geológico do estado do Ceará: projeto geologia e recursos minerais do estado do Ceará. Fortaleza: CPRM, 2020. 1 mapa, color. Escala 1:500.000.

RICHARDS, L. A. Diagnosis and improvement of saline and alkaline soils. [s. l.], 1954.

SANTOS, E. M. *et al.* Modeling water quality in the brazilian semiarid region using remote sensing: support for water management. **Environmental Monitoring and Assessment**, v. 197, n. 8, p. 891, 2025.

SEIGERMAN, C. K. *et al.* At the extremes: Assessing interrelations among the impacts of and responses to extreme hydroclimatic events in Ceará, Northeast Brazil. **Journal of Hydrology**, v. 632, p. 130850, 2024.

SILVA, F. O. da; CAMARGO, A. F.; TREICHEL, H. Thermotolerant coliform bacteria present in water bodies. **Brazilian Applied Science Review**, v. 8, n. 1, p. 42–67, 2024.

SILVA, M. B. D.; MAIA, R. P. Caracterização morfoestrutural do alto curso da Bacia Hidrográfica do Rio Jaguaribe, Ceará-Brasil. **Revista Brasileira de Geomorfologia**, v. 18, n. 3, 2017.

Sitote, Y. M., & Gebremedhine, M. G. (2024). Comprehensive Review of Eutrophication in Freshwater Ecosystems: Causes, Effects, Assessment, and Management Strategies. doi: 10.20944/preprints202409.0704.v1

SOUZA, C. A. de *et al.* Análise comparativa da qualidade de água para irrigação em três sistemas hídricos conectados no semiárido. **Revista Brasileira de Agricultura Irrigada - RBAI**, v. 10, n. 6, p. 1011–1022, 2017.

TAGAR, S. *et al.* Surface Water Analysis for Physical Parameters, Fecal Indicator Bacteria, and Identification of the Origin of Contamination. **Water, Air, & Soil Pollution**, v. 236, n. 2, p. 118, 2025.

TERAMOTO, E. H.; STRADIOTO, M. R.; CHANG, H. K. Geochemical simulation to assess the rock–water interaction in crystalline aquifers in São Paulo State, Southeastern Brazil. **Sustainable Water Resources Management**, v. 9, n. 5, p. 162, 2023.

THAPA, R. *et al.* An evaluation of irrigation water suitability in the Dwarka river basin through the use of GIS-based modelling. **Environmental Earth Sciences**, v. 76, n. 14, p. 471, 2017.

TINÔCO, I. C. M. *et al.* Characterization of Rainfall Patterns in the Semiarid Brazil. **Anuário do Instituto de Geociências**, v. 41, n. 2, p. 397–409, 2018.

ROJAS, L. V., *et al.* Quality and management status of the drinking water supplies in a semiarid region of Northeastern Brazil. **Journal of Environmental Science and Health, Part A**, v. 55, n. 10, p. 1247–1256, 2020.

VALE, T. M. C. D. *et al.* Climate and water balance influence on agricultural productivity over the Northeast Brazil. **Theoretical and Applied Climatology**, v. 155, n. 2, p. 879–900, 2024.

VAN GEEN, A. *et al.* Fecal Contamination of Shallow Tubewells in Bangladesh Inversely Related to Arsenic. **Environmental Science & Technology**, v. 45, n. 4, p. 1199–1205, 2011.

WADI, D. *et al.* Assessment and feasibility of the potential artificial groundwater recharge in semi-arid crystalline rocks context, Biteira district, Sudan. **Scientific African**, v. 17, p. e01298, 2022.

WHO, 2019. Progress on drinking water, sanitation and hygiene. World Health Organization.

WU, C. *et al.* Hydrogeochemical Characterization and Its Seasonal Changes of Groundwater Based on Self-Organizing Maps. **Water**, v. 13, n. 21, p. 3065, 2021.

ZHANG, Y. *et al.* Small-Scale Irrigation: Improving Food Security under Changing Climate and Water Resource Conditions in Ethiopia. **Journal of Water Resources Planning and Management**, v. 150, n. 8, p. 04024028, 2024.

GENERAL CONCLUSIONS

The changes in the landscape over the last 37 years in Iguatu-CE city have negatively impacted the plant life on the ground, increasing the areas covered by monoculture pasture. These changes of land cover, combined with atypical periods of severe and/or prolonged drought, have hampered agricultural production in the city.

Agricultural practices adopted in the studied areas, in tandem with the soil's granulometric composition, directly influenced the biological composition and the most recalcitrant fractions of soil organic matter, demonstrating the greater effectiveness of intercropping compared to monoculture.

Climate seasonality, linked to the geological composition of the watershed and the type of water source, has resulted in differences in the physical and chemical composition of water resources, with an increase in salt levels during the dry season, which corresponds to the period of highest water use for irrigation in the region.

Table Supplementary 1. Physicochemical parameters of groundwater (G) and surface water (river-R and Orós reservoir-OR), during the dry and rainy seasons, in the municipality of Iguatu, Ceará, Brazil.

Dry period

Sites	**pH**	**EC**	**Na^{+}**	**K^{+}**	**Ca^{2+}**	**Mg^{2+}**	**CO_3^{2-}**	**HCO_3^{-}**	**SO_4^{2-}**	**Cl^{-}**	**Turbidity**	**TDS**
	water	**dSm^{-1}**	**mmol**	**mmol**	**Mmol**	**mmol**	**mmol**	**mmol**	**mgL^{-1}**	**mmol**	**NTU**	**mg/L**
G1	7.7±0.0	0.40±0.00	1.35±0.14	0.21±0.01	1.55±0.05	1.99±0.07	0.34±0.01	3.49±0.09	1.9±0.7	2.3±0.1	5.77±0.20	0.17±0.00
G2	7.8±0.0	0.45±0.00	1.43±0.15	0.20±0.00	1.62±0.00	2.46±0.03	0.27±0.04	3.54±0.01	1.3±0.1	2.0±0.0	19.8±1.27	0.20±0.00
G3	7.3±0.3	0.79±0.00	2.53±0.00	0.36±0.00	2.88±0.05	2.21±0.01	0.15±0.00	4.52±0.01	1.4±0.0	3.5±0.3	10.04±0.27	0.29±0.00
G4	6.7±0.0	0.40±0.01	1.56±0.04	0.11±0.00	1.19±0.08	2.05±0.25	0.13±0.00	2.28±0.29	68.5±0.3	2.1±0.1	69.7±4.97	0.20±0.00
OR5	7.8±0.0	0.31±0.00	0.76±0.00	0.22±0.00	1.22±0.03	2.31±0.17	0.20±0.00	3.20±0.08	0.5±0.1	1.9±0.1	6.18±0.31	0.13±0.00
G6	7.1±0.0	0.87±0.00	3.41±0.00	0.39±0.00	2.21±0.07	2.36±0.09	0.17±0.01	4.77±0.14	24.1±0.9	5.0±0.0	1.15±0.01	0.29±0.00
R7	9.6±0.0	0.43±0.00	1.97±0.01	0.20±0.00	0.89±0.05	2.23±0.15	0.31±0.01	2.19±0.07	11.9±3.0	4.6±0.2	13.51±4.27	0.17±0.00
G8	7.2±0.0	0.98±0.00	3.07±0.02	0.02±0.00	2.55±0.27	3.97±0.30	0.28±0.02	6.96±0.01	15.4±0.3	2.9±0.1	0.72±0.11	0.31±0.01
G9	7.0±0.0	0.93±0.00	3.86±0.00	0.10±0.00	1.70±0.06	2.58±0.02	0.14±0.01	5.25±0.06	26.8±0.5	6.2±0.1	0.43±0.04	0.31±0.00
G10	6.9±0.0	0.74±0.00	2.37±0.02	0.20±0.00	2.49±0.00	2.57±0.00	0.12±0.00	4.77±0.12	14.0±0.8	3.1±0.1	10.97±0.83	0.28±0.00
R11	7.9±0.0	0.37±0.00	1.31±0.01	0.15±0.00	1.14±0.03	1.97±0.08	0.17±0.02	3.16±0.11	2.8±0.1	2.1±0.1	4.22±0.05	0.14±0.00
R12	7.5±0.2	0.84±0.08	3.34±0.23	0.75±0.31	1.48±0.02	1.96±0.09	0.22±0.03	3.77±0.15	31.5±2.3	4.3±0.3	11.88±5.38	0.34±0.00
R13	8.8±0.0	0.46±0.00	1.79±0.00	0.17±0.00	1.30±0.00	1.97±0.01	0.24±0.02	3.18±0.04	2.4±0.4	3.0±0.1	6.59±2.49	0.17±0.00

Rainy period

Sites	**pH**	**EC**	**Na^{+}**	**K^{+}**	**Ca^{2+}**	**Mg^{2+}**	**CO_3^{2-}**	**HCO_3^{-}**	**SO_4^{2-}**	**Cl^{-}**	**Turbidity**	**TDS**
	water	**dSm^{-1}**	**mmol**	**mmol**	**Mmol**	**mmol**	**mmol**	**mmol**	**mgL^{-1}**	**mmol**	**NTU**	**mg/L**
G1	7.7±0.1	0.36±0.02	0.15±0.00	0.02±0.00	1.77±0.04	0.80±0.05	0.00±0.00	2.50±0.00	2.59±1.03	1.0±0.0	1.28±0.29	0.17±0.00
G2	7.1±0.0	0.38±0.00	0.14±0.00	0.03±0.00	1.54±0.07	1.30±0.08	0.00±0.00	3.85±0.07	1.42±0.58	1.0±0.0	1.66±0.04	0.22±0.00
G3	7.3±0.0	0.70±0.01	0.28±0.01	0.03±0.00	2.55±0.04	1.89±0.14	0.00±0.00	4.65±0.02	0.87±0.10	1.5±0.3	8.35±0.46	0.43±0.01
G4	6.9±0.0	0.25±0.00	0.13±0.01	0.03±0.01	1.23±0.08	1.07±0.11	0.00±0.00	2.70±0.10	31.39±0.18	0.8±0.0	1.77±0.13	0.18±0.01
OR5	7.0±0.0	0.26±0.00	0.12±0.00	0.02±0.00	1.08±0.01	1.23±0.08	0.00±0.00	3.05±0.15	4.93±2.39	0.7±0.1	9.85±0.18	0.63±0.04
G6	6.8±0.0	0.72±0.01	0.37±0.01	0.03±0.00	2.08±0.09	1.72±0.15	0.00±0.00	4.60±0.05	22.56±0.06	2.2±0.0	2.27±0.08	0.48±0.02
R7	7.9±0.0	0.33±0.00	0.15±0.00	0.02±0.00	1.57±0.04	1.44±0.02	0.00±0.00	2.65±0.07	1.17±0.28	1.0±0.0	13.75±1.18	0.25±0.00
G8	7.0±0.0	0.94±0.01	0.35±0.00	0.01±0.00	2.90±0.03	4.02±0.07	0.00±0.00	6.45±0.02	15.98±0.34	2.1±0.1	2.62±0.09	0.57±0.01
G9	6.8±0.1	0.93±0.01	2.65±0.06	0.01±0.00	1.52±0.02	1.98±0.02	0.00±0.00	3.85±0.07	25.18±0.84	3.0±0.0	1.82±0.32	0.68±0.00
G10	6.6±0.0	0.39±0.00	0.18±0.04	0.02±0.00	2.29±0.46	1.89±0.24	0.00±0.00	4.00±0.15	27.95±26.93	1.5±0.3	2.10±0.05	0.70±0.00
R11	7.6±0.0	0.34±0.00	0.17±0.02	0.02±0.00	2.08±0.22	0.49±0.12	0.00±0.00	3.80±0.15	8.14±2.84	1.5±0.3	7.85±0.23	0.32±0.00
R12	7.9±0.1	0.35±0.00	0.11±0.00	0.02±0.00	1.82±0.06	1.37±0.01	0.00±0.00	2.90±0.05	2.08±0.64	1.1±0.1	4.83±0.46	0.31±0.01
R13	8.1±0.0	0.34±0.00	0.12±0.00	0.02±0.00	1.56±0.01	1.06±0.05	0.00±0.00	3.20±0.15	0.87±0.24	1.0±0.0	11.28±1.41	0.29±0.01

Source: ?????? Mean±standard error of the mean. EC= Electrical Conductivity; Na^{+}= Sodium; K^{+}= Potassium; Ca^{2+}= Calcium; Mg^{2+}= Magnesium; CO_3^{-2-}= Carbonate; HCO_3^{-}= Bicarbonate; Cl^{-} = Chloride; SO_4^{2-}= Sulfate; TDS= Total Dissolved Solids.

Table Supplementary 2. Micronutrient and metal content of groundwater (G) and surface water (river-R and Orós reservoir-OR), during the dry and rainy seasons, in the municipality of Iguatu, Ceará, Brazil.

Dry period								
Sites	Cu*	Mn	Fe	Zn	Cr	Ni	Cd	Pb
	mg L^{-1}							
G1	0.014±0.008	0.033±0.007	0.154±0.180	0.000±0.000	0.000±0.000	0.000±0.000	0.000±0.000	0.000±0.000
G2	0.026±0.011	0.046±0.005	0.788±0.075	0.000±0.000	0.000±0.000	0.000±0.000	0.000±0.000	0.000±0.000
G3	0.023±0.010	1.650±0.043	0.410±0.044	0.000±0.000	0.000±0.000	0.000±0.000	0.000±0.000	0.000±0.000
G4	0.098±0.015	0.052±0.003	5.738±0.221	0.000±0.000	0.000±0.000	0.000±0.000	0.000±0.000	0.000±0.000
OR5	0.034±0.001	0.000±0.000	0.050±0.001	0.000±0.000	0.000±0.000	0.000±0.000	0.000±0.000	0.000±0.000
G6	0.021±0.012	0.009±0.001	0.000±0.000	0.000±0.000	0.000±0.000	0.000±0.000	0.000±0.000	0.000±0.000
R7	0.068±0.029	0.000±0.000	0.274±0.158	0.000±0.000	0.000±0.000	0.000±0.000	0.000±0.000	0.000±0.000
G8	0.042±0.008	0.000±0.000	0.000±0.000	0.000±0.000	0.000±0.000	0.000±0.000	0.000±0.000	0.000±0.000
G9	0.051±0.010	0.035±0.004	0.000±0.000	0.000±0.000	0.000±0.000	0.000±0.000	0.000±0.000	0.000±0.000
G10	0.081±0.009	0.071±0.005	0.405±0.011	0.000±0.000	0.000±0.000	0.000±0.000	0.000±0.000	0.000±0.000
R11	0.075±0.004	0.086±0.011	0.071±0.020	0.000±0.000	0.000±0.000	0.000±0.000	0.000±0.000	0.000±0.000
R12	0.027±0.009	0.008±0.004	0.248±0.140	0.000±0.000	0.011±0.006	0.136±0.078	0.000±0.000	0.000±0.000
R13	0.117±0.044	0.003±0.002	0.283±0.115	0.000±0.000	0.000±0.000	0.000±0.000	0.000±0.000	0.000±0.000
Rainy period								
Sites	Cu	Mn	Fe	Zn	Cr	Ni	Cd	Pb
	mg L^{-1}							
G1	0.007±0.001	0.043±0.017	0.200±0.026	0.004±0.001	0.000±0.000	0.000±0.000	0.000±0.000	0.000±0.000
G2	0.018±0.009	0.054±0.011	0.102±0.051	0.000±0.000	0.002±0.001	0.000±0.000	0.000±0.000	0.000±0.000
G3	0.063±0.014	1.167±0.553	0.125±0.019	0.000±0.000	0.000±0.000	0.000±0.000	0.000±0.000	0.000±0.000
G4	0.044±0.014	1.210±0.605	0.049±0.025	0.000±0.000	0.008±0.003	0.000±0.000	0.000±0.000	0.000±0.000
OR5	0.036±0.018	0.002±0.001	0.186±0.093	0.000±0.000	0.010±0.005	0.000±0.000	0.000±0.000	0.000±0.000
G6	0.049±0.009	0.009±0.004	0.079±0.034	0.000±0.000	0.000±0.000	0.000±0.000	0.000±0.000	0.000±0.000
R7	0.040±0.020	0.012±0.002	0.213±0.072	0.004±0.002	0.000±0.000	0.000±0.000	0.000±0.000	0.000±0.000
G8	0.070±0.022	0.000±0.000	0.197±0.098	0.000±0.000	0.000±0.000	0.000±0.000	0.000±0.000	0.000±0.000
G9	0.023±0.012	0.029±0.014	0.000±0.000	0.000±0.000	0.000±0.000	0.000±0.000	0.000±0.000	0.000±0.000
G10	0.044±0.022	0.026±0.008	0.101±0.027	0.000±0.000	0.000±0.000	0.000±0.000	0.000±0.000	0.000±0.000
R11	0.045±0.010	0.029±0.006	0.144±0.072	0.000±0.000	0.000±0.000	0.000±0.000	0.000±0.000	0.000±0.000
R12	0.000±0.000	0.000±0.000	0.057±0.004	0.000±0.000	0.000±0.000	0.000±0.000	0.000±0.000	0.000±0.000
R13	0.024±0.012	0.000±0.000	0.062±0.027	0.000±0.000	0.000±0.000	0.000±0.000	0.000±0.000	0.000±0.000
WHO**	2.0	0.4	0.3	3.0	0.05	0.07	0.003	0.01

Source: ???????? *Cu: Copper; Mn: Manganese; Fe: Iron: Zn: Zinc; Cr: Chromium; Ni: Nickel; Cd: Cadmium; Pb: Lead. WHO (World Health Organization). **Limits presented by the World Health Organization for water contamination.

Table Supplementary 3. Physicalchemical parameters of water quality compared to the limits presented by the World Health Organization (WHO, 2019), highlighting the locations with values above the permitted level in the dry and rainy seasons.

Parameter	WHO Limit	Exceedances
pH	6.5–8.5	R7 (9.6) in dry (alkaline); R13 (8.8) in dry.
EC (dSm^{-1})	< 0.75 (low salinity)	G8 (0.98), G6 (0.87) in dry; G8 (0.94) in rainy.
Na^{+}	< 200 mg/L (~8.7 mmol)	All below, but G9 (3.86 mmol/L in dry) requires monitoring.
SO_4^{2-}	< 250 mg/L	G4 (68.5 mg/L in dry) below, but close to irrigation thresholds.
Cl^{-}	< 250 mg/L (~7 mmol)	All below.
Turbidity	< 5 NTU	G4 (69.7 NTU), G2 (19.8 NTU) in dry; R7 (13.75 NTU) in rainy.

Source: ??????? * pH = hydrogen potential, EC= EC: Electrical Conductivity, Na^{+}= Sodium, Chloride; SO_4^{2-}= Sulfate.

Table Supplementary 4. Physicochemical parameters of water quality and tolerated limits for irrigation according to Ayers and Westcot (1985) criterials.

Parameter	Tolerable limit for irrigation	Observed risks
EC (dS/m)	< 3 (low risk)	All below, but G8 (0.98 in dry) may affect sensitive crops.
Na^+	SAR < 3 (low risk)	SAR not calculated here, but Na^+ in G9 (3.86 mmol/L) may require monitoring.
Cl^-	< 10 mmol/L	All below.
SO_4^{2-}	< 20 mmol/L (~1920 mg/L)	All below.
TDS (mg/L)	< 2000 (low risk)	All below.
EC (dS/m)	< 3 (low risk)	All below, but G8 (0.98 in dry) may affect sensitive crops.

Source: ?????? * pH = hydrogen potential, EC= EC: Electrical Conductivity, Na^+= Sodium, Chloride; SO_4^{2-}= Sulfate.